FLORIDA MUSEUM OF NATURAL HISTORY

BULLETIN

A NEW SPECIES OF *TELEOCERAS* (MAMMALIA, RHINOCEROTIDAE) FROM THE LATE HEMPHILLIAN OF TENNESSEE

Rachel A. Short, Steven C. Wallace, and Laura G. Emmert

Vol. 56, No. 5, pp. 183–260 **April 27, 2019**
ISSN 2373-9991

UNIVERSITY OF FLORIDA **GAINESVILLE**

The **FLORIDA MUSEUM OF NATURAL HISTORY** is Florida's state museum of natural history, dedicated to understanding, preserving, and interpreting biological diversity and cultural heritage.

The **BULLETIN OF THE FLORIDA MUSEUM OF NATURAL HISTORY** is an on-line, open-access, peer-reviewed journal that publishes results of original research in zoology, botany, paleontology, archaeology, and museum science. New issues of the Bulletin are published at irregular intervals, and volumes are not necessarily completed in any one year. Volumes contain between 150 and 300 pages, sometimes more. The number of papers contained in each volume varies, depending upon the number of pages in each paper, but four numbers is the current standard. Multi-author issues of related papers have been published together, and inquiries about putting together such isues are welcomed. Address all inquiries to the Editor of the Bulletin.

The electronic edition of this article conforms to the requirements of the amended International Code of Zoological Nomenclature, and hence the new names contained herein are available under that Code. This published work and the nomenclatural acts it contains have been registered in ZooBank, the online registration system for the ICZN. The ZooBank Publication number for this issue is B925B0D2-740E-440A-AB1A-0D480B9C963D.

ISSN: 2373-9991

Publication Date: April 27, 2019. This number concludes volume 56.
This and other recent issues of the Bulletin can be freely downloaded at:
https://www.floridamuseum.ufl.edu/bulletin/publications/

Send communications about this publication to:

Editor of the Bulletin; Florida Museum of Natural History; University of Florida; P.O. Box 117800; Gainesville, FL 32611-7800 USA

FAX: 352-846-0287; Email: bulletin@flmnh.ufl.edu
URL: https://www.floridamuseum.ufl.edu/bulletin/home/

A NEW SPECIES OF *TELEOCERAS* (MAMMALIA, RHINOCEROTIDAE) FROM THE LATE HEMPHILLIAN OF TENNESSEE

Rachel A. Short[1,2], Steven C. Wallace[2,3], and Laura G. Emmert[2]

ABSTRACT

A new species of rhinoceros, *Teleoceras aepysoma* n. sp., is described from the late Hemphillian-aged Gray Fossil Site of eastern Tennessee. Fossils from a minimum of six individuals, including two nearly complete, articulated skeletons, have been found at the Gray Fossil Site. Availability of such complete specimens enables a thorough morphological description of the new species. Furthermore, the diagnostic characters of *T. aepysoma* necessitate an emended diagnosis for the tribe Teleoceratini and genus *Teleoceras.* Cranial features, such as lack of rugose bone for a horn on the dorsal surface of the unfused nasals and pronounced supraorbital tubercles positioned on the frontals dorsal to the orbits, support the establishment of a new species. Additionally, linear measurements and proportions show that *T. aepysoma* has relatively longer forelimb elements and, thus, a more elevated body than previously described species of *Teleoceras*.

Key words: *Teleoceras*, new species, Hemphillian, morphology, Gray Fossil Site, Tennessee.

TABLE OF CONTENTS

[1]Department of Ecosystem Science and Management, Texas A&M University, College Station, Texas 77843, USA <rachel.a.short@tamu.edu>
[2]Don Sundquist Center of Excellence in Paleontology, East Tennessee State University Museum of Natural History, Gray, Tennessee 37615, USA <wallaces@mail.etsu.edu>, <zlsg5@goldmail.etsu.edu>
[3]Department of Geosciences, East Tennessee State University, Johnson City, Tennessee 37614, USA

Short, R. A., S. C. Wallace, and L. G. Emmert. 2019. A new species of *Teleoceras* (Mammalia, Rhinocerotidae) from the late Hemphillian of Tennessee. Bulletin of the Florida Museum of Natural History 56(5):183–260.

INTRODUCTION

Teleoceras is a wide-spread Miocene rhinoceros that has been reported in North American faunas from the late Hemingfordian to the latest Hemphillian North American Land Mammal Ages (NALMA) (Prothero, 1998, 2005; Tedford et al., 2004). In 2000, late Miocene fossils were found during road construction near Gray, Tennessee (Fig. 1A–B; Wallace and Wang, 2004), and the Gray Fossil Site (GFS) was established at the location. In 2004, two nearly complete, articulated rhinoceros skeletons (Figs. 1C, 2) were discovered and provisionally referred to *Teleoceras* cf. *T. hicksi* (Wallace, 2006). To date, the GFS has produced a minimum of six individuals of *Teleoceras* based on the presence of four adult left astragali, a subadult femur, and a juvenile, possibly fetal, tibia and fibula pair (Wallace, 2006); however, this number is likely to increase as excavations continue.

At the GFS, fossil material is found primarily in an organic-rich clay deposit that filled a large sinkhole system in the Knox Group Limestone (Wallace and Wang, 2004). The locality was not a single sinkhole but instead a series of collapsed sinkholes that formed a large basin and, subsequently, a pond, which likely served as a watering hole for local fauna (Whitelaw et al., 2008; Zobaa et al., 2011). The pond filled with finely laminated lacustrine sediments and isolated gravel lenses over 4,500–11,000 years to an estimated depth of 30–40 m (Shunk et al., 2006, 2009). These fine laminations have contributed to the preservation of many completely or partially articulated fossils.

To date, the GFS is one of three Hemphillian fossil localities east of the Mississippi River and outside of Florida along with the Pipe Creek Sinkhole of Indiana and the Mauvilla local fauna of Alabama (Farlow et al., 2001; Prothero, 2005; Hulbert and Whitmore, 2006). Taxa from the GFS are a mix of North American and Eurasian lineages, and there are genera from warm habitats, including *Alligator*, *Tapirus*, and *Heloderma*, as well as

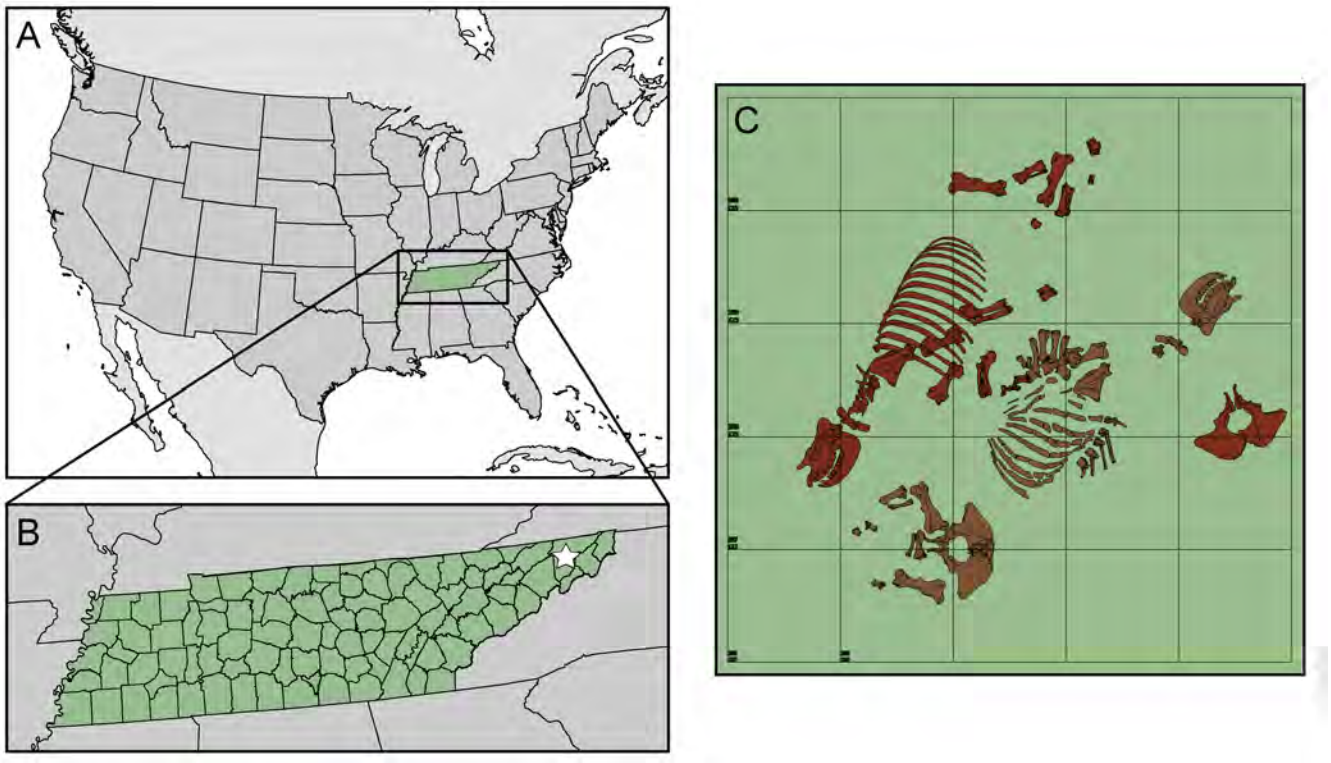

Figure 1. Geography of the Gray Fossil Site. A, Tennessee; B, Gray, Tennessee indicated with the white star; C, positions of ETMNH 601 and ETMNH 609 at time of excavation with 1 m^2 grid.

Figure 2. Mounted cast of ETMNH 609 on public display at the East Tennessee State University Museum of Natural History, Gray, Tennessee.

genera related to modern taxa from cool habitats, such as *Arctomeles*, *Pristinailurus*, and *Gulo* (Wallace and Wang, 2004; Mead et al., 2012; Samuels et al., 2018). The GFS has been biochronologically constrained to 4.5–4.9 Ma based on fauna including *Teleoceras, Plionarctos*, *Gulo sudorus*, *Tapirus polkensis*, and three species of tayassuids (Wallace and Wang, 2004; Hulbert et al., 2009; Doughty et al., 2018; Samuels et al., 2018).

During the late Miocene, the North American climate was warmer and drier than today. Expansion of grasslands was producing more open habitats across much of the continent's center (Strömberg and McInerney, 2011). Yet, in a palynological assessment, Ochoa et al. (2012, 2016) found that 90% of the flora at the GFS was *Quercus*, *Carya*, and *Pinus*. Despite being deposited during a time of climatic and environmental change, it is believed that the landscape surrounding the GFS remained a forest, possibly as a refugium, throughout its depositional history, and that resident *Teleoceras* adopted a browsing ecology (Wallace and Wang, 2004; DeSantis and Wallace, 2008).

Appearance of *Teleoceras* in the North American fossil record has been used, along with other taxa, to indicate the beginning of the late Hemingfordian NALMA (He2, ~17.5 Ma), and its disappearance, with other taxa, indicates the termination of the Hemphillian NALMA (Hh4, ~4.8 Ma; Tedford et al., 2004). Most recently, Prothero (2005) recognized nine species of *Teleoceras*: *T. americanum* (Yatkola and Tanner, 1979), *T. medicornutum* Osborn, 1904, *T. meridianum* (Leidy, 1865), *T. brachyrhinum* Prothero, 2005, *T. major* Hatcher,

1894, *T. proterum* (Leidy, 1885), *T. fossiger* (Cope, 1878), *T. hicksi* Cook, 1927, and *T. guymonense* Prothero, 2005.

Previous work on *Teleoceras* has focused on skulls and dentition, which has caused much confusion and uncertainty (Prothero, 2005); relatively little work has been done on postcranial elements (Mead, 2000; Prothero, 2005). With two nearly complete skeletons available, we present the results of a morphometric comparison of *Teleoceras* from the GFS and the other nine species, recognize the GFS specimens as a new species, and offer a detailed, thorough bone-by-bone description of the *Teleoceras* from the GFS.

MATERIALS AND METHODS

Morphological descriptions of the GFS population were written with the aid of Barone (1999), Flower (1876), McFadyean (1908), Osborn (1898a), and Prothero (2005). Dental morphology is modified from Garutt (1994) and Prothero (2005), and linear measurements come from Prothero (2005). Five cranial measurements (i.e., distance from P2 to occiput, distance from lambdoid crest to nasals, width at zygoma, width of occiput, and height of occiput) and six dental measurements (i.e., lengths of P2–M3, P2–4, M1–3, p3–m3, p3–4, and m1–3) captured skull morphology (Fig. 3). Four postcranial linear measurements (i.e., length, proximal width, distal width, and midshaft width) were taken on humeri, radii, ulnae, femora, tibiae, third metacarpals, and third metatarsals (Fig. 4). Three linear measurements (i.e., length, midshaft width, and width of the sustentaculum) were taken on calcanea (Fig. 4). Measurements were obtained with an osteometric board and recorded to the nearest 0.1 of a millimeter or calipers and recorded to the nearest 0.01 of a millimeter. Mean values from the GFS were plotted with existing data (Prothero, 2005; Appendix 1) in scatter plot matrices using R Software (R Core Team, 2016).

Abbreviations

ETMNH, East Tennessee State University Museum of Natural History; **GFS**, Gray Fossil Site, Gray, Tennessee; **NALMA**, North American Land Mammal Age.

RESULTS

Skulls from the GFS are larger than those of other species of *Teleoceras* with a greater length from P2 to the occiput and greater widths across the zygoma and occiput (Fig. 5; Table 1). Yet, the GFS skulls maintain the characteristically brachycephalic skull of the genus relative to *Aphelops* and *Peraceras*. Dental measurements are consistent across the genus except for upper tooth row lengths of *T. fossiger* and *T. proterum*, which are considerably longer than those of other species (Fig. 5).

Postcranial measurements of the GFS specimens are provided in Table 2. Humeri from the GFS have a greater length, midshaft width, and distal width than other species (Fig. 6). The GFS humeri consistently plot outside of the cluster created by other species of *Teleoceras*. Radii from the GFS have a greater length than other species (Fig. 6). However, radial distal and midshaft widths from the GFS plot within the cluster of the other *Teleoceras* species. Ulnae from the GFS have a greater length and midshaft width than other species and plot considerably beyond the cluster of *Teleoceras* species (Fig. 7).

Interestingly, the proportional differences observed in the forelimb elements are not evident in the hind limb or podial elements. Femora from the GFS have a slightly greater length than femora of other species (Fig. 8), but the midshaft width and distal width plot within the cluster of *Teleoceras* species. Tibiae from the GFS are within the cluster of *Teleoceras* species for length, midshaft width, and distal width (Fig. 8). Podial elements are also within the cluster of *Teleoceras* species, which is to be expected from a genus characterized by derived, yet conservative, podial morphology (Prothero, 2005; Fig. 9). Third metapodials from the GFS have a slightly greater proximal width, and calcanea from the GFS have a slightly greater length and are one of the widest at the sustentaculum. *Teleoceras* calcanea form a nearly linear trend with the GFS at the largest end and, interestingly, this corresponds closely to taxonomy through time.

Skulls and limb elements of the GFS *Teleoceras* are proportionally different from the currently recognized nine species. In addition to unique

Figure 3. Skull and dental linear measurements. 1, height of occiput; 2, lambdoid crest to nasals; 3, width at zygoma; 4, width of occiput; 5, P2 to occiput; 6, P2−M3; 7, P2−P4; 8, M1−M3. Lower dentition was measured similarly: p2−m3, p2−p4, and m1−m3. Measurements are from Prothero (2005).

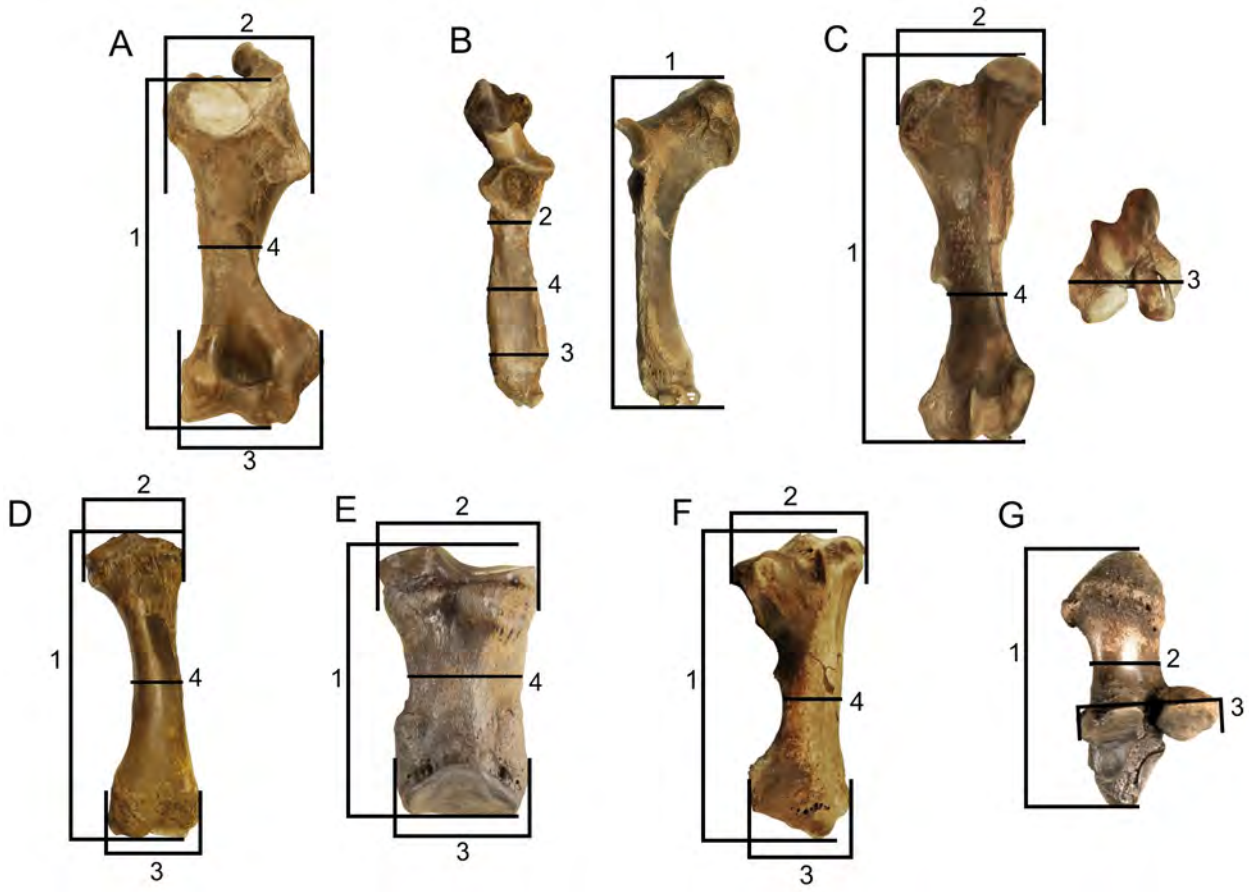

Figure 4. Postcranial linear measurements. A, humerus; B, ulna; C, femur; D, radius; E, third metacarpal; F, tibia; G, calcaneum. For A–F: 1, maximum length; 2, maximum proximal width; 3, maximum distal width; 4, midshaft width. For G: 1, maximum length; 2, midshaft width; 3, width of the sustentaculum. Measurements are modified from Prothero (2005).

morphological characters, these features warrant emended diagnoses of Teleoceratini and *Teleoceras* as well as the designation of a new species (Table 3).

SYSTEMATIC PALEONTOLOGY

Class MAMMALIA Linnaeus, 1758
Order PERISSODACTYLA Owen, 1848
Family RHINOCEROTIDAE Owen, 1845
Tribe TELEOCERATINI Hay, 1902

Emended diagnosis.—Retained characters from Prothero (2005:94): "robust, flattened carpals, tarsals, and metapodials…a very brachycephalic skull with a flaring lambdoid crest and broad zygomatic arches…nasals that are U-shaped in cross-section, with or without a small terminal horn… a strong, lobal antecrochet on the upper molars, and an elongate calcaneal tuber." Rejected characters from Prothero (2005) are provided in the remarks below.

Remarks.—Presence of most characters of Teleoceratini supports placing the GFS specimens in this tribe rather than the subfamily Aceratheriinae (Table 3). Aceratherines, including *Peraceras* and *Aphelops*, were the only other North American rhinoceroses during the late Neogene. Aceratherines are characterized by reduced premaxillae, reduced medial flanges of lower tusks, narrow skulls, and long legs. The GFS fossils exhibit several distinct features (see diagnosis below) that not only warrant

erection of the new species, but also call in to question some of the characters used to define the tribe. The new species described below justifies removing the following characters from the tribe diagnosis of Prothero (2005:94): "short, stumpy limbs… [and] a nasal incision retracted to anterior P3 (not as far as in aceratheriines)." The latter character is not evident on examined skulls of *Teleoceras* and is believed to be poorly defined.

Genus *TELEOCERAS* Hatcher, 1894

Emended diagnosis.—Retained characters from Prothero (2005:94): "medium- to large-sized teleoceratin rhinos with hypsodont teeth, strong antecrochets, greatly reduced premolars with dP1/p1 lost and occasional loss of P2/p2, thick cement on teeth, narrow nasals with strongly downturned lateral edges, enlarged premaxilla and I1, broad zygomatic arches, flaring lambdoid crests (skull semicircular in posterior view)…lower tusk (i2) shaped like a teardrop in cross-section, and…barrel-shaped trunk." Rejected characters from Prothero (2005) are provided in the remarks below.

Included species.—*T. americanum* (Yatkola and Tanner, 1979); *T. medicornutum* Osborn, 1904; *T. brachyrhinum* Prothero, 2005; *T. meridianum* (Leidy, 1865); *T. fossiger* (Cope, 1878); *T. proterum* (Leidy, 1885); *T. hicksi* Cook, 1927; *T. guymonense* Prothero, 2005; *T. aepysoma* n. sp.

Remarks.—*Teleoceras* is the only North American genus of Teleoceratini, and presence of most characters supports referring the GFS specimens to this genus (Table 3). The GFS fossils exhibit several distinct features (see diagnosis below) that not only warrant erection of the new species, but also call in to question some of the characters used to define the genus. Specifically, the new species justifies removing the following characters from the generic diagnosis of Prothero (2005:94): "a small terminal nasal horn and fused nasals…teleoceratin body proportions…and short, robust limbs."

TELEOCERAS AEPYSOMA n. sp.

Teleoceras sp. Parmalee et al. (2002); Wallace and Wang (2004); Shunk (2006)

Teleoceras cf. *T. hicksi* Shunk et al. (2006); DeSantis and Wallace (2008); Hulbert et al. (2009)

Teleoceras sp. nov Wallace et al. (2014)

Diagnosis.—*Teleoceras aepysoma* has

Table 1. *Teleoceras aepysoma* cranial measurements (mm). See Figure 3 for measurement schematic.

	Mean	ETMNH 601	ETMNH 609
Skull			
height of occiput	196.54	201.63	191.45
lambdoid crest to nasals	455.49	493.39	417.59
width at zygoma	357.18	377.15	337.21
width of occiput	235.61	246.29	224.94
P2 to occiput	519.76	530.74	508.78
Dentition			
P2–M3	265.99	264.45	267.54
P2–P4	116.29	114.06	118.53
M1–M3	158.85	162.42	155.29
p3–m3	246.84	249.44	244.24
p3–p4	82.33	82.21	82.46
m1–m3	165.74	167.60	163.89

Table 2. *Teleoceras aepysoma* postcranial measurements (mm). See Figure 4 for measurement schematic. For the metacarpal, the mean is calculated from the means of individuals to prevent duplicating values for ETMNH 601 and ETMNH 609. Unavailable measurements are indicated with dashes, and unavailable elements are indicated with a gray background.

	Mean	ETMNH 601 Right	ETMNH 601 Left	ETMNH 609 Right	ETMNH 609 Left	ETMNH 8271 Right
Humerus						
Length	392.5	--	--	392.0	393.0	
Proximal Width	157.6	161.0	--	150.0	158.5	
Distal Width	154.1	161.5	161.5	146.8	146.8	
Midshaft Width	76.08	77.27	75.58	74.02	77.44	
Ulna						
Length	388.8	403.5	401.0	372.0	378.5	
Proximal Width	53.21	57.78	58.45	45.88	50.74	
Distal Width	66.72	68.59	67.54	66.97	63.78	
Midshaft Width	59.20	60.50	59.80	58.57	57.91	
Radius						
Length	310.6	328.3	321.8	296.5	295.8	
Proximal Width	100.4	101.8	103.0	99.0	98.0	
Distal Width	97.9	103.0	103.5	93.3	91.8	
Midshaft Width	48.84	51.89	52.22	45.36	45.89	
MC3						
Length	125.6	140.3	139.0	118.0	118.5	119.0
Proximal Width	69.8	77.0	75.0	67.0	66.0	67.0
Distal Width	64.8	73.5	73.0	60.3	59.5	61.3
Midshaft Width	52.11	58.03	58.55	48.65	48.79	49.32
Femur						
Length	491.6	505.8	513.3	472.3	475.0	
Proximal Width	190.4	200.0	196.8	183.3	181.5	
Distal Width	134.4	140.5	139.8	129.0	128.5	
Midshaft Width	69.99	75.21	73.13	66.15	65.50	
Tibia						
Length	271.5	--	290.8	253.0	251.5	
Proximal Width	112.2	122.0	117.5	103.3	105.8	
Distal Width	90.1	94.3	94.8	87.0	84.3	
Midshaft Width	51.44	--	53.35	51.41	47.67	
Calcaneum						
Length	140.2	149.5	151.0	130.0	130.3	
Midshaft Width	44.30	48.20	44.56	41.54	42.91	
Width at Sustentaculum	77.06	81.67	79.56	75.52	71.50	

Table 2. Continued.

MT3					
Length	105.2	114.5	113.0	96.3	97.0
Proximal Width	54.3	56.0	57.5	52.0	51.5
Distal Width	59.8	64.3	66.5	53.8	54.5
Midshaft Width	45.53	49.73	50.11	40.89	41.41

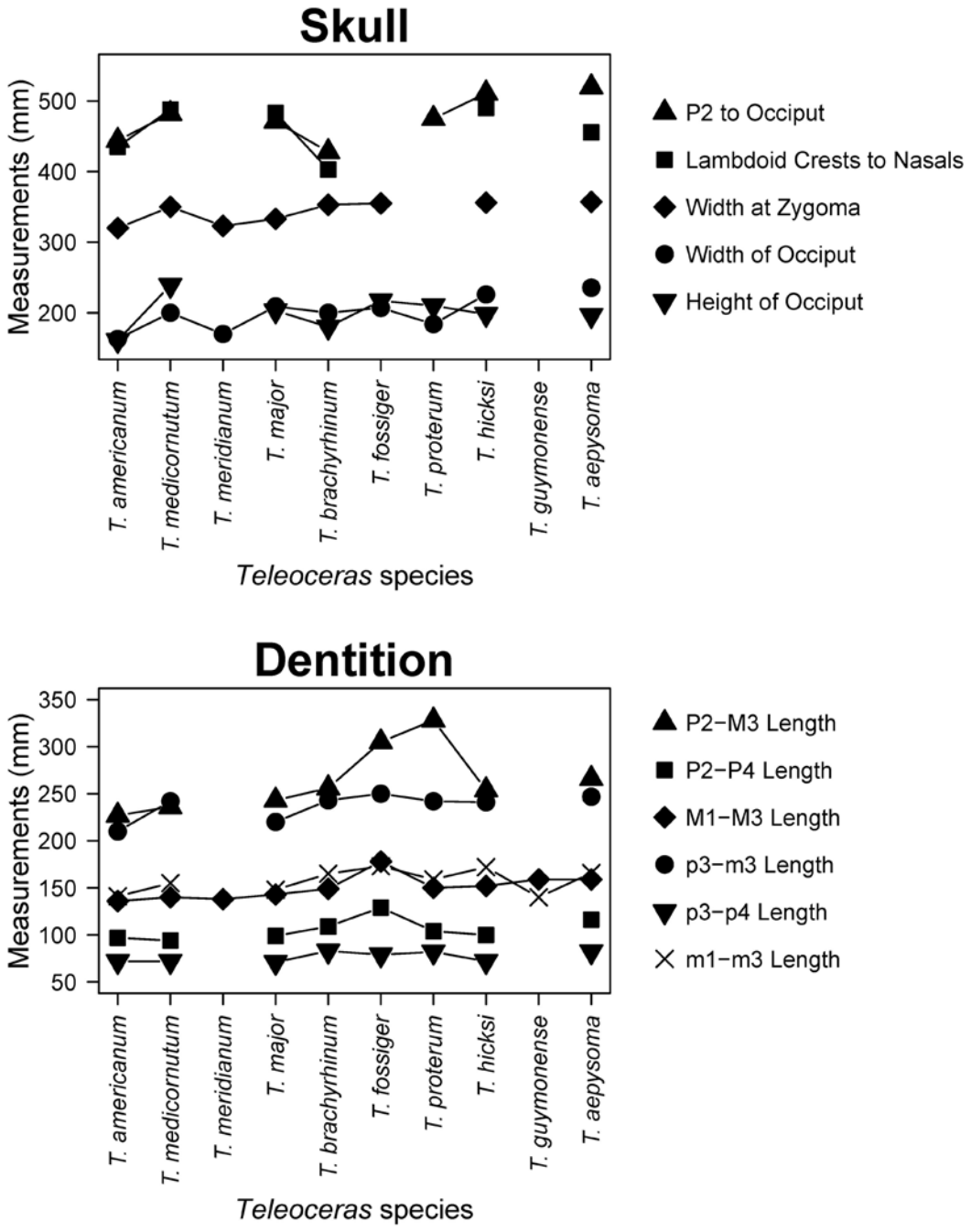

Figure 5. Measurements of *Teleoceras* skulls and dentition. See Figure 3 for measurement schematic. *Teleoceras aepysoma* data are compared to data from Prothero (2005; see Appendix 1).

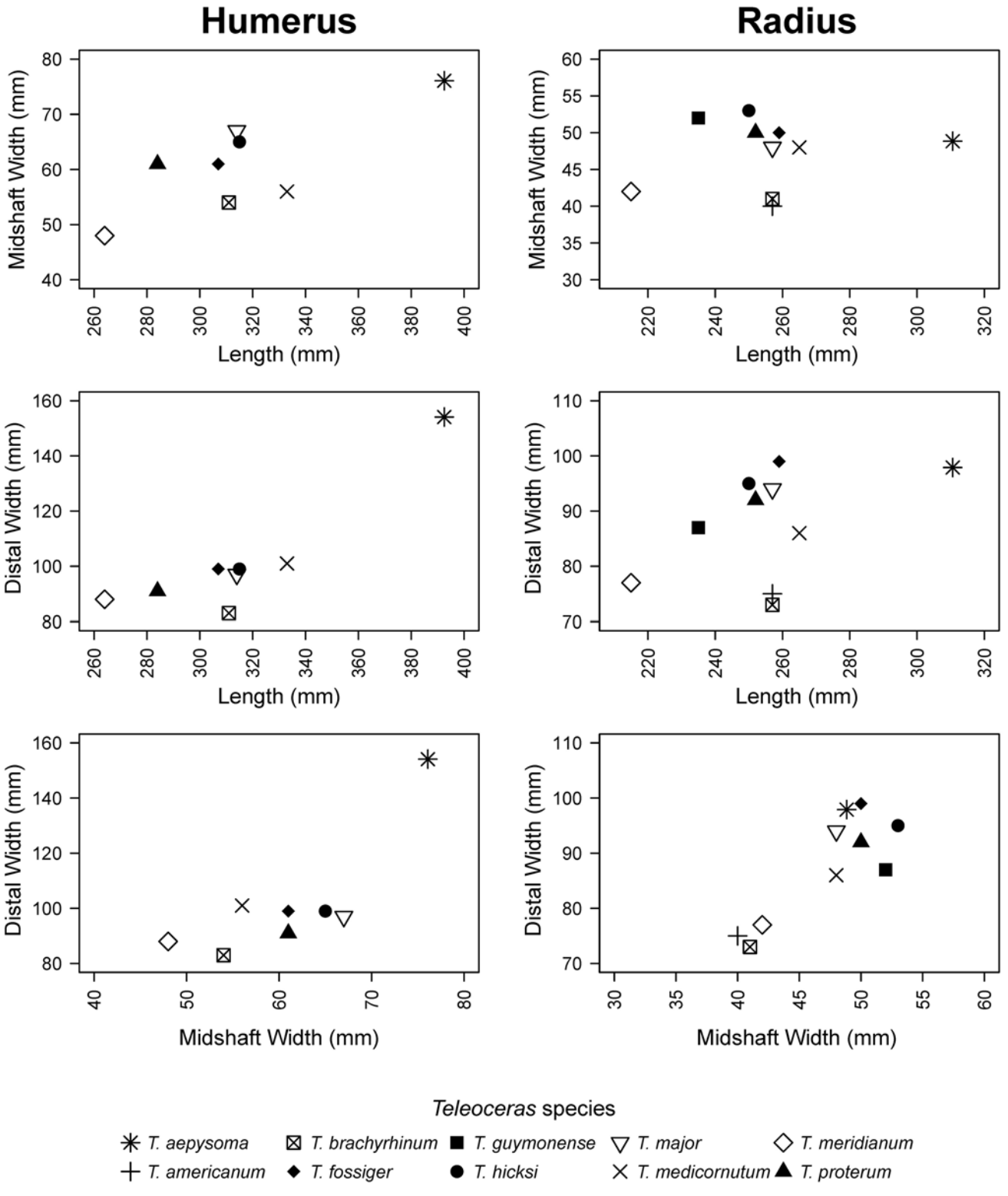

Figure 6. Measurements of *Teleoceras* humeri and radii. See Figure 4 for measurement schematic. *Teleoceras aepysoma* data are compared to data from Prothero (2005; see Appendix 1).

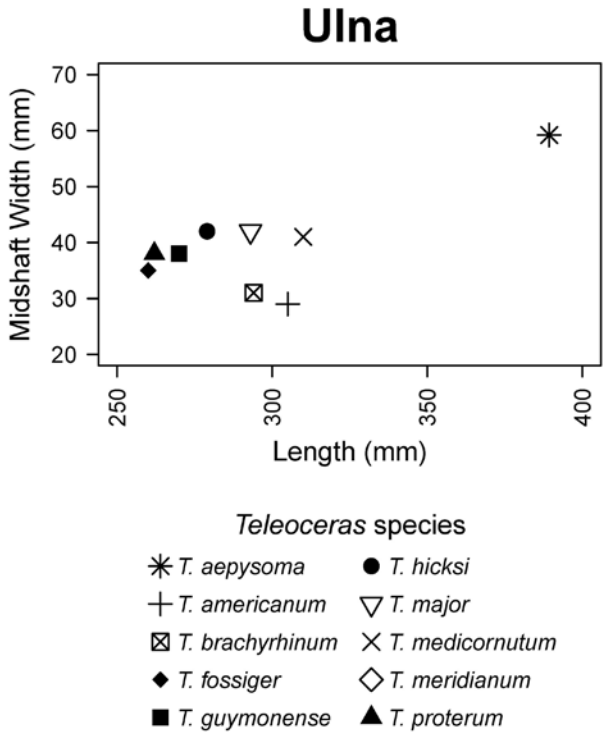

Figure 7. Measurements of *Teleoceras* ulnae. See Figure 4 for measurement schematic. *Teleoceras aepysoma* data are compared to data from Prothero (2005; see Appendix 1).

large skulls with a greater length from P2 to the occiput and greater widths across the zygoma and the occiput than other species of *Teleoceras*. As adults, male *T. aepysoma* have unfused nasals, lack evidence of a nasal horn, and have extensive dorsal tubercles superior to the orbits (supraorbital tubercles). Forelimb bones (i.e., humerus, radius, and ulna) of *T. aepysoma* are longer than in other species of *Teleoceras*. Humeri and ulnae also have greater midshaft widths and distal widths. In the hind limbs, femora are slightly longer than other species of *Teleoceras.* As a result of the longer limb bones, the body of *T. aepysoma* is more elevated, especially at the front end, than is typical of the genus. Characters are provided in Table 3.

Etymology.—"*Aepy*," Greek for high or tall, and "*soma*," Greek for body; referring to the elevated stance of this species relative to congenerics.

Types.—Holotype, ETMNH 609, complete skeleton, missing only one distal phalanx. Paratype, ETMNH 601, nearly complete skeleton. Type locality is the Gray Fossil Site, Gray, Washington County, Tennessee, USA (Fig. 1). A cast of the holotype is on public display at the ETMNH (Fig. 2). A paratype is assigned because of its better-preserved skull (Fig. 10).

Zoobank Nomenclatural Act.—D3CCE3BC-98AA-4D98-8727-86999FC6D248.

Occurrence.—Latest Hemphillian, late Miocene to early Pliocene. *Teleoceras aepysoma* is currently only known from the Gray Fossil Site, Gray, Washington County, Tennessee.

Referred specimens.—Partial skeleton: ETMNH 19280; Cranial: ETMNH 12175, 17351, 17352, 17353, 21659; Dentition: ETMNH 566, 780, 781, 3763, 5235, 7894, 12487, 13914; Vertebra: ETMNH 559, 573, 3751, 12175, 13510, 17354; Rib: ETMNH 3747, 3752, 3754, 4286, 6037, 6649, 6749, 7291, 7294, 8173, 8182, 8636, 10959, 12242, 14174, 14710, 14894, 17355, 17356; Humerus: ETMNH 5057, 6648; Ulna: ETMNH 502, 8762; Partial manus: ETMNH 8271; Trapezium: ETMNH 13236; Magnum: ETMNH 8516; Femur: ETMNH 3721; Tibia with fibula: ETMNH 19025; Astragalus: ETMNH 1901, 6647, 14175; Mesocuneiform: ETMNH 3749; Metapodial: ETMNH 565; Podial: ETMNH 62; Phalanx: ETMNH 80, 107, 564, 712, 713, 743, 769, 3755, 4381, 5233, 11651, 12175, 12450, 12776, 12777, 13031, 13968, 17357.

Remarks.—All specimens from the GFS are well-preserved with minimal breakage or other distortion. Two nearly complete skeletons have been recovered along with isolated elements from other individuals. ETMNH 609 is smaller and is only missing the distal phalanx of the left hind fourth digit. ETMNH 601 is a larger individual, but is less complete than ETMNH 609. ETMNH 601 has the skull, dentition, and most of the appendicular skeleton, though it is more damaged than that of ETMNH 609; however, ETMNH 601 is missing most of the axial skeleton. ETMNH 19280 is a partial skeleton that includes a fragmented dentary with fragmented teeth, partial vertebrae and ribs, right distal tibia and fibula, left third metatarsal,

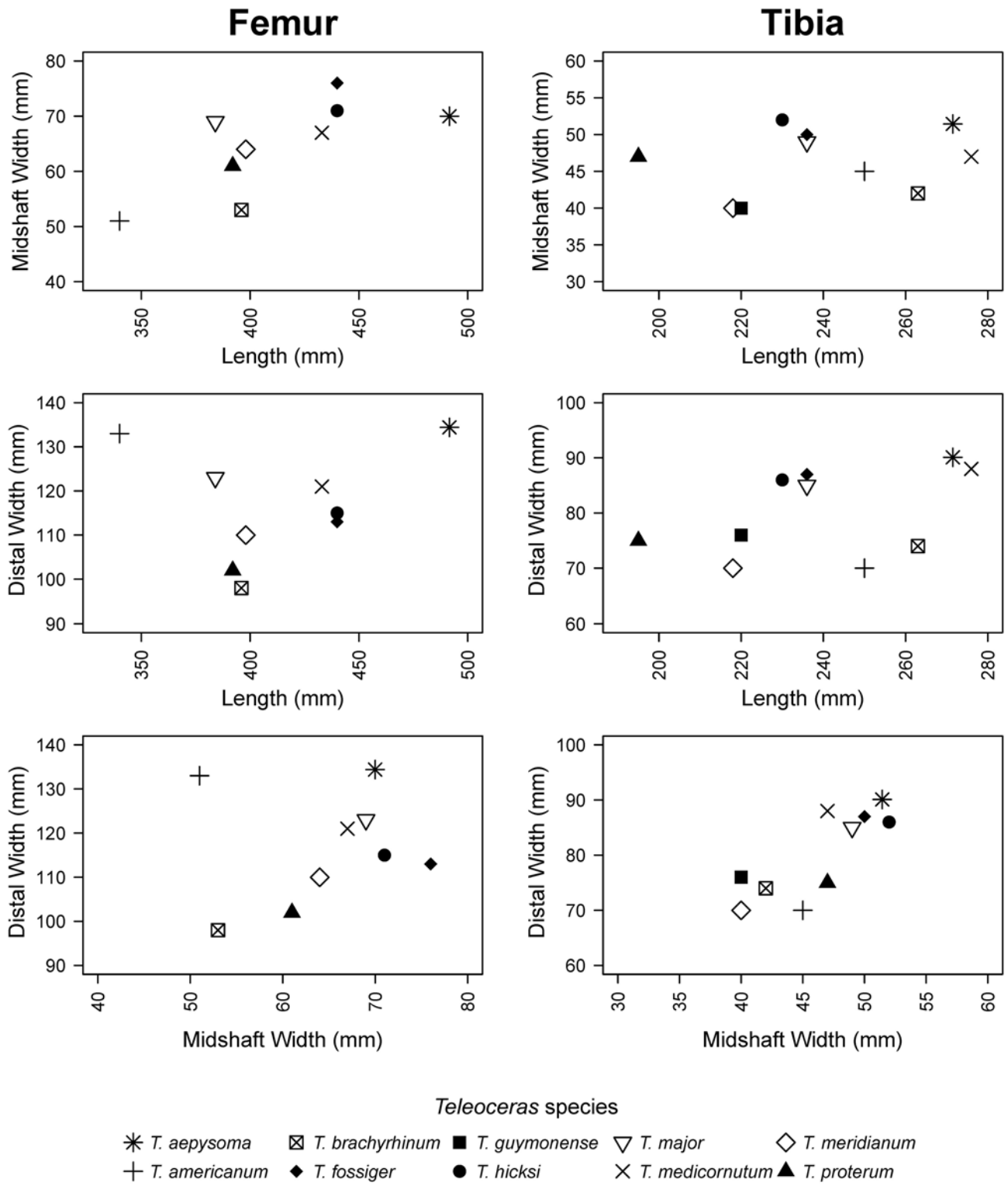

Figure 8. Measurements of *Teleoceras* femora and tibiae. See Figure 4 for measurement schematic. *Teleoceras aepysoma* data are compared to data from Prothero (2005; see Appendix 1).

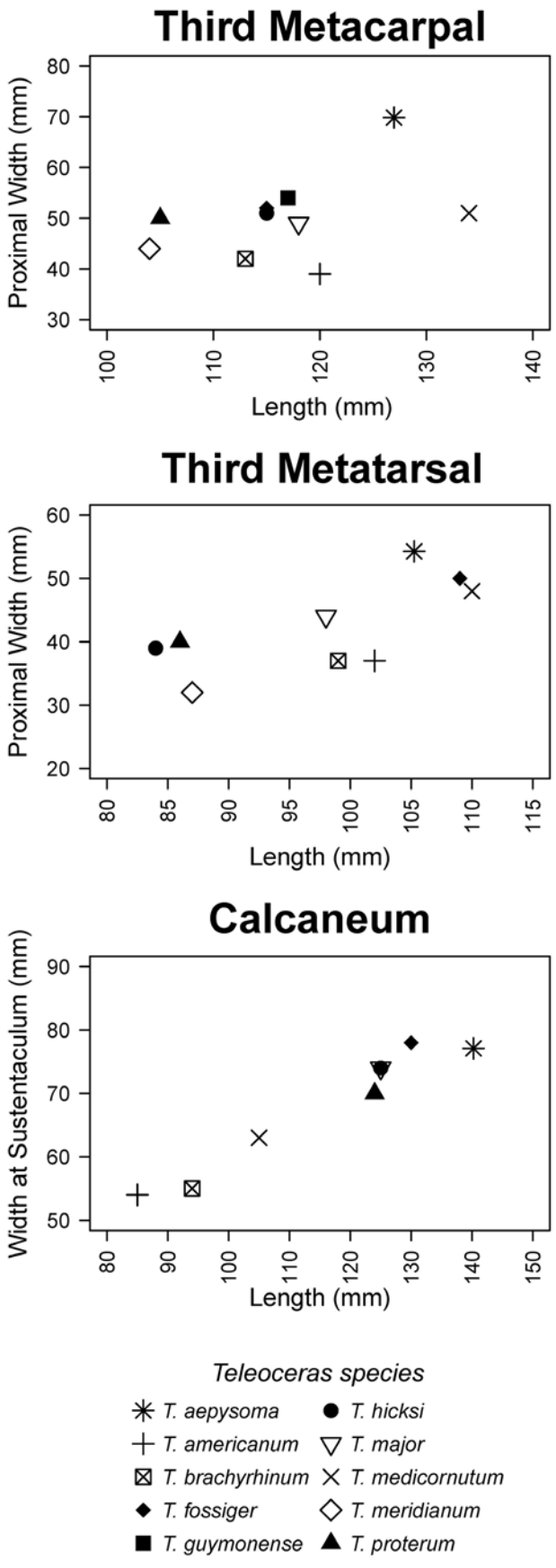

and associated unidentified fragments.

Both ETMNH 609 and ETMNH 601 are considered males because of their large, tusk-like i2s. This is in contrast to the smaller i2s found in female rhinoceroses (Osborn, 1898a, 1898b; Voorhies and Stover, 1978; Dinerstein, 1991). Both skeletons are also adults based on the degree of epiphyseal fusion and tooth wear. The upper tooth row of ETMNH 609 matches age class XI of Hitchins (1978) and the lower tooth row matches age class X. The larger ETMNH 601 matches age class XIII of Hitchins (1978) on the upper teeth and age class XII on the lower teeth. Using Mihlbachler's (2003) life span percentages, ETMNH 609 was at the beginning of an age class marking 25–35% of its potential life span and ETMNH 601 was at the beginning of an age class marking 35–52% of its potential life span. In extant *Diceros*, these life span percentages refer to 8–12 years old and 11–18 years old, respectively (Hitchins, 1978).

Mass estimates suggest *Teleoceras aepysoma* is quite large. Using equations based on the circumferences of the humerus and femur (Anderson et al., 1985), the mass of ETMNH 609 is estimated to be 1488 kg and 1335 kg, respectively, and that of ETMNH 601 is estimated to be 2330 kg and 2147 kg. These same equations produced mass estimates of 702 kg and 568 kg for *T. proterum* from the Love Bone Bed (MacFadden and Hulbert, 1990). The substantially greater mass estimates for *T. aepysoma* are corroborated by calculations using the calcaneum and constants from two modern rhino taxa (*Ceratotherium simum* and *Diceros bicornis*) (Christiansen, 2002). Mass was estimated separately for each constant and then averaged. Using this method, the estimated masses of ETMNH 609 and ETMNH 601 are 1544 kg and 2268 kg, respectively.

Figure 9. Measurements of *Teleoceras* podial elements. See Figure 4 for measurement schematic. *Teleoceras aepysoma* data are compared to data from Prothero (2005; see Appendix 1).

Table 3. Morphological characters of Teleoceratini, *Teleoceras*, and *T. aepysoma* n. sp. Teleoceratini synapomorphies and *Teleoceras* characters are quoted from Prothero (2005:94). Those that are present in *Teleoceras aepysoma* are indicated with '*,' those absent are indicated with 'X,' and one that is questionably defined is indicated by '?.'

Synapomorphies of Teleoceratini	***T. aepysoma***
1. short, stumpy limbs	X
2. robust, flattened carpals, tarsals, and metapodials	*
3. very brachycephalic skull	*
4. flaring lambdoid crest	*
5. broad zygomatic arches	*
6. nasals that are U-shaped in cross-section	*
7. nasals with or without a small terminal horn	*
8. nasal incision retracted to anterior P3 (not as far as in aceratheriines)	?
9. strong, lobal antecrochet on the upper molars	*
10. elongate calcaneal tuber	*
Characters of *Teleoceras*	***T. aepysoma***
1. hypsodont teeth	*
2. strong antecrochets	*
3. greatly reduced upper and lower premolars	*
4. deciduous p1s lost and occasional loss of p2s	*
5. thick cement on teeth	*
6. narrow nasals with strongly downturned lateral edges	*
7. enlarged premaxilla and I1	*
8. broad zygomatic arches	*
9. flaring lambdoid crests (skull semicircular in posterior view)	*
10. small terminal nasal horn	X
11. fused nasals	X
12. i2 (tusk) shaped like a teardrop in cross-section	*
13. teleoceratine body proportions of a barrel-shaped trunk and short, robust limbs	X
New Characters of *Teleoceras aepysoma*	
1. greater length from P2 to the occiput than other species	
2. greater widths across the zygoma and the occiput than other species	
3. unfused nasals	
4. no evidence of a nasal horn	
5. extensive dorsal tubercles superior to the orbits	
6. humerus, radius, ulna, and femur with greater lengths than other species	
7. humerus and ulna with greater midshaft and distal widths than other species	
8. more elevated body than considered typical of the genus	

Figure 10. Cranium of ETMNH 601 in three views. The upper tusks are removed in this image. A, right lateral view; B, dorsal view; C, ventral view. Anterior is to the right in all three. Scale bar = 10 cm.

MORPHOLOGICAL DESCRIPTION

Cranium

Nasal.—Anteriorly, the nasals are round in cross-section and, when visible, articulate along a coarsely serrated suture (Fig. 11). No evidence of a horn attachment is present on the smooth dorsal surface. Ventrally, the surface is concave and has an anteroposterior ethmoid crest. Nasals become progressively thicker in cross-section toward the anterior suture. ETMNH 609 has only slightly more anteriorly upturned nasals than the straight nasals of ETMNH 601.

Frontal.—Dorsally, the frontals are flat except for laterally extending supraorbital tubercles positioned dorsal to the orbits that are unique to this taxon (Fig. 12).

Parietal.—Laterally, the parietals are inflated around the braincase (Fig. 13). A broad concavity is present at the articulation between the squamosal and the parietal and dorsal to the external auditory meatus. Paired temporal crests extend posteromedially from the supraorbital tuberosities of the frontals until they nearly merge dorsally, before separating at the lambdoid crest; the temporal crests of ETMNH 601 merge to form a sagittal table.

Premaxilla.—Premaxillae of ETMNH 601 are complete and are nearly articulated at their anterior-most point (Fig. 14). Anteroventrally-oriented tusk alveoli are present and support the I1s. Premaxillae of ETMNH 601 are medially flattened, laterally flared, dorsally rounded, and posteroventrally pinched. No nasal or palatine processes are present and there is no evidence of an incisive foramen. Both premaxillae of ETMNH 609 have been entirely reconstructed so that the upper tusks occlude with the lower tusks.

Maxilla.—Except for the incisors, the maxilla supports the entirety of the upper tooth row (Fig. 15). Though the facial surfaces are present, most of the internal maxilla of ETMNH 601 is missing. Between the premaxillae articulations, the maxillae are concave to form a rounded incisive cleft at the anterior end of the palate. On the lateral surface, there is a concavity anterior to the lacrimal and ventral to the nasal.

Posterolaterally, the maxilla expands laterally to articulate with the jugal and form the anterior zygomatic arch. The maxillary tuberosity continues posteromedially to the jugal articulation at the end of the tooth row. A superior maxillary sinus is within the maxillary tuberosity. A facial crest is bordered by a groove between the maxillary tuberosity and the jugal articulation. Both ETMNH 601 and ETMNH 609 have anteriorly deep maxillary palates that rise to the level of the tooth alveoli at the posterior end.

Lacrimal.—This small bone forms the anterior edge of the orbit (Fig. 16). Though the facial surface is rugose, the orbital surface is smooth. There is a laterally-directed lacrimal foramen just beneath a laterally-protruding lacrimal tubercle.

Jugal.—The jugal articulates with the maxilla superior to the M1 and M2 (Fig. 17). With the squamosal, the jugal forms the broad and rugose zygomatic arch. Minimal roughness is present on the facial surface, but along the ventral edge of the orbit, the jugal is smooth. There are heavy rugosities on the medial side of the zygomatic arch.

Squamosal.—Like the jugal, the medial surface of the squamosal has prominent muscle scarring (Fig. 18). The posterolateral squamosal is more rugose along the medial curve from the zygomatic arch to the parietal articulation and, in doing so, forms the lateral boundary of the temporal fossa. A transversely elongate glenoid fossa has an open angle and is only slightly concave. Anterior to the glenoid fossa, the articular tubercle is round, but it appears pinched anteriorly. Post-glenoid processes are nearly straight and elongate but are shorter than the paroccipital processes of the occipital. These two processes fuse ventral to the external auditory meatus to form the mastoid crest but are then separated by a ‘V’-shaped notch. Dorsal to the external auditory meatus, the squamosal and occipital bones fuse to form the lambdoid crest. There is no evidence of external auditory bullae.

Occipital.—On the posteroventral surface, the triangular (in posterior view), convex occipital condyles are lateral to the foramen magnum (Fig. 19). On the ventral surface, the paired hypoglossal foramina are anterior to each of the occipital

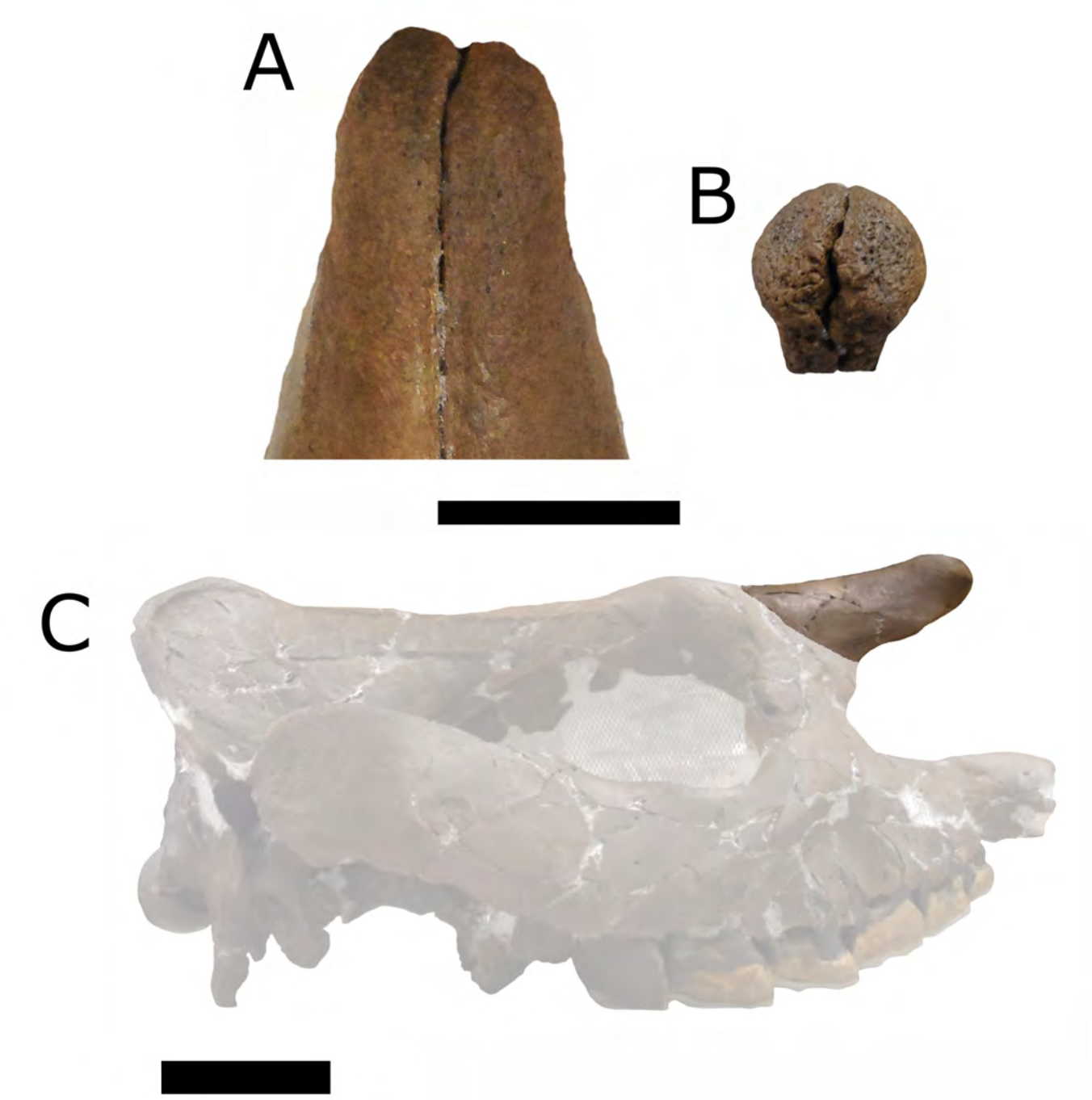

Figure 11. Nasals of ETMNH 601. A, dorsal view; B, anterior view; C, right lateral view. In A and B, the scale bar = 5 cm. In C, the scale bar = 10 cm.

condyles and medial to each paroccipital process. Most of the occipital extends in the same plane as the occipital condyles and only the dorsal-most lambdoid crest extends more posteriorly. Edges of the occipital form the lambdoid crest with the squamosal and parietals. At the ventral point of the external auditory meatus, the lambdoid crest meets the crest of the post-glenoid process and then continues as the paroccipital process. ETMNH 609 has an asymmetrical lambdoid crest that may be due to pathology but further examination is needed.

Basicranium.—Because of the large amount of fusion, it is difficult to discern the individual bones of the basicranium, so it will be described

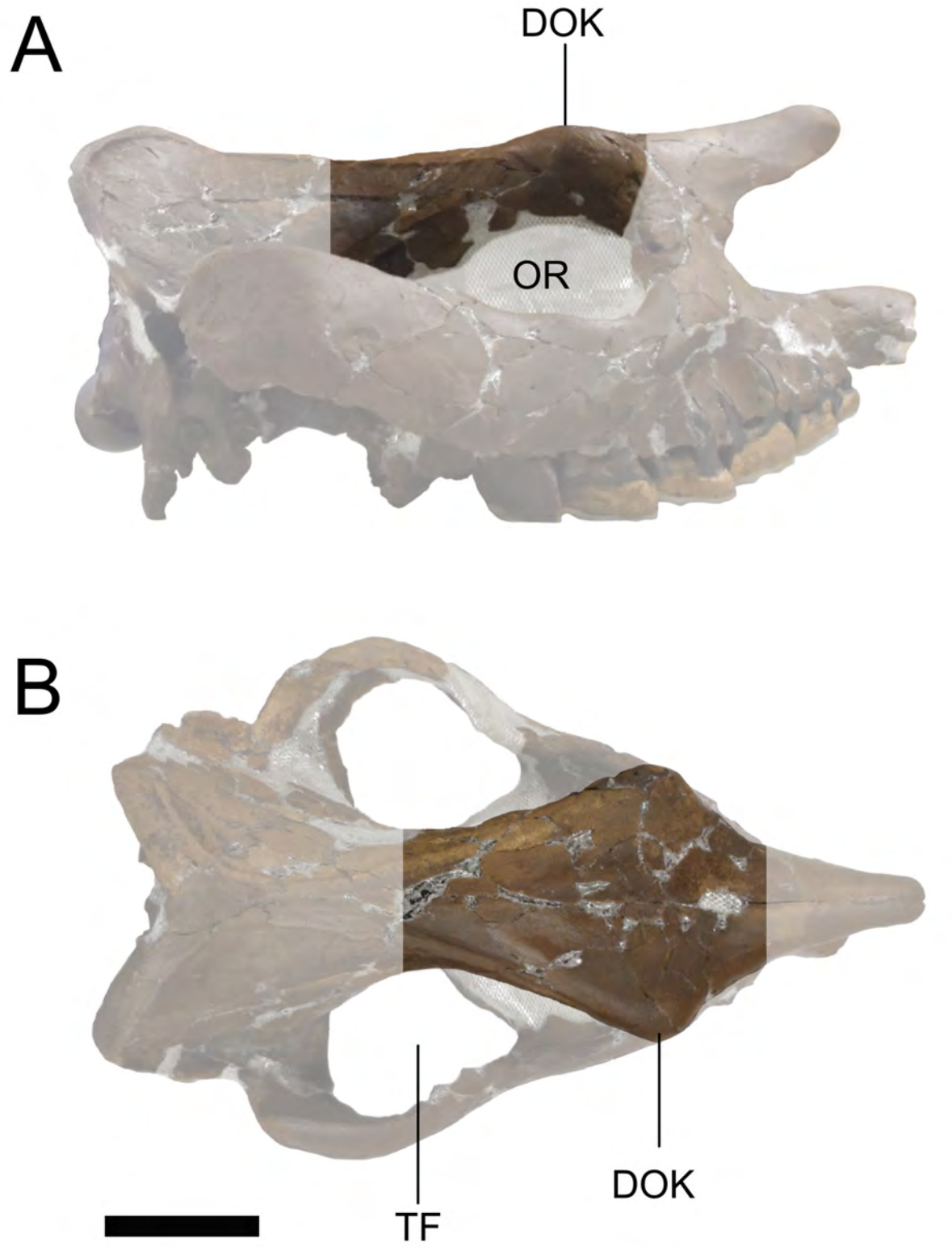

Figure 12. Frontals of ETMNH 601. A, right lateral view; B, dorsal view. Abbreviations: DOK, dorsal orbit knobs; OR, orbit; TF, temporal fossa. Scale bar = 10 cm.

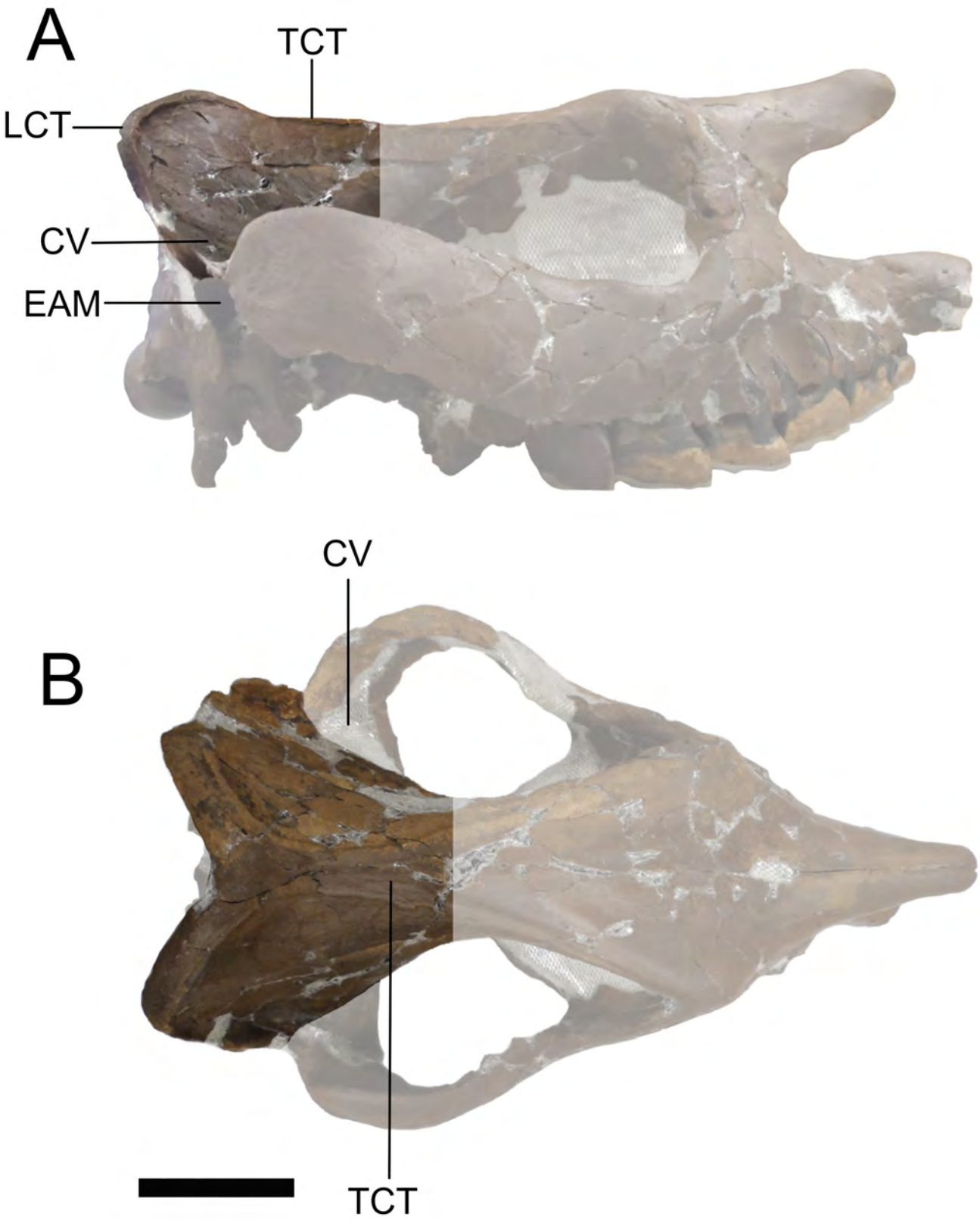

Figure 13. Parietals of ETMNH 601. A, right lateral view; B, dorsal view. Abbreviations: CV, concavity; EAM, external auditory meatus; LCT, lambdoid crest; TCT, temporal crest. Scale bar = 10 cm.

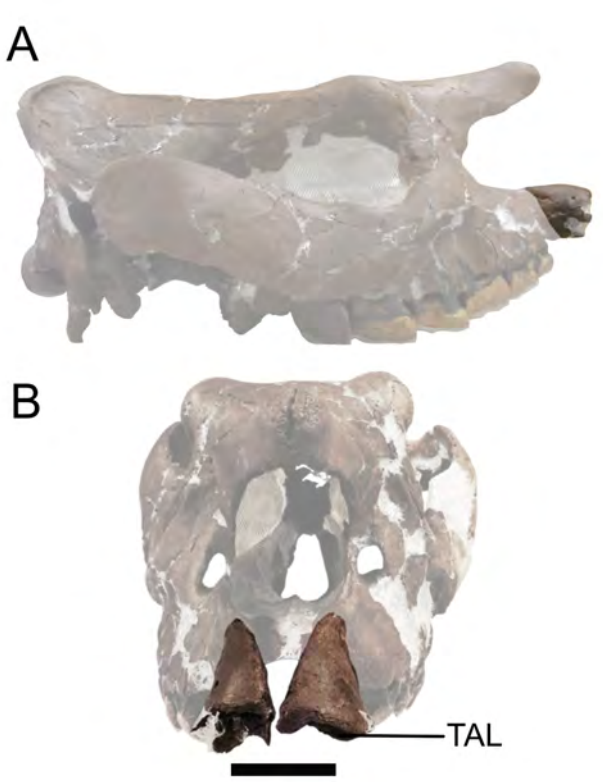

Figure 14. Premaxillae of ETMNH 601. Views: A, right lateral; B, anterior. Abbreviations: TAL, tusk alveolus. Scale bar = 10 cm.

here as a region (Fig. 20). Ventrally, the basicranium is in poor condition on both crania. There is a ventral muscle tubercle anterior to what is most likely the articulation between the occipital and the basisphenoid. Each lateral side of this region has an alisphenoid canal that is bridged by bone, likely the alisphenoid, with prominent surficial ridges. A dorsal opening to this canal is anterior and the canal gently curves posteroventrally.

Pterygoid.—Pterygoid processes are directed posteroventrally and almost to the height of the M3 (Fig. 21).

Palatine.—Almost all of the palatine of ETMNH 601 has been repaired with mesh making it nearly impossible to describe any morphology (Fig. 22).

Vomer.—The unpaired vomer is missing from both skulls.

Hyoid Apparatus.—The basihyoid is round but is dorsoventrally compressed and lacks a lingual process (Fig. 23). The left thyrohyoid of ETMNH 601 is present and it extends posterolaterally from the basihyoid. A rugose knob forms the articulation and the thyrohyoid tapers so that it is mediolaterally compressed. The ceratohyoid is short with rounded sides, and it would articulate between the basihyoid and the epihyoid; though, no epihyoids are present. Finally, the stylohyoid articulates with the epihyoid and the tympanohyoid cartilage. The stylohyoid is the largest of the hyoid bones and is mediolaterally compressed with a medial fossa at the proximal end. There are no tympanohyoids present. North American rhinoceros hyoids were previously only known from *Teleoceras major* at Ashfall Fossil Beds State Historical Park (Prothero, 2005).

Mandible.—Overall, the mandible is much longer than it is tall and the intermaxillary space is 'V'-shaped (Fig. 24). A shallow, sloping symphysis with a broad lingual surface is present between the dentaries and extends posteriorly to the middle of the p4. Angles of the dentaries are flared laterally and are rugose, especially on ETMNH 601, which is likely due to increased muscle attachment associated with a more advanced age. Each lateral surface has a broad and shallow masseteric fossa that is dorsal to the angular rugosities, which are present on both the medial and lateral side of the dentary. Though there are no angular processes, shallow mandibular incisures separate thin, rounded coronoid processes from transversely long and convex articular condyles. Posterior to each articular condyle, there is a second convex surface that merges with the lateral articular condyle and slopes medioventrally.

Below the medial edge of the tusks, there are variable foramina. A short diastema is transversely pinched behind the tusks and separates the tusks from the p2, if present, or the p3. A mental foramen is found inferior to the anterior root of the p4. An inferior mandibular foramen is on the internal pterygoid fossa of the ramus at the same level as the tooth row.

Dentition

Along each upper tooth row, there is a modified incisor and six lophodont cheek teeth. Along each lower tooth row, there is a modified incisor and five functional, lophodont cheek teeth.

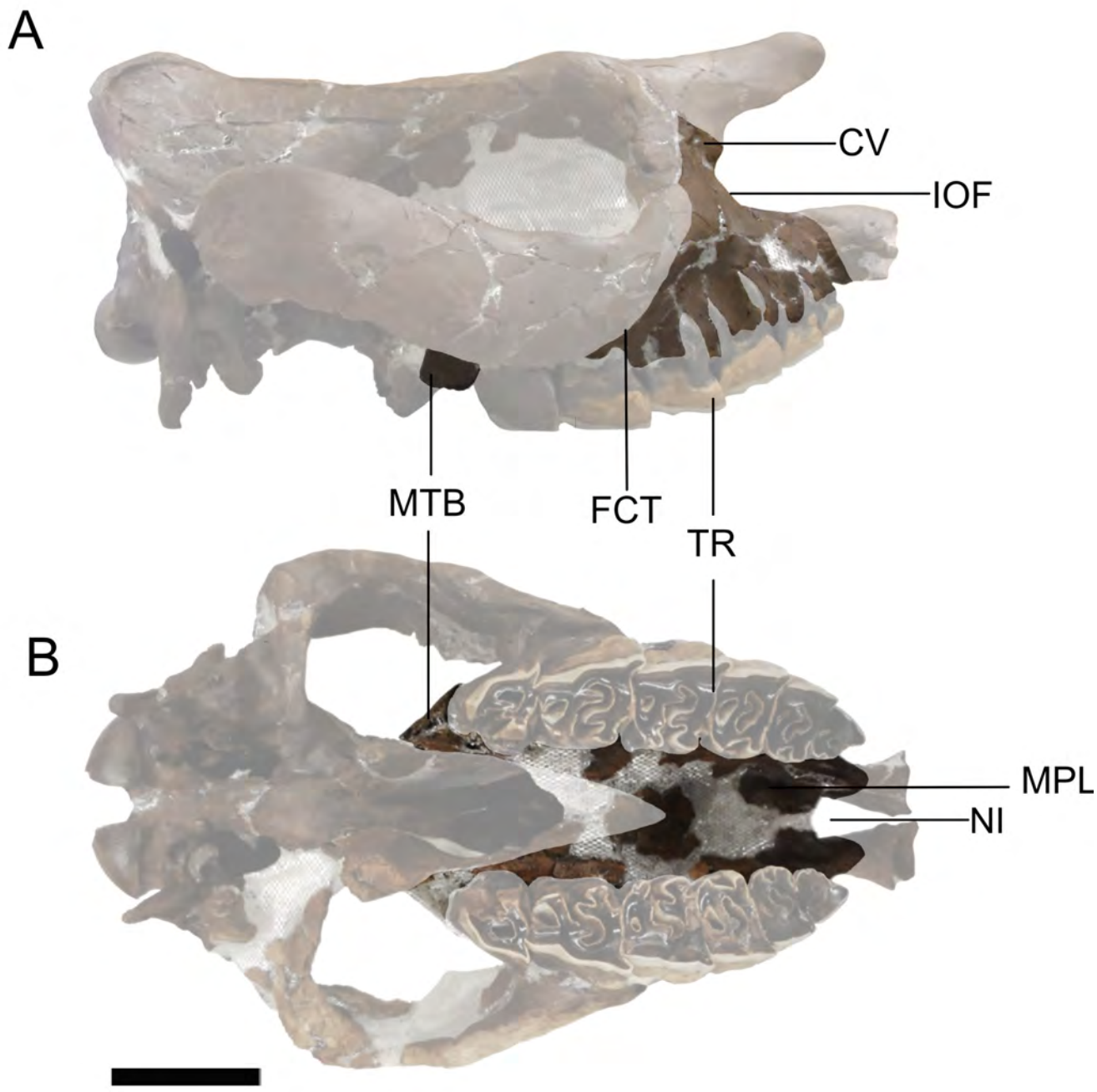

Figure 15. Maxillae of ETMNH 601. Views: A, right lateral; B, ventral. Abbreviations: CV, concavity; FCT, facial crest; IOF, infraorbital foramen; MPL, maxillary palate; MTB, maxillary tuberosity; NI, nasal incision; TR, tooth row. Scale bar = 10 cm.

Some lower dentitions include vestigial p2s that are not functional. Dental nomenclature is provided in Figure 25.

Upper Incisors.—Upper tusks are modified I1s that are smaller than the lower tusks (Fig. 26). These upper tusks are ovate, elongate mediodorsally to lateroventrally, and function to hone the lower tusks during occlusion. Similar upper tusks are present in other species of *Teleoceras*, while these are lacking in *Aphelops* and *Peraceras*, the other common late Neogene rhinoceroses of North America (Prothero, 2005).

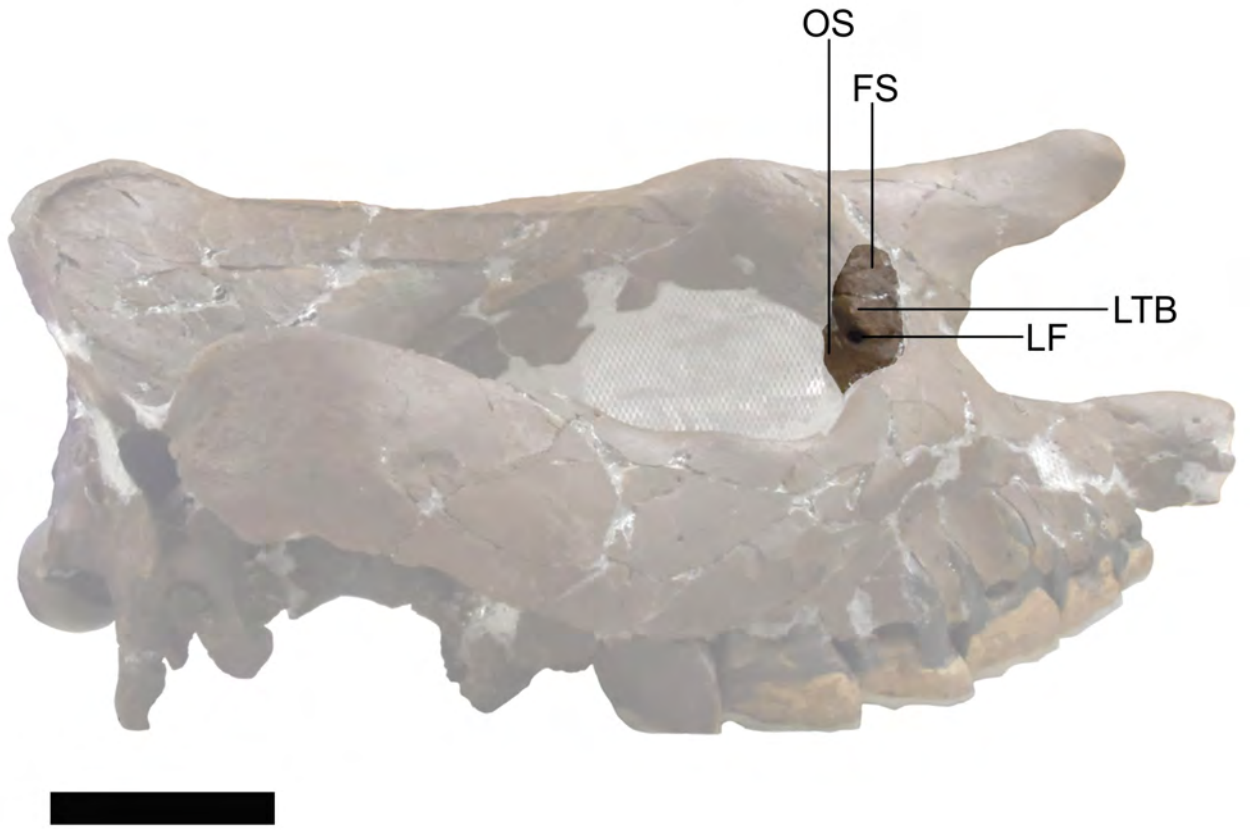

Figure 16. Right lacrimal of ETMNH 601 in lateral view. Abbreviations: FS, facial surface; LF, lacrimal foramen; LTB, lacrimal tuberosity; OS, orbital surface. Scale bar = 10 cm.

Upper Cheek Teeth.—Occlusal surfaces of the upper cheek teeth make the 'π' shape that is characteristic of rhinoceroses (Fig. 27). Upper premolars are rectangular with the longest axis oriented labiolingually, and, though the M1 is nearly square, the M2 is longer anteroposteriorly. M3s are smaller and form a triangular shape because the crochet is folded within the antecrochet. The P2s have very small crochets, and P3–M3 have large crochets and antecrochets. In all of the premolars, the ectoloph is either shorter than or equal in length to the protoloph and metaloph. Three lophs of the M1s are subequal in length whereas the ectolophs of the M2s are longer than both the protolophs and the metalophs of the same tooth. On the M3s, there are no metalophs, and the ectolophs are approximately the same length or longer than the protolophs. On P3–M3, the anterior parastyle overlays the posterior metastyle of the previous tooth. All upper cheek teeth have slight depressions lined by cingula on the anterior and lingual sides of the protocone, and all molars have a slight paracone fold on their labial surfaces. On some teeth, small folds of enamel protrude into the fossettes (e.g., P4 of ETMNH 609, Fig. 27B).

Lower Incisors.—Lower tusks are i2s that have a tear-drop shaped cross-section with the point directed medially (Fig. 28). Complete tusks of ETMNH 609 and ETMNH 601 have concave wear surfaces caused by occlusion with the upper tusks resulting in a sharp edge and apex.

Lower Cheek Teeth.—Most often, p1 and p2 are absent from *Teleoceras* dentition. There are no p1s present in *T. aepysoma*; however, presence of the p2 is variable. ETMNH 601 does not have p1 or p2 on either side; however, ETMNH 609 has a small vestigial p2 (Fig. 29) that was first noted by Wallace (2006), and ETMNH 21659 has both the

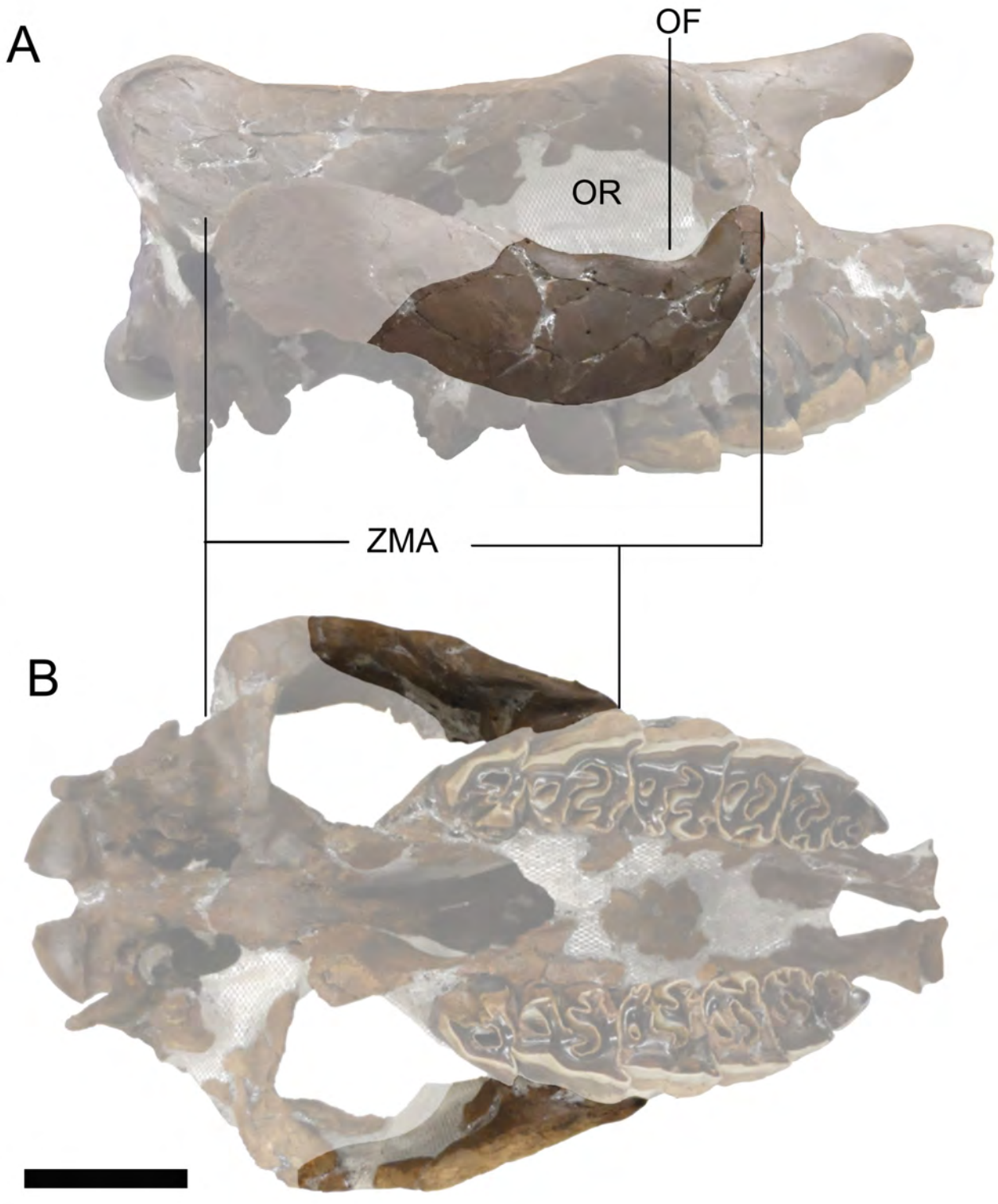

Figure 17. Jugals of ETMNH 601. Views: A, right lateral; B, ventral. Abbreviations: OF, orbital floor; OR, orbit; ZMA, zygomatic arch. Scale bar = 10 cm.

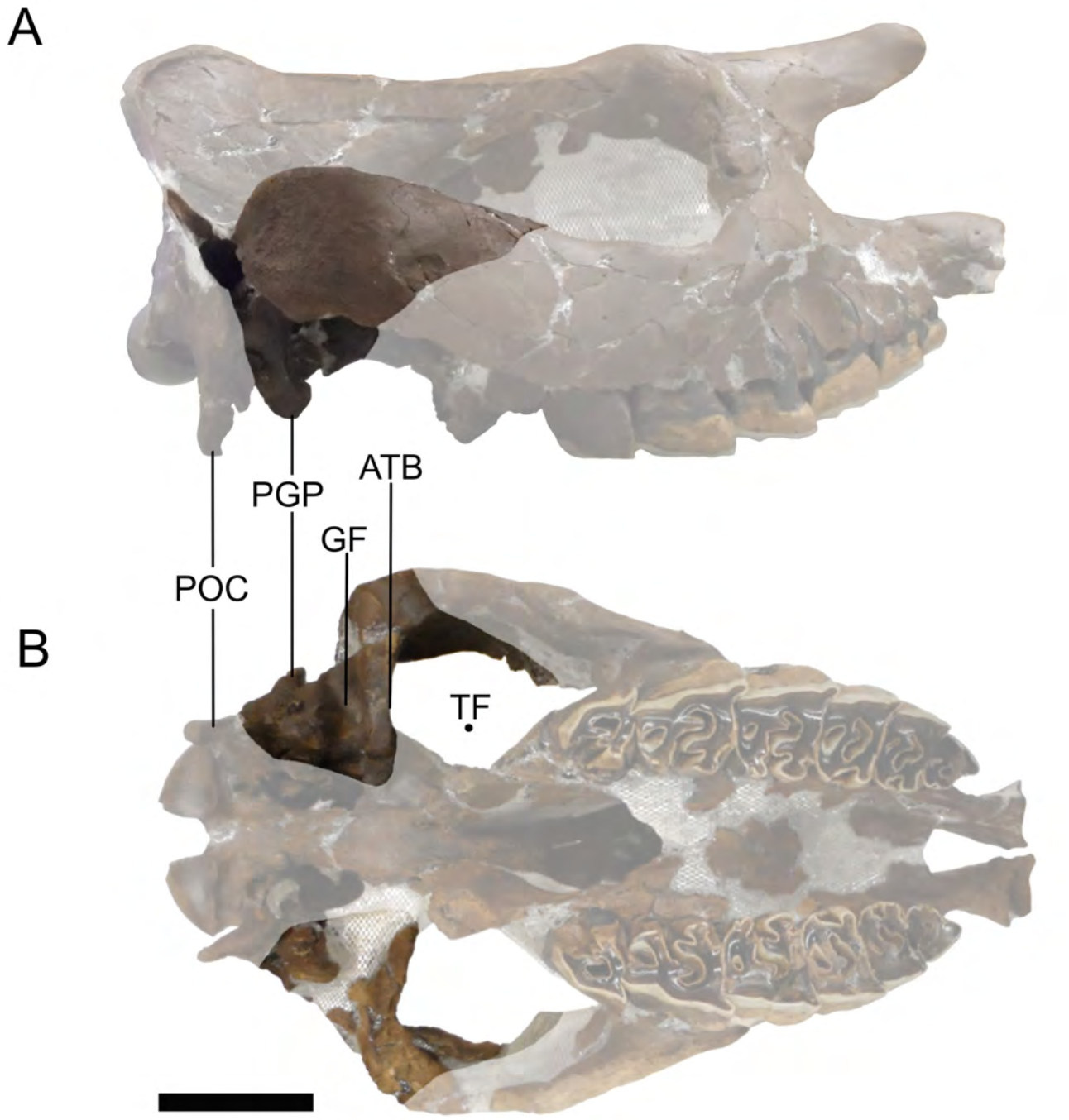

Figure 18. Squamosals of ETMNH 601. Views: A, right lateral; B, ventral; Abbreviations: ATB, anterior tubercle; GF, glenoid fossa; PGP, post-glenoid process; POC, paroccipital process; TF, temporal fossa. Scale bar = 10 cm.

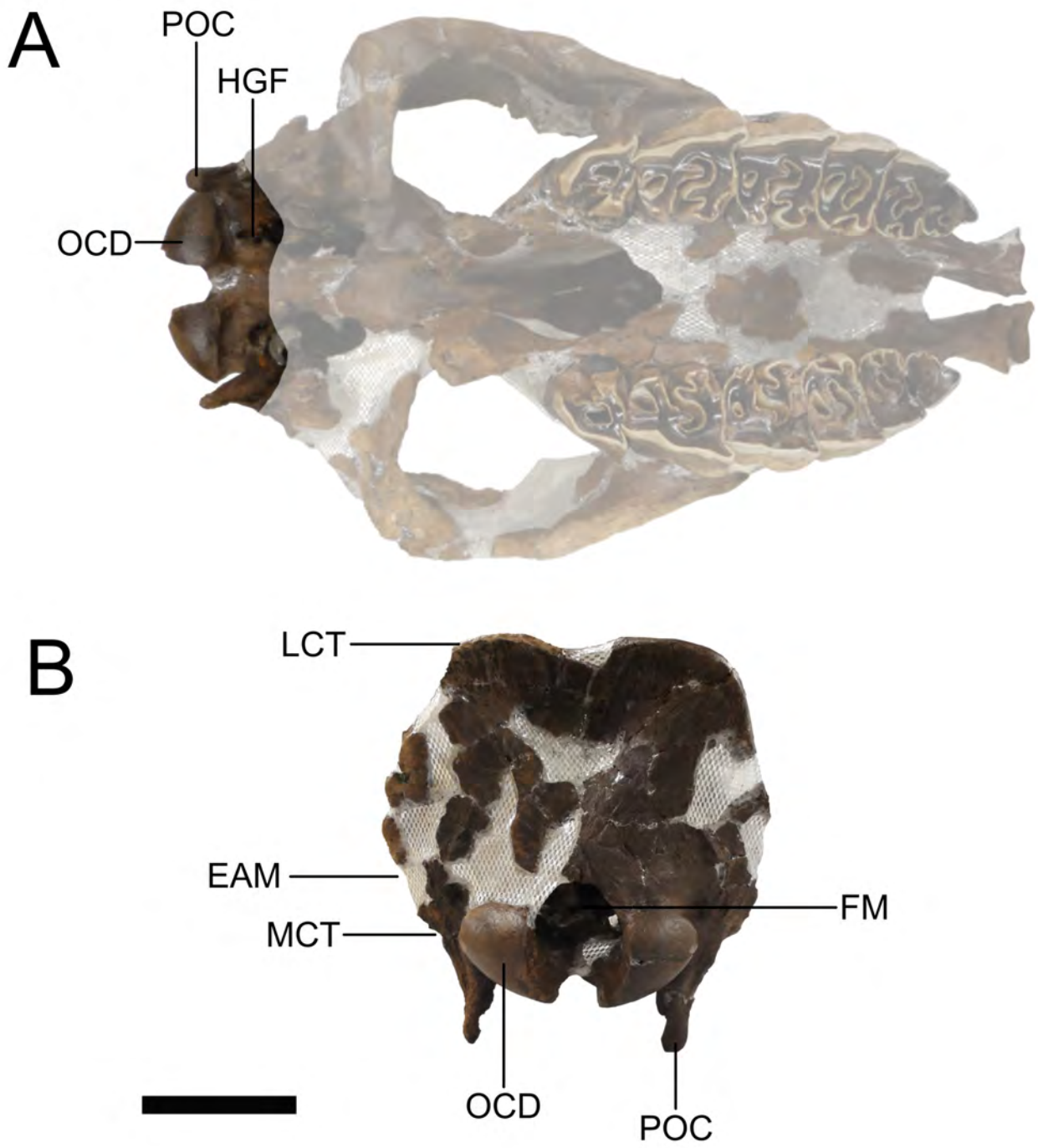

Figure 19. Occipital of ETMNH 601. Views: A, ventral; B, posterior. Abbreviations: EAM, external auditory meatus; FM, foramen magnum; HGF, hypoglossal foramen; LCT, lambdoid crest; MCT, mastoid crest; OCD, occipital condyles; POC, paroccipital process. Scale bar = 10 cm.

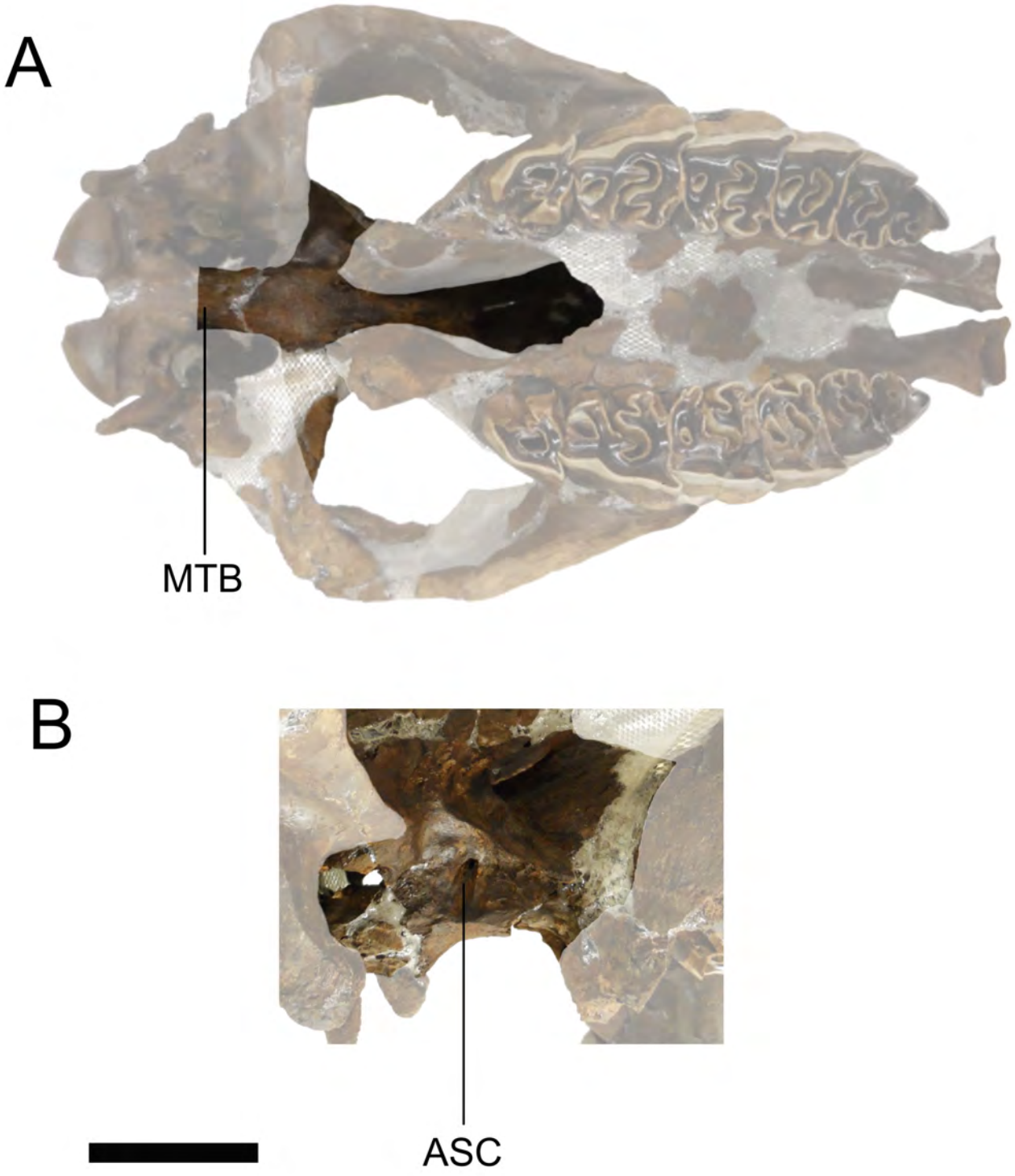

Figure 20. Basicranium of ETMNH 601. Views: A, ventral; B, right ventrolateral, beneath zygomatic arch, with arrows pointing at both ends of the alisphenoid canal. Abbreviations: ASC, alisphenoid canal; MTB, muscle tubercle. Scale bar = 10 cm.

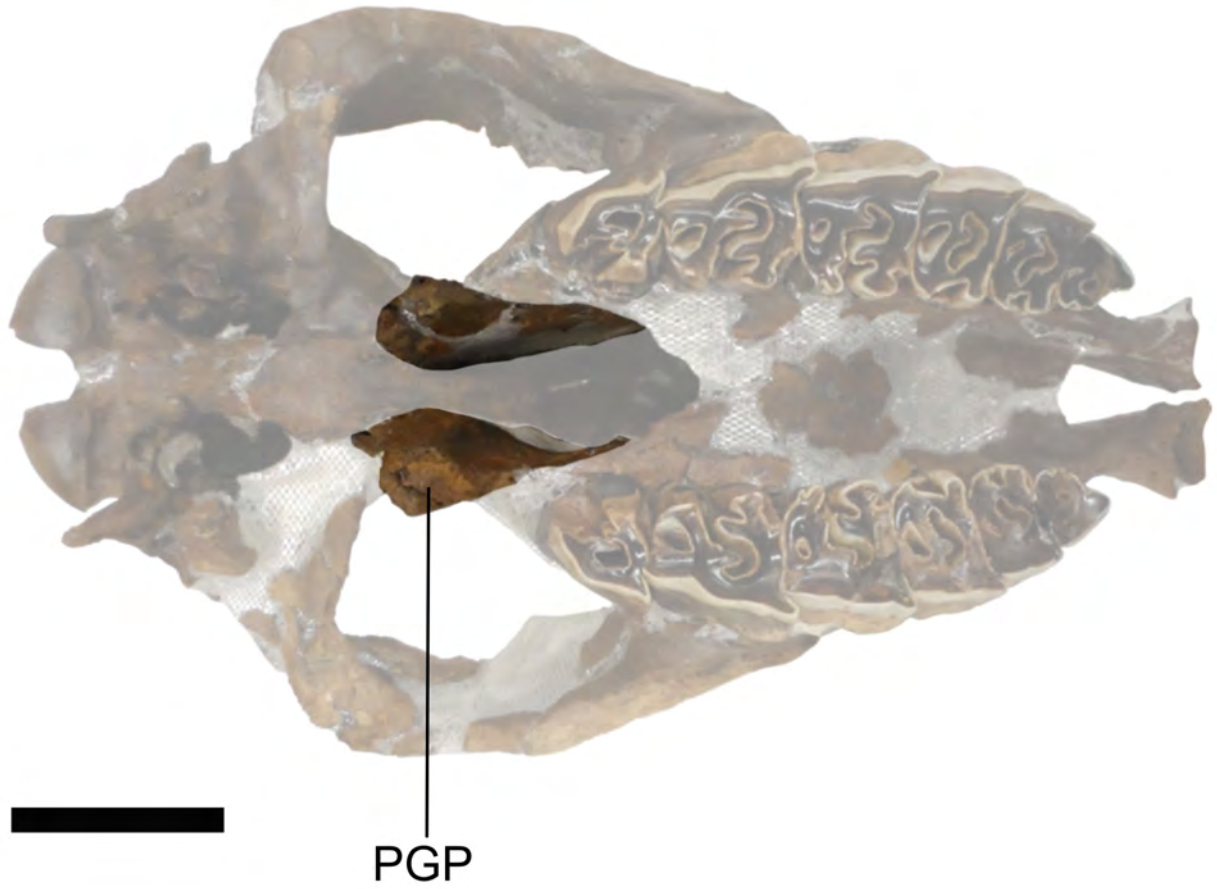

Figure 21. Pterygoids of ETMNH 601 in ventral view. Abbreviation: PGP, pterygoid process. Scale bar = 10 cm.

right and left p2s. Lower premolars have the 'W' shape that is characteristic of rhinoceroses and lack significant cingula (Fig. 30).

Vertebrae and Other Axial Elements

Atlas.—A round dorsal tubercle is present along the midline of the dorsal arch, which narrows caudally (Fig. 31). A minimal ventral tubercle mirrors the odontoid process of the axis. The ventral arch is more robust than the dorsal arch. Dorsally, the neural canal is round and, ventrally, it is 'U'-shaped. At the base of the dorsal arch, lateral vertebral foramina are located slightly more cranially. Transverse foramina are present on the medioventral surface of the transverse processes. At the lateral-most ends of the transverse processes, there is a great amount of rugose bone present on ETMNH 601 that is not present on ETMNH 609; likely this is because ETMNH 601 is the older and larger of the two individuals. On the cranial surface, articular surfaces for the occipital condyles are craniomedially depressed to form a pair of concave tear-drop shaped facets that narrow ventromedially. Caudal articular surfaces are ovate with the elongate axis extended mediolaterally from the ventral neural canal to the transverse vertebral foramina.

Axis.—Axes are taller and wider than they are long and have large rounded odontoid processes for articulation with the atlas (Fig. 32). Caudally, the centrum is concave as typically seen in the opisthocoelous vertebrae of perissodactyls. Dorsally, the neural canal is domed, but, ventrally, it is flattened. Transverse foramina are present; though they are completely closed on ETMNH 601 and only partially closed on ETMNH 609.

Figure 22. Palatines of ETMNH 601 in ventral view. Scale bar = 10 cm.

Figure 23. Hyoid apparatus of ETMNH 601 with ceratohyoid from ETMNH 609. Image in dorsal view with anterior to the right. Abbreviations: BAS, basihyoid; CER, ceratohyoid; STY, stylohyoid; THY, thyrohyoid. Scale bar = 10 cm.

Only minimal transverse processes are present. Prezygapophyses are expanded mediolaterally from the odontoid process. Postzygapophysis processes extend laterally and caudally to form ovate facets. Deep cranial notches are present dorsal to the prezygapophyses and caudal vertebral notches are rounded between the ventral postzygapophyses and the dorsal centrum.

Third–Seventh Cervical Vertebrae.—Dorsally, the neural canal is domed and, ventrally, it is flattened along the dorsal side of the centrum (Fig. 33). On the ventral surface of the centra, there is no evidence of any hemal structures. Round prezygapophyses are present on the dorsal surface of the anterior prominences of the vertebrae. These articulate with the round postzygapophyses that are present on the ventral surface of the posterior prominences. Through the cervical series, the neural spines transition from short to pronounced, and the transverse processes vary from a simple, laterally-flared extension on the third cervical vertebra to a larger, lateral process with dorsal and ventral

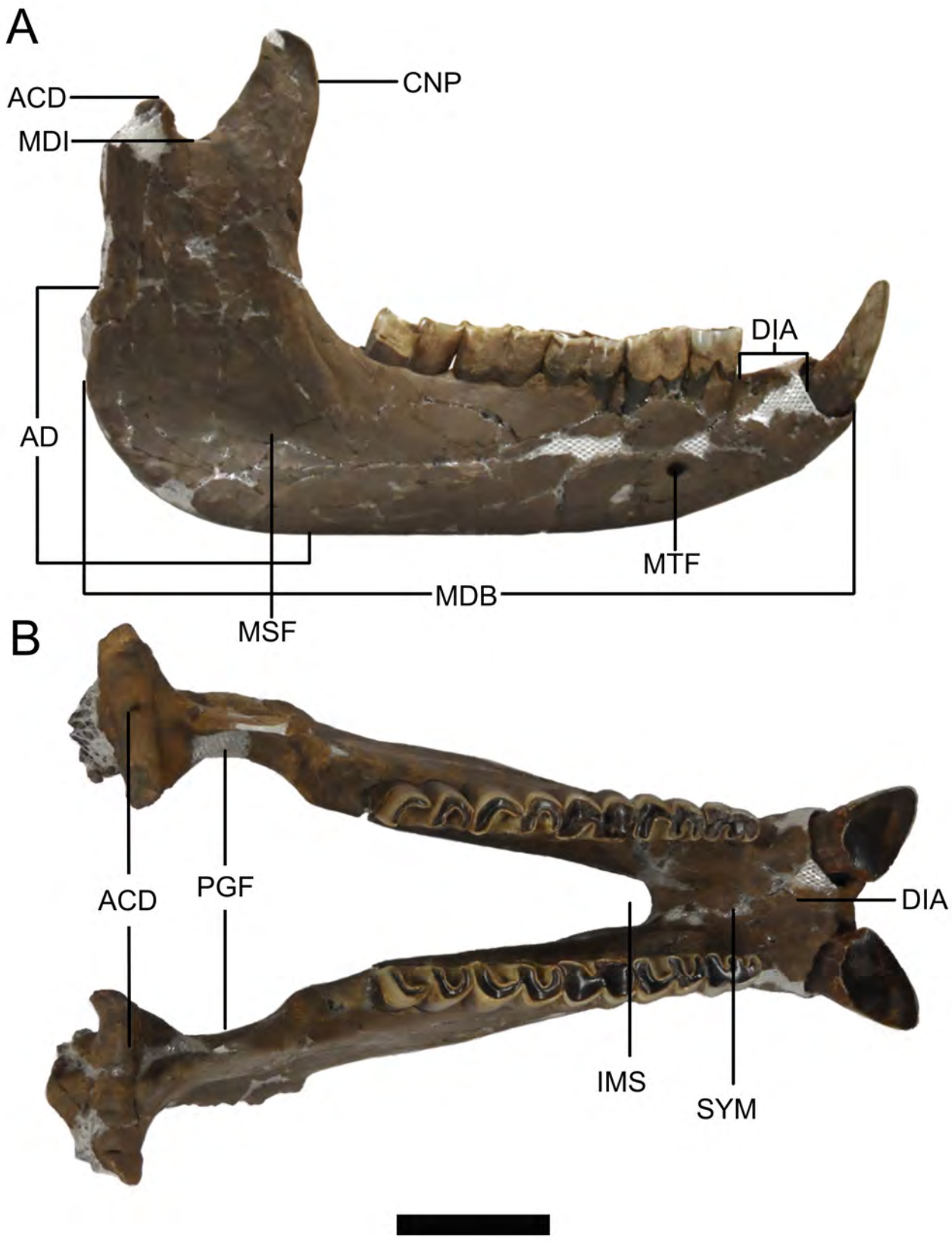

Figure 24. Mandible of ETMNH 601. Views: A, right lateral; B, dorsal. Abbreviations: ACD, articular condyle; AD, angle of dentary; CNP, coronoid process; DIA, diastema; IMS, intermaxillary space; MDB, mandibular body; MDI, mandibular incisure; MSF, masseteric fossa; MTF, mental foramen; PGF, pterygoid fossa; SYM, symphysis. Scale bar = 10 cm.

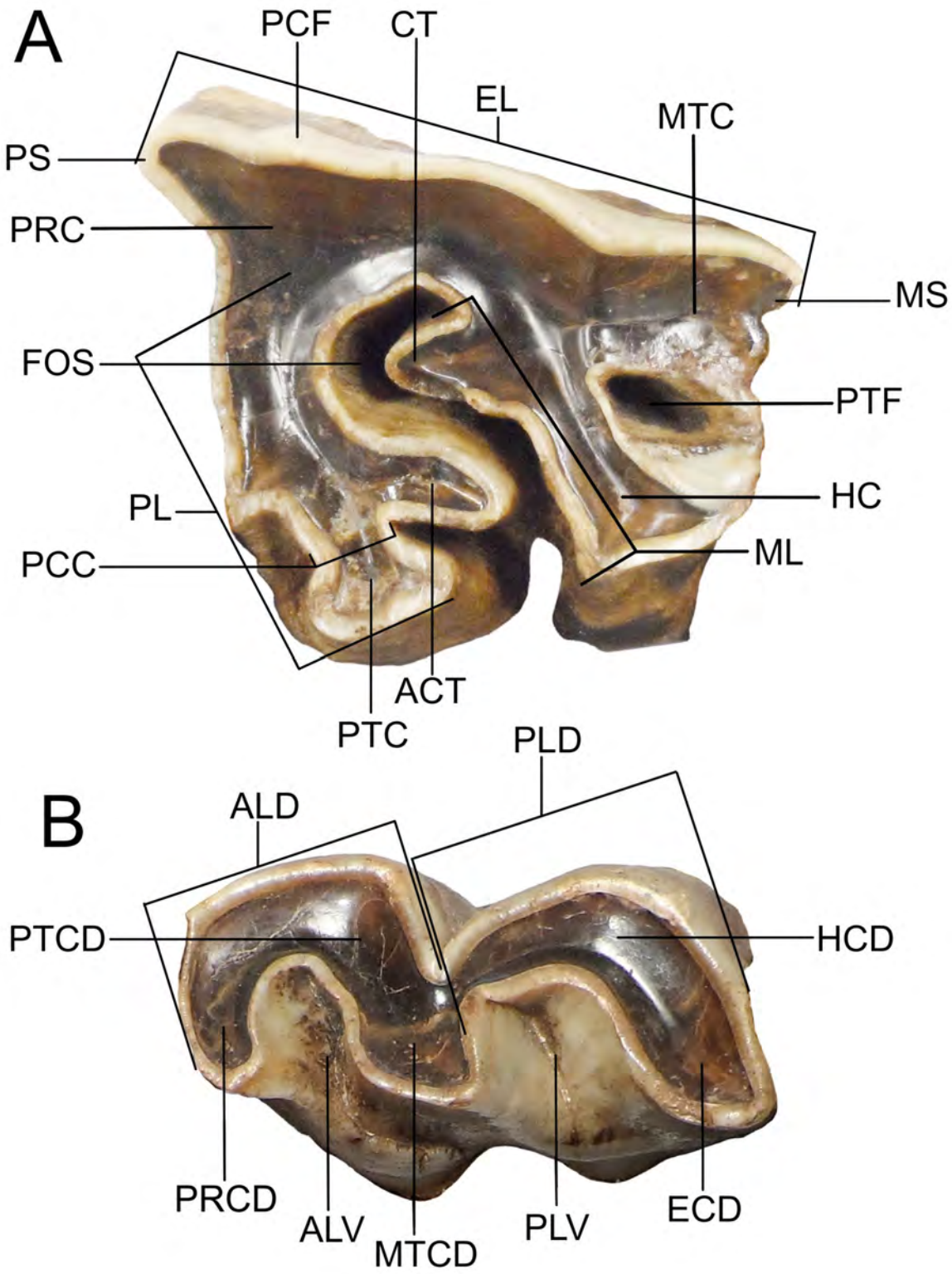

Figure 25. Dental morphology and nomenclature. A, Left M2 of ETMNH 601; B, Right m2 of ETMNH 601. Abbreviations: ACT, antecrochet; ALD, anterior lophid; ALV, anterior lingual valley; CT, crochet; ECD, entoconid; EL, ectoloph; FOS, fossette; HC, hypocone; HCD, hypoconid; ML, metaloph; MS, metastyle; MTC, metacone; MTCD, metaconid; PCC, protocone constriction; PCF, paracone fold; PLD, posterior lophid; PL, protoloph; PLV, posterior lingual valley; PRC, paracone; PRCD, paraconid; PS, parastyle; PTC, protocone; PTCD, protoconid; PTF, post-fossette.

Figure 26. Left I1 tusks with occlusal surface down. A, ETMNH 601; B, ETMNH 609. Scale bar = 5 cm.

extensions on the sixth cervical vertebra. Characteristic transverse foramina are found just lateral to the centra at the origin of the transverse processes. The seventh cervical vertebrae resemble the third through sixth except there is a longer neural spine, a lack of transverse foramina lateral to the centrum, and the transverse processes are missing the ventral processes.

Thoracic Vertebrae.—ETMNH 609 has 18 thoracic vertebrae that articulate with 18 pairs of ribs, all of which were articulated when the specimen was found (Figs. 1C, 34). ETMNH 601 has an incomplete thoracic series with only 10 fragmented and concreted vertebrae present. Neural spine height arcs throughout the thoracic series with the third thoracic as the apex until the height becomes consistent at the thirteenth thoracic. In addition to height, the neural spines become more caudally directed through the series. Thoracic neural canals change from triangular at the anterior end of the series to round at the posterior end. Thoracic centra also change from round at the anterior end to heart-shaped at the posterior end. Between the neural spine and the transverse process, the dorsal vertebral arch is more obtuse in the anterior thoracics and becomes more acute in the posterior thoracics.

On the first two thoracic vertebrae, the prezygapophyses resemble those on the cervical vertebrae, but, beginning with the third thoracic, the prezygapophyses are smaller in size and are at the base of the anterior neural spine. Through the craniocaudal progression, the dorsal notch between the prezygapophyses becomes narrower and extends more caudally as the prezygapophyses shift medially. Small postzygapophyses are at the

Figure 27. Right upper cheek teeth (P2–M3) in occlusal view with anterior to the right. A, ETMNH 601; B, ETMNH 609. Scale bar = 10 cm.

base of the posterior neural spine for articulation with the prezygapophyses of the subsequent vertebra. First and second thoracic vertebrae have prominent transverse processes and articulate with small ribs. Third through eighteenth thoracic vertebrae have small transverse processes and articulate with larger ribs. There are three articular surfaces for ribs—the articular facet for the anterior rib head, the articular facet for the posterior rib head, and the costal fovea. Throughout the thoracic series, the size and shape of these facets varies and, in some cases, the anterior articular facet and the costal fovea merge. The eighteenth thoracic lacks the posterior articular facet. On the posterior surface of each vertebra, caudal notches separate the transverse processes from the posterior articular facets.

Lumbar Vertebrae.—There are only three lumbar vertebrae on ETMNH 609; however, none are preserved on ETMNH 601 (Fig. 35). This is in contrast to many North American rhinocerotids who typically have five lumbar vertebrae (Prothero, 2005); though, modern rhinos are known to have variable vertebral counts both across and within species (Heller, 1914). Lumbar neural spines are thin, anteroposteriorly wide, and angled posteriorly. Lumbar neural canals are triangular, and they widen through the series. Lumbar vertebrae have considerably more acoelous centra than the thoracic vertebrae. The posterior centrum of the last lumbar is oval for articulation with the sacrum. The first lumbar vertebra has tighter anterodorsal processes for articulation with the last thoracic; these are more wide-set on the last lumbar. Prezygapophyses are small ovals on either side of the medial notch. Oval postzygapophyses are on the ventral side of the neural spine and on either side of the

Figure 28. Left i2 tusks in occlusal view. A, ETMNH 609; B, ETMNH 601. Scale bar = 10 cm.

dorsal notch. Transverse processes are smallest on the first lumbar vertebrae and largest on the second. On the third lumbar vertebra, the transverse processes have flat, rugose articular surfaces on their caudal surfaces for articulation with the wings of the sacrum.

Sacrum.—Four sacral vertebrae fused to form the triangular sacrum that is wide cranially and narrows caudally (Fig. 36). ETMNH 609 has a complete sacrum but very little of the sacrum of ETMNH 601 is preserved. Sacral foramina are present on either side of the neural spines and between each adjacent pair of sacral vertebrae. The neural canal appears to be triangular, but this may be an effect of preservation because part of the dorsal surface has collapsed into the caudal portion of the canal. Ovate centra are transversely elongated and dorsoventrally shortened. The first sacral vertebra has bulbous prezygapophyses for articulation with the third lumbar vertebra. Rugose cranial margins of the sacral wings are flattened and turned dorsally so that their dorsal surfaces articulate with the ventral ilia. Caudal notches are smaller than cranial notches and form minimal postzygapophyses that articulate with the first caudal vertebra.

Caudal Vertebrae.—ETMNH 609 has 21 caudal vertebrae and ETMNH 601 has 23 (Fig. 37). Through the caudal series, the vertebrae change from a typical vertebral morphology to a more general, non-descript morphology. The first four caudals have distinct neural spines, which become progressively minimized through the caudal series. Transverse processes are present on the cranial-most caudals and become smaller until they are simple protuberances just over midway through the caudal series before being lost completely. A dorsoventrally compressed, triangular neural canal curves laterally over the centrum on the anterior caudals, and approximately midway through the series, the neural canal is more round and opened by the posterior progression of the dorsal neural canal notch. The first three caudal vertebrae have small round remnants of pre- and postzygapophyses; however, after the third caudal, the only articulation between caudals occurs at the centra.

Sternebrae.—Sternebrae of ETMNH 609 include the long manubrium with a triangular protuberance, one short sternebra that is compressed on the craniocaudal axis and expanded at both ends, and one round sternebra (Fig. 38).

Ribs.—ETMNH 609 has 18 pairs of ribs and ETMNH 601 only has incomplete fragments that do not produce an accurate count. Overall, the ribs are rather unremarkable in their morphology; although, ETMNH 601 has two ribs with pathologies (Fig. 39). In addition, each complete skeleton has pieces of ossified costal cartilage that are characteristically very porous.

Forelimb

Scapula.—Robust scapulae are nearly triangular in shape with a slightly convex cranial border that is rugose, especially at the proximal angle where it meets the heavily rugose vertebral border (Fig. 40). A concave vertebral border extends

Figure 29. Vestigial left p2 of ETMNH 609. Tooth of interest is indicated by the rectangle. Scale bar = 10 cm.

Figure 30. Left lower cheek teeth (p3–m3) in occlusal view with anterior to the right. A, ETMNH 601; B, ETMNH 609. Scale bar = 10 cm.

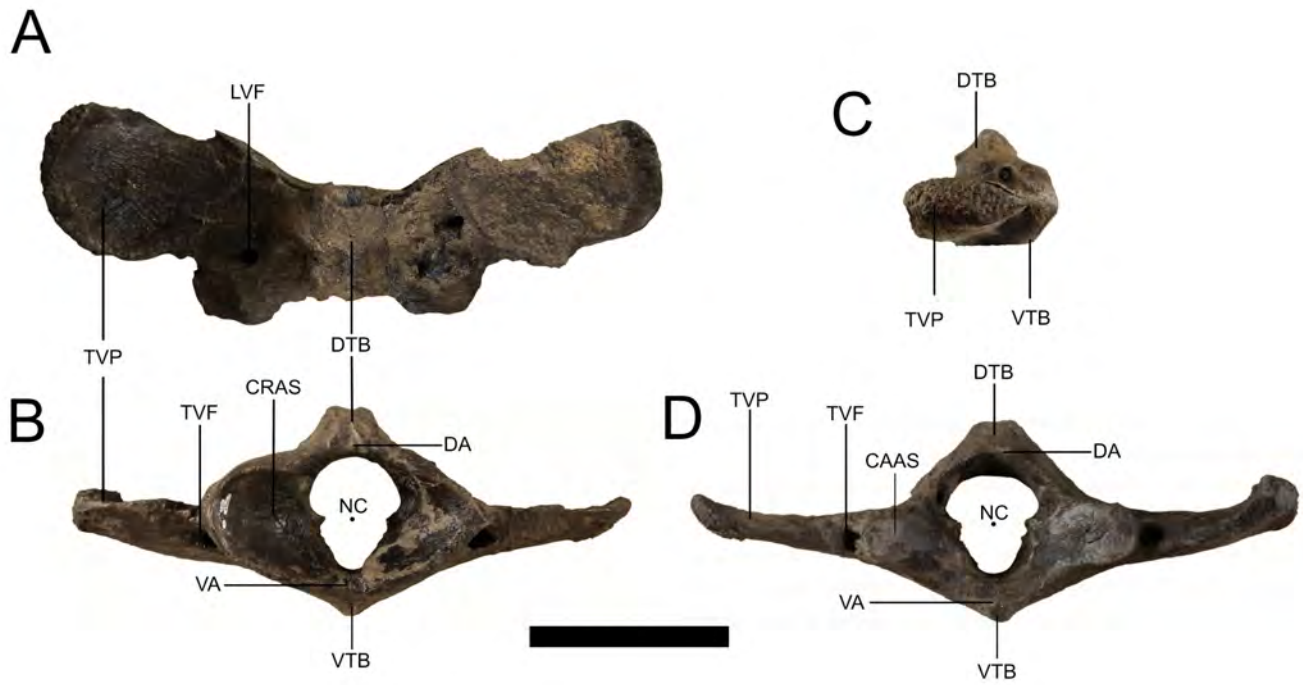

Figure 31. Atlas of ETMNH 609. Views: A, dorsal; B, anterior; C, left lateral; D, posterior. Abbreviations: CAAS, caudal articular surface; CRAS, cranial articular surface; DA, dorsal arch; DTB, dorsal tubercle; LVF, lateral vertebral foramen; NC, neural canal; TVF, transverse foramen; TVP, transverse process; VA, ventral arch; VTB, ventral tubercle. Scale bar = 10 cm.

to form a prominent, rugose angle with the rather straight caudal border. A wide scapular neck separates the broad scapular blade from the distal site of articulation. An ovate and gently concave glenoid fossa forms the distal end of the scapula and articulates with the humeral head. The glenoid fossa has well-defined edges, except the craniolateral edge, which is modified into a rounded surface as if folded toward the coracoid process to create an extra point of articulation with the proximal head of the humerus.

The scapular spine extends nearly the length of the element from just distal of the vertebral point to just proximal of the glenoid fossa. The spine is prominently elevated and curves over the infraspinous fossa toward the caudal angle. Distally, the scapular spine is more elevated, but it slopes to the level of the fossae as it extends proximally. A heavily rugose spinal tuber is triangular but has a rounded apex directed caudally. Medially, the underside of the spine is marked by a depression. Laterally, the smaller supraspinous fossa is depressed near the scapular spine and raised at the cranial border. In the same view, the larger infraspinous fossa is nearly flat, except for a slight raise along the caudal border.

Humerus.—The articular head extends posterodistally, so that it curves onto the posterior surface of the humerus (Fig. 41). On the proximal surface, there is a depression posterior to the lesser and intermediate tuberosities and anterior to the humeral head for articulation with the craniolateral portion of the scapula's glenoid fossa. The greater tuberosity extends proximomedially and with a distinct curvature; the greater tuberosity is broken off of both humeri of ETMNH 601. The convexity of the lesser tuberosity is a slight knob on the medial side of the humeral head. Both the greater and lesser tuberosities are rugose, which indicates strong muscle attachments. A tightly rounded bicipital groove separates the greater tuberosity and the intermediate tubercle. The intermediate tubercle is

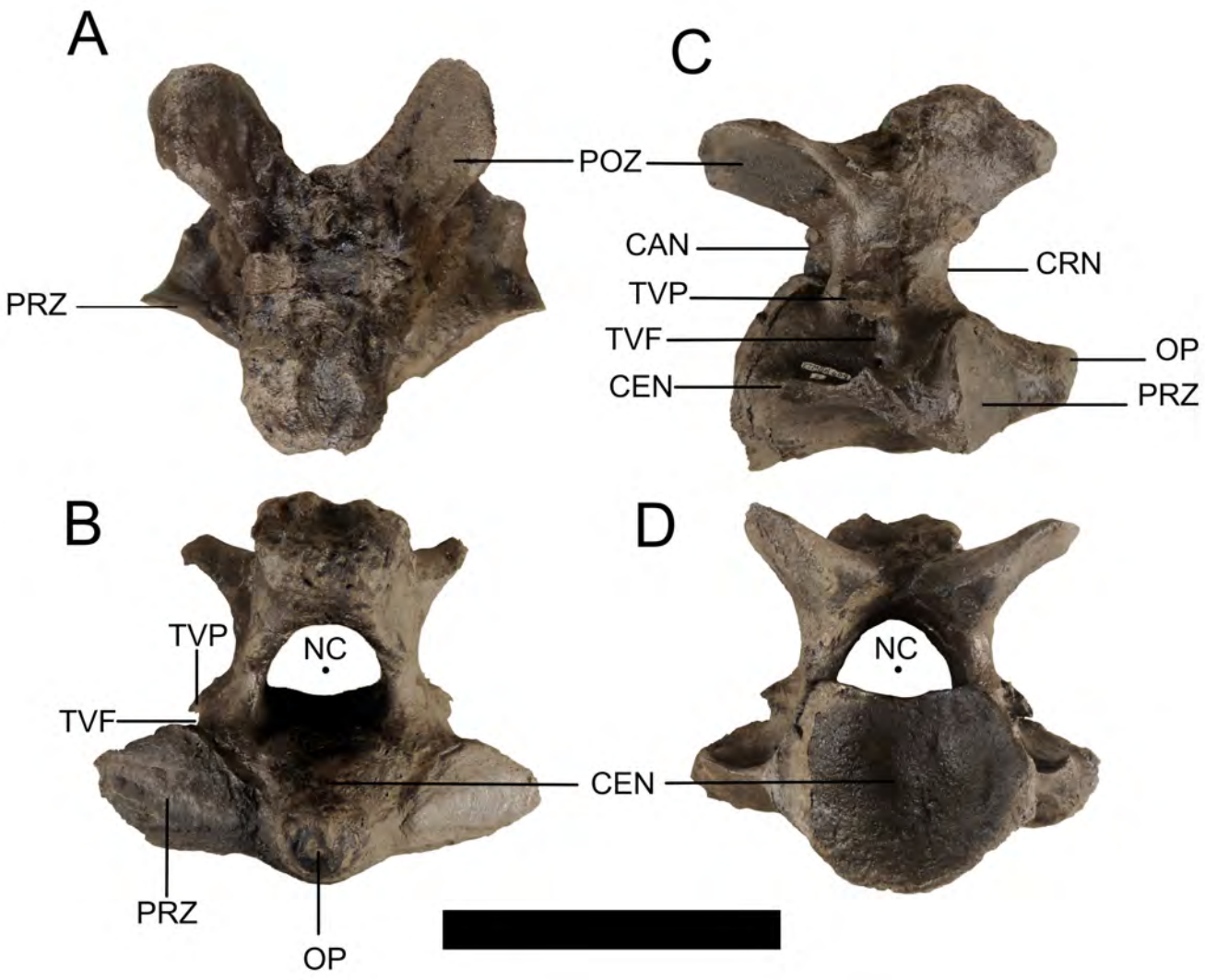

Figure 32. Axis of ETMNH 609. Views: A, dorsal; B, left lateral; C, anterior; D, posterior. Abbreviations: CAN, caudal notch; CEN, centrum; CRN, cranial notch; NC, neural canal; OP, odontoid process; PRZ, prezygapophyses; POZ, postzygapophyses; TVF, transverse foramen; TVP, transverse process. Scale bar = 10 cm.

not as prominent as that seen in *Equus* and, for that reason, was not considered to be present in rhinos by Hermanson and MacFadden (1992). It is being considered as a feature here because it is distinct from the greater and lesser tuberosities and, within rhinos, *Teleoceras* has a large intermediate tubercle (Mihlbachler, 2013, pers. comm.).

In medial view, rugose bone extends from the lesser tuberosity almost to the medial epicondyle. In lateral view, the deltoid tuberosity is distal to the greater tuberosity and, though the deltoid tuberosity is small, it is a rugose projection that is directed posteriorly. A pronounced humeral crest originates at the deltoid tuberosity and curves distomedially. Anterodistally, a larger, medial coronoid fossa and a smaller, lateral radial fossa are proximal to the trochlea and capitulum, respectively, and are divided by a very slight ridge. The wide trochlea extends more proximally than the narrow capitulum, giving the appearance of a rotated articular surface. Articular surfaces of the trochlea and capitulum curve around the distal end, narrow, and merge before terminating at the distal edge of the olecranon fossa. Epicondyles are robust, and the

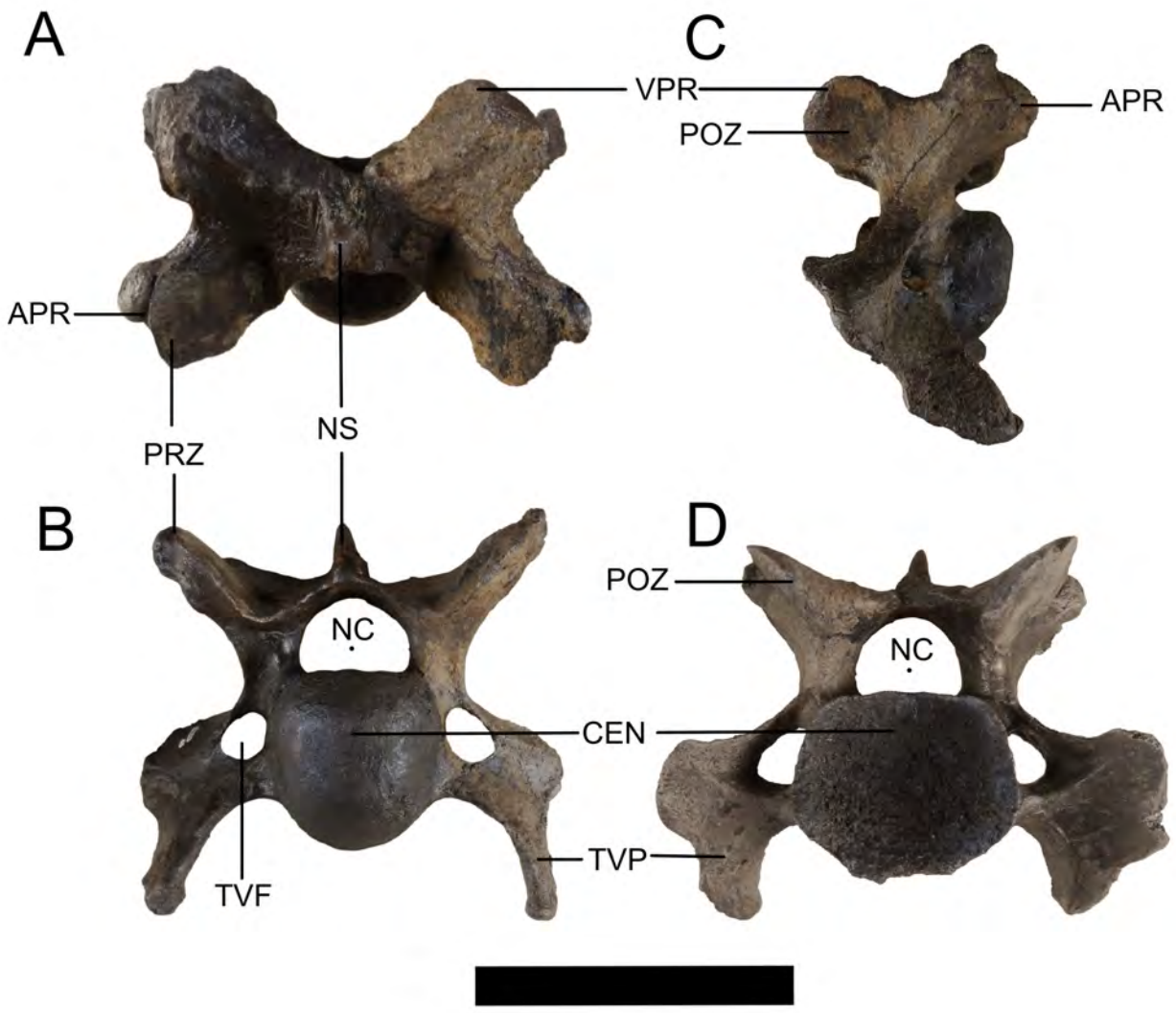

Figure 33. Fourth cervical vertebra of ETMNH 609. Views: A, dorsal; B, anterior; C, right lateral; D, posterior. Abbreviations: APR, anterior prominence; CEN, centrum; NC, neural canal; NS, neural spine; POZ, postzygapophyses; PRZ, prezygapophyses; TVF, transverse foramen; TVP, transverse process. Scale bar = 10 cm.

medial epicondyle is relatively slender in contrast to the expanded lateral epicondyle. The epicondyles form the sides of the olecranon fossa, which is a deep, rounded depression that is proximally open to the diaphysis. From the lateral epicondyle, the epicondylar crest extends proximally to the midpoint of the posterior diaphysis.

Ulna.—At the proximal end, the olecranon process is robust with heavy rugosities and numerous foramina (Fig. 42). A prominent anconeal process slants laterally at its proximal point, which is marked with a 'V'-shaped depression. A broad trochlear notch slants laterally at its proximal end. Two articular processes extend from the distal trochlear notch; the medial of which is wider and longer than the lateral. A deep, rugose radial notch is present between the medial and lateral processes of the trochlear notch. The articular surface of the trochlear notch has a slight concave curvature for articulation with the humerus; the radius acts as a stabilizer for this joint.

Ulnar diaphyses are triangular in cross section with the apex along the posterior surface. The ulna has its narrowest point at its proximal

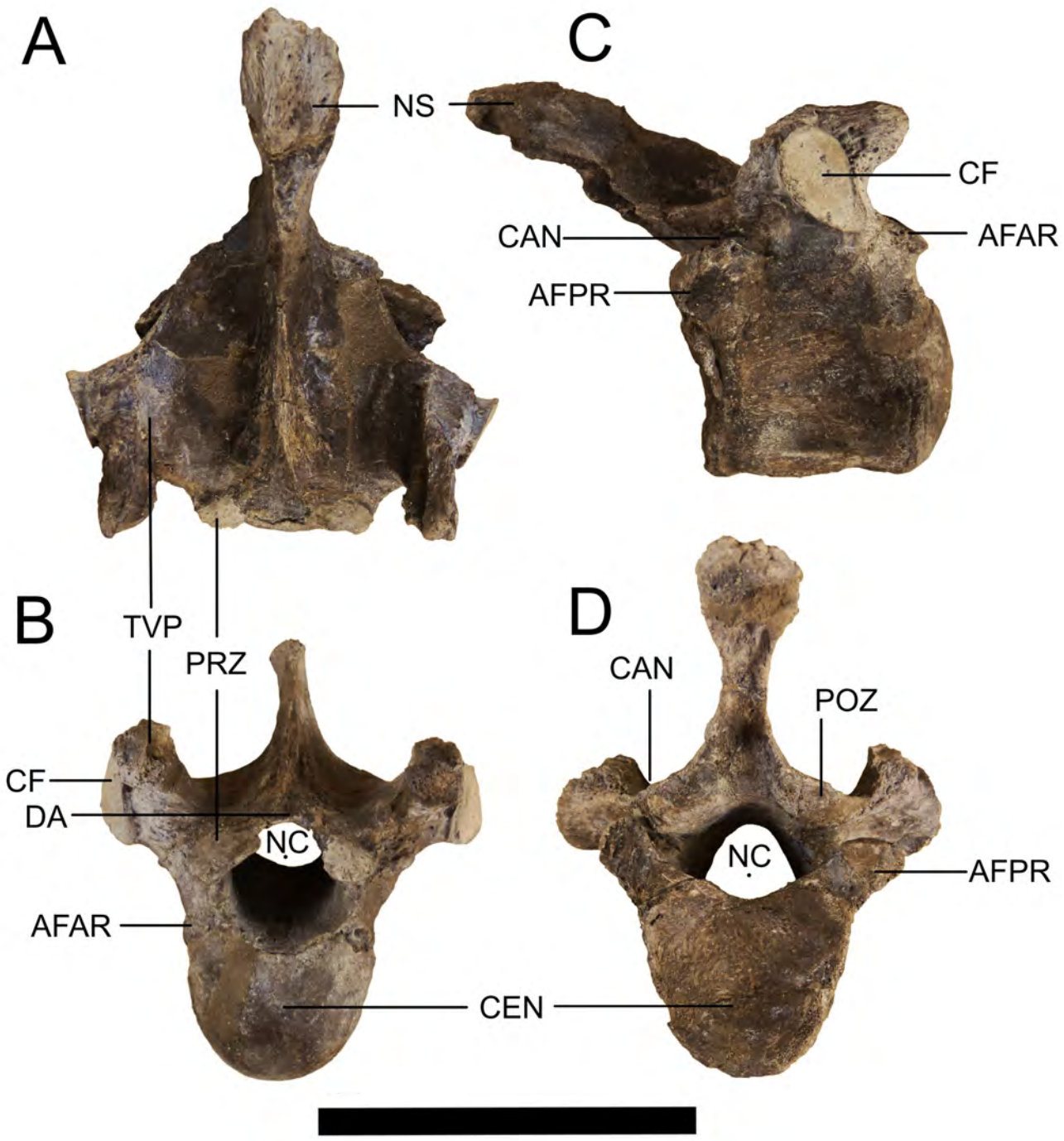

Figure 34. Sixteenth thoracic vertebra of ETMNH 609. Views: A, dorsal; B, right lateral; C, anterior; D, posterior. Abbreviations: AFAR, articular fossa for anterior rib; AFPR, articular fossa for posterior rib; CAN, caudal notch; CEN, centrum; CF, costal fossa; DA, dorsal arch; NC, neural canal; NS, neural spine; POZ, postzygapophyses; PRZ, prezygapophyses; TVP, transverse process. Scale bar = 10 cm.

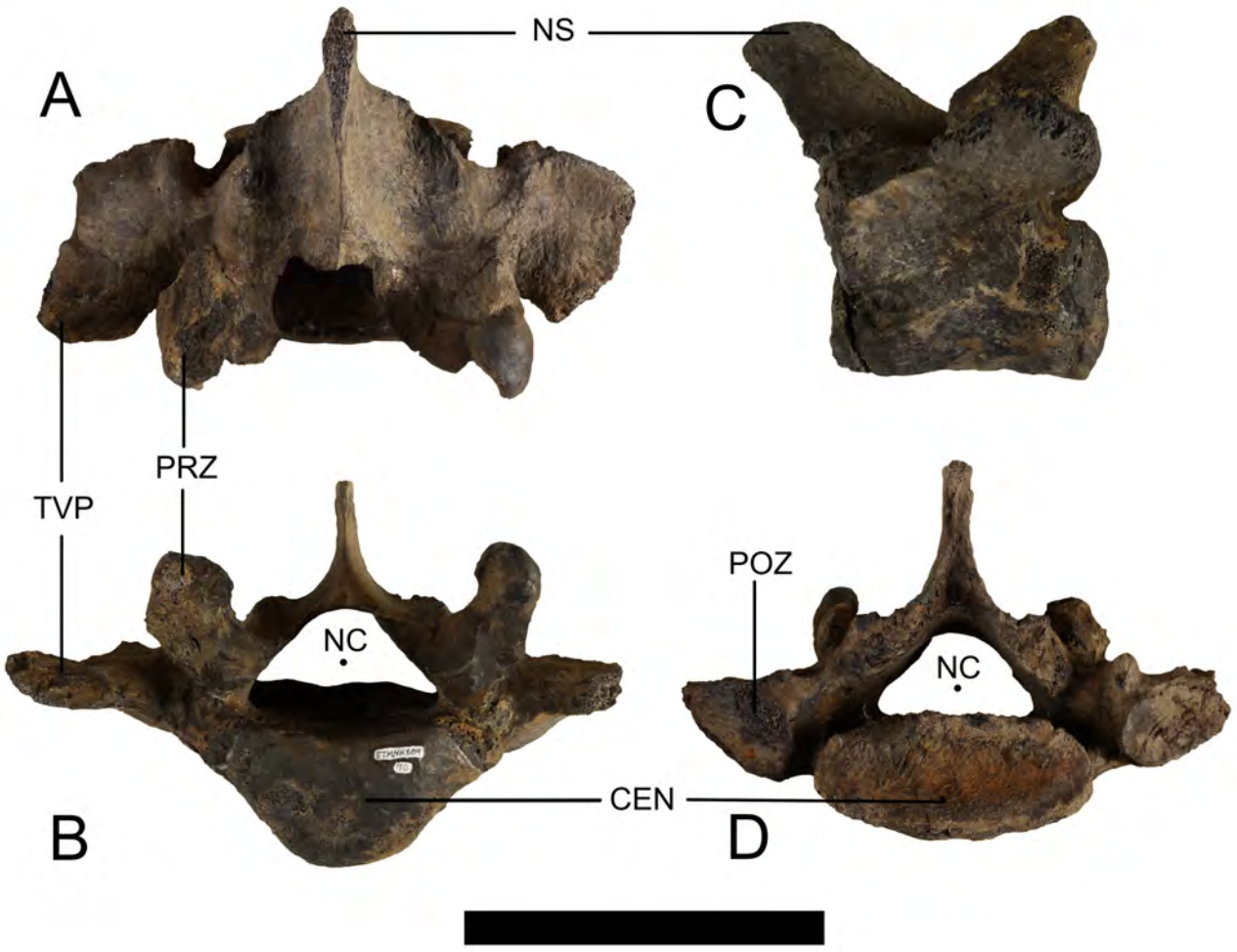

Figure 35. Third lumbar vertebra of ETMNH 609. Views: A, dorsal; B, anterior; C, right lateral; D, posterior. Abbreviations: CEN, centrum; NC, neural canal; NS, neural spine; PRZ, prezygapophyses; POZ, postzygapophyses; TVP, transverse process. Scale bar = 10 cm.

end just distal to the radial notch and broadens distally. At the distal end, the diaphysis narrows to form the styloid process, which articulates with the cuneiform and the radius. In distal view, the articular surface for the cuneiform is slanted from anterolateral to posteromedial with a central concavity that extends parallel to the slant of the facet. On the proximomedial surface of the styloid process, a small facet extends along the medial edge of the ulna providing a point of articulation with the radius.

Radius.—The neck of the radius narrows more on the lateral side to form a diaphyseal curve but is only slightly narrowed on the medial side (Fig. 43). There is a small anteroposterior ridge between the two proximal articular surfaces for the capitulum and trochlea of the humerus. This ridge is offset laterally creating a larger medial articular facet for the trochlea. Also proximally, on the posterior surface, there is a rugose site for attachment to the ulna. A triangular articular surface on the proximolateral side is slightly depressed for articulation with the corresponding facet on the anterior surface of the ulna. On the proximoanterior surface of the radius, there is a radial tuberosity that is rugose but not depressed on the GFS specimens; this feature can form a pronounced fossa on some *Teleoceras*.

Distally, there is a triangular area of rugose bone on the posterolateral surface that fits into the

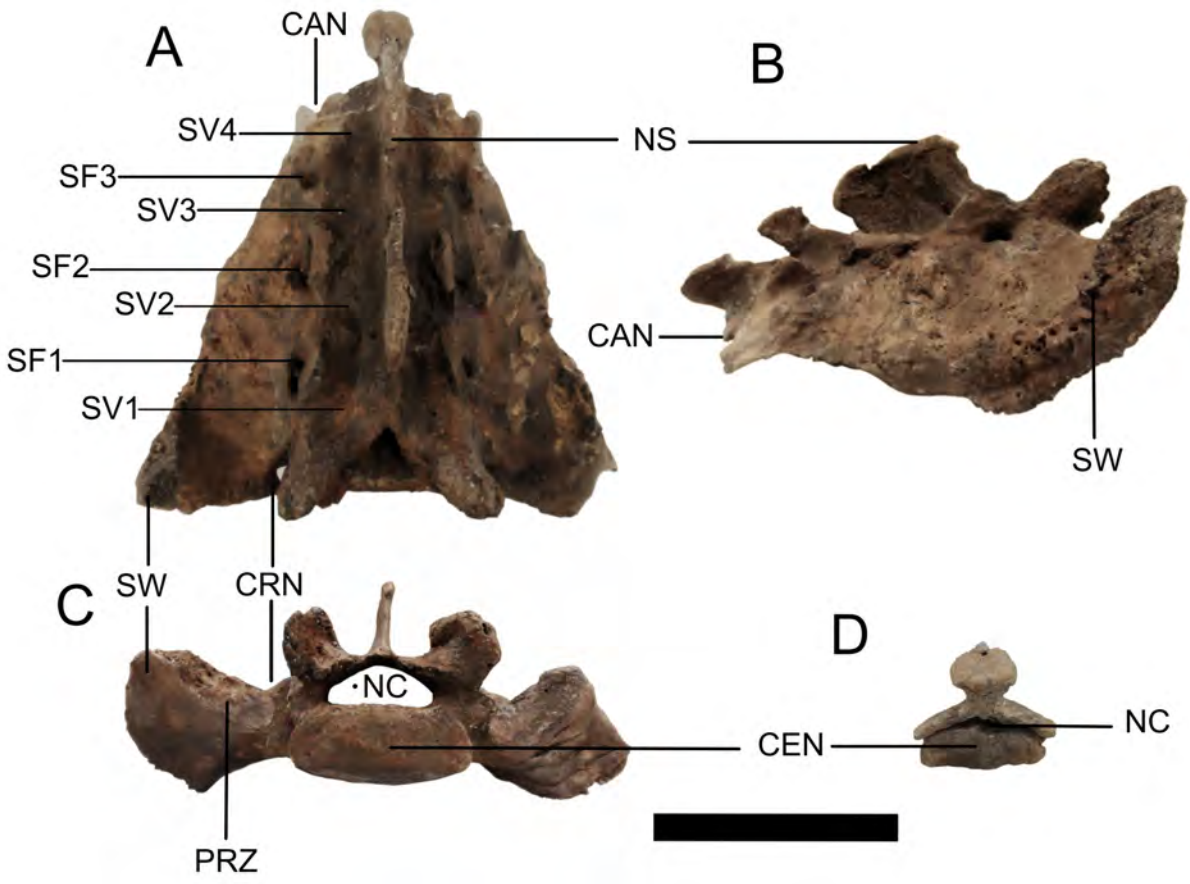

Figure 36. Sacrum of ETMNH 609. Views: A, dorsal; B, anterior; C, right lateral; D, posterior. Abbreviations: CAN, caudal notch; CEN, centrum; CRN, cranial notch; NC, neural canal; NS, neural spine; PRZ, prezygapophyses; SF1–3, sacral foramina 1–3; SV1–4, sacral vertebrae 1–4; SW, sacral wing. Scale bar = 10 cm.

corresponding area of the ulna. A small, rounded articular facet is along the posterolateral edge for articulation with the ulna. Medially adjacent to that facet is a narrow articular surface for articulation with the cuneiform. Two additional articular facets are on the very distal surface and are separated by a ridge as they slant from anterolateral to posteromedial. A smaller lateral articular surface is depressed on the posterior portion for articulation with the lunar and the more rounded medial articular surface is depressed on the anterior portion for articulation with the scaphoid; together, these form a continuous depression across the slant of the articular surfaces. No remnant of a styloid process is present on the distal radius.

Scaphoid.—The scaphoid is the largest of the carpal bones (Figs. 44, 45). Proximally, there is a concave, rounded articular surface for the radius. The medial corner of this surface folds over its raised point to form an articular surface extension. Where the lateral corner is raised, it forms an edge with an anteroproximal articular surface for the lunar. Posterior to the radial facet is the rugose posterior process with a second, round articular surface for the lunar on the lateral side. On the posterior side of the lateral extension, there is a third, round articular surface for the lunar. This facet folds over into the triangular laterodistal articular surface for the magnum. A raised ridge is formed by this laterodistal and the mediodistal articular surfaces. The mediodistal articular surface for the trapezoid is saddled over the distal surface and extends on both the anterior and posterior surfaces.

Lunar.—Overall, the lunar is anteroposte-

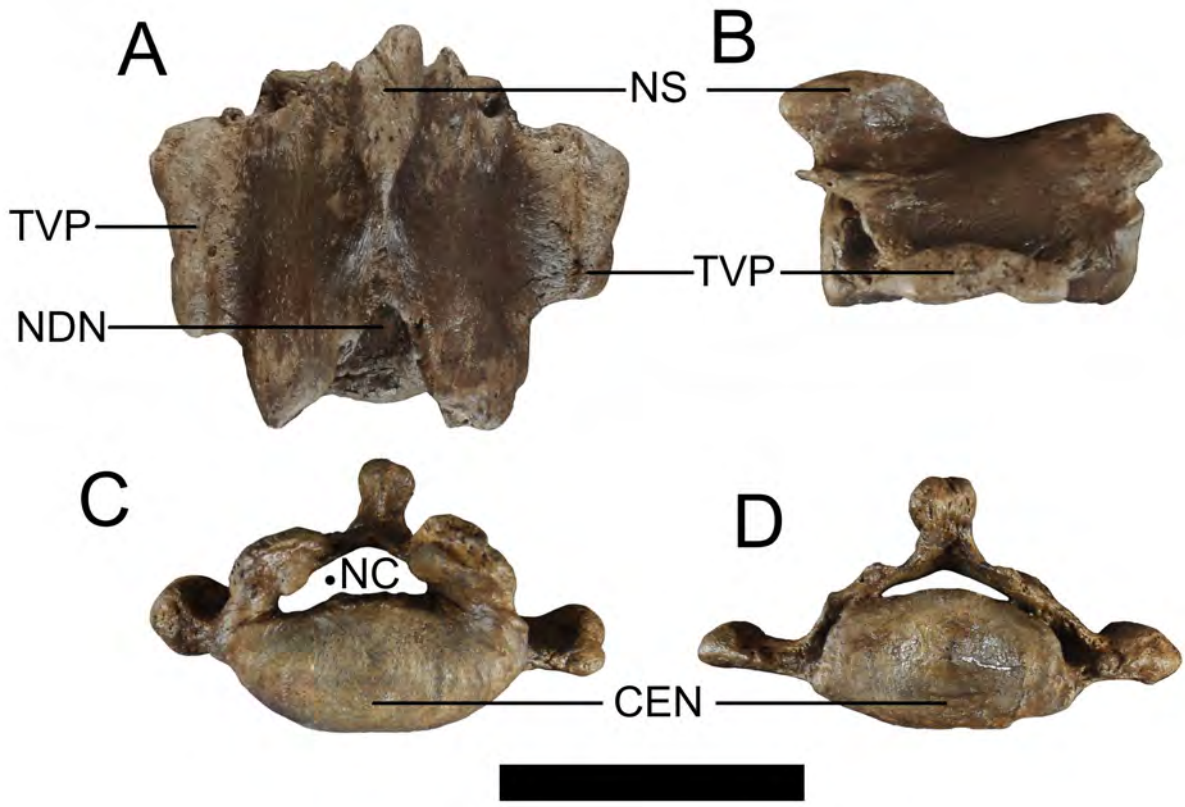

Figure 37. Third caudal vertebra of ETMNH 609. Views: A, dorsal; B, right lateral; C, anterior; D, posterior. Abbreviations: CEN, centrum; NC, neural canal; NDN, neural dorsal notch; NS, neural spine; TVP, transverse process. Pre- and post-zygapophyses are not visible in this figure. Scale bar = 10 cm.

riorly elongate and mediolaterally narrow (Figs. 44, 46). Most of the articular surfaces are on the anterior two-thirds of the lunar as the posterior one-third forms a rugose process. On the proximomedial side of the process, there is an articular surface that is one of the three points of articulation with the scaphoid. Proximally, the lunar has a large, convex articular surface for articulation with the radius. Posteriorly, this articular surface slopes distally onto the lunar process, whereas the anterior portion slopes along the anterior surface. Distally, the lunar has two concave articular surfaces joined at a slightly elevated ridge. The medial facet is a small tear-drop situated more posteriorly for articulation with the magnum. The lateral facet is posteriorly square and anteriorly flared, and it articulates with the unciform. On the medial side, there are two additional articular surfaces for the scaphoid. The proximal of these is elongate antero-

Figure 38. Sternebrae of ETMNH 609. Scale bar = 10 cm.

Figure 39. Ribs of ETMNH 601 showing pathology. Scale bar = 10 cm.

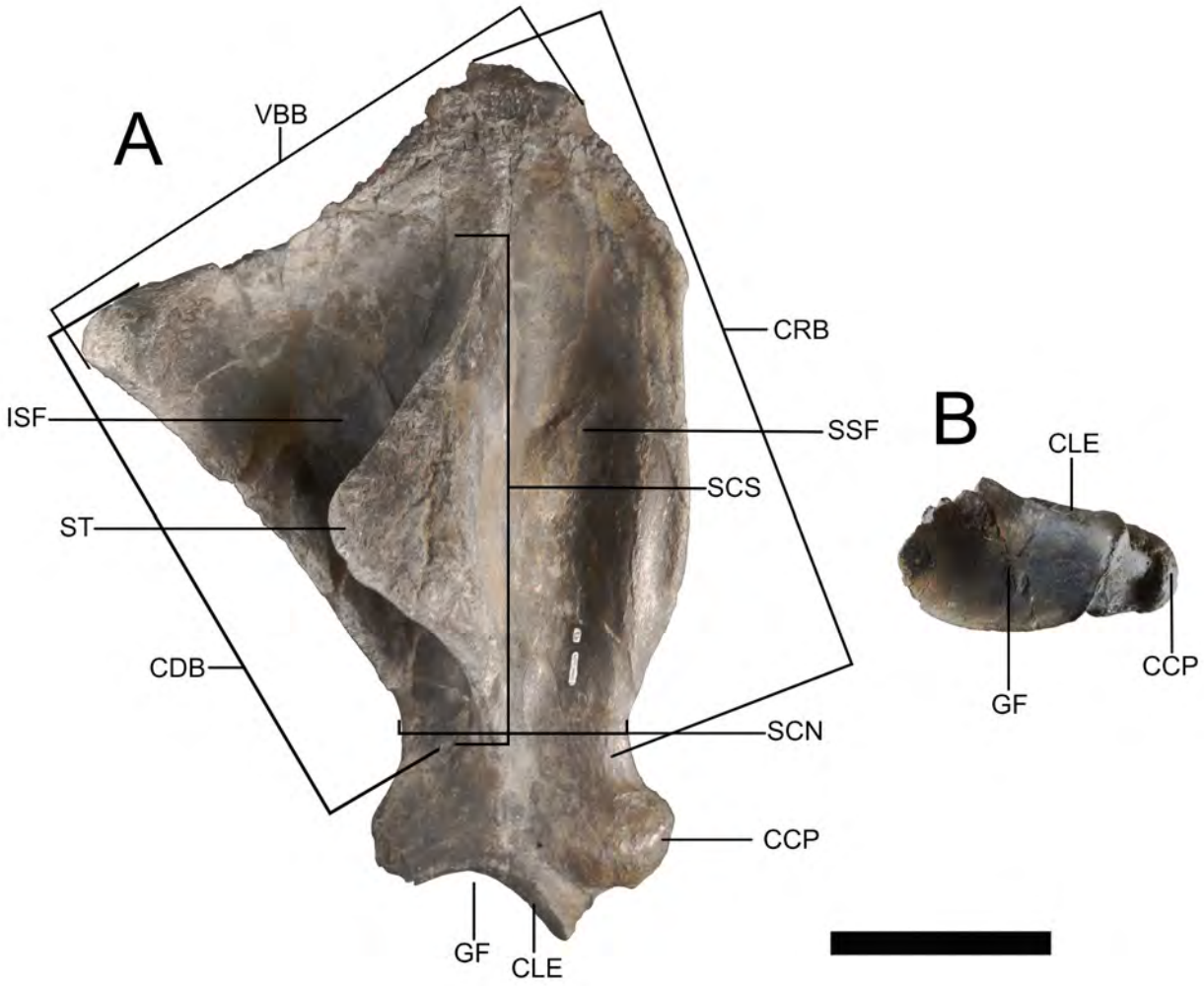

Figure 40. Right scapula of ETMNH 609. Views: A, lateral; B, distal. Abbreviations: CCP, coracoid process; CDB, caudal border; CLE, craniolateral edge; CRB, cranial border; GF, glenoid fossa; ISF, infraspinous fossa; SCN, scapular neck; SCS, scapular spine; SSF, supraspinous fossa; ST, spinous tuber; VBB, vertebral border. Scale bar = 10 cm.

posteriorly, and the distal one is proximally domed and distally square. On the lateral side, there are also two articular surfaces for articulation with the cuneiform. The proximal of these is oval, and the distal one is thin and oblong.

Cuneiform.—Proximodistal and anteroposterior axes of the cuneiform are long, whereas the mediolateral axis is short (Figs. 44, 47). There is rugose bone extending anteroposteriorly on the distal portion of the lateral side. A proximal articular surface is saddle-like for articulation with the styloid process of the ulna. Laterally, this articular surface curves distally, and medially, it terminates at a ridge with a rectangular articular surface for the lunar. A square articular surface with a rounded anterolateral corner is present on the distal end of the cuneiform for articulation with the unciform. Medially, this ulnar articular surface folds proximally and creates a small, domed articular surface for the lunar. On the posterior side, an oblong articular surface is present for articulation with the pisiform. This articular surface forms a lateral ridge as it joins the lateral portion of the proximal articular surface.

Pisiform.—The pisiform appears to be pinched mediolaterally because it curves medi-

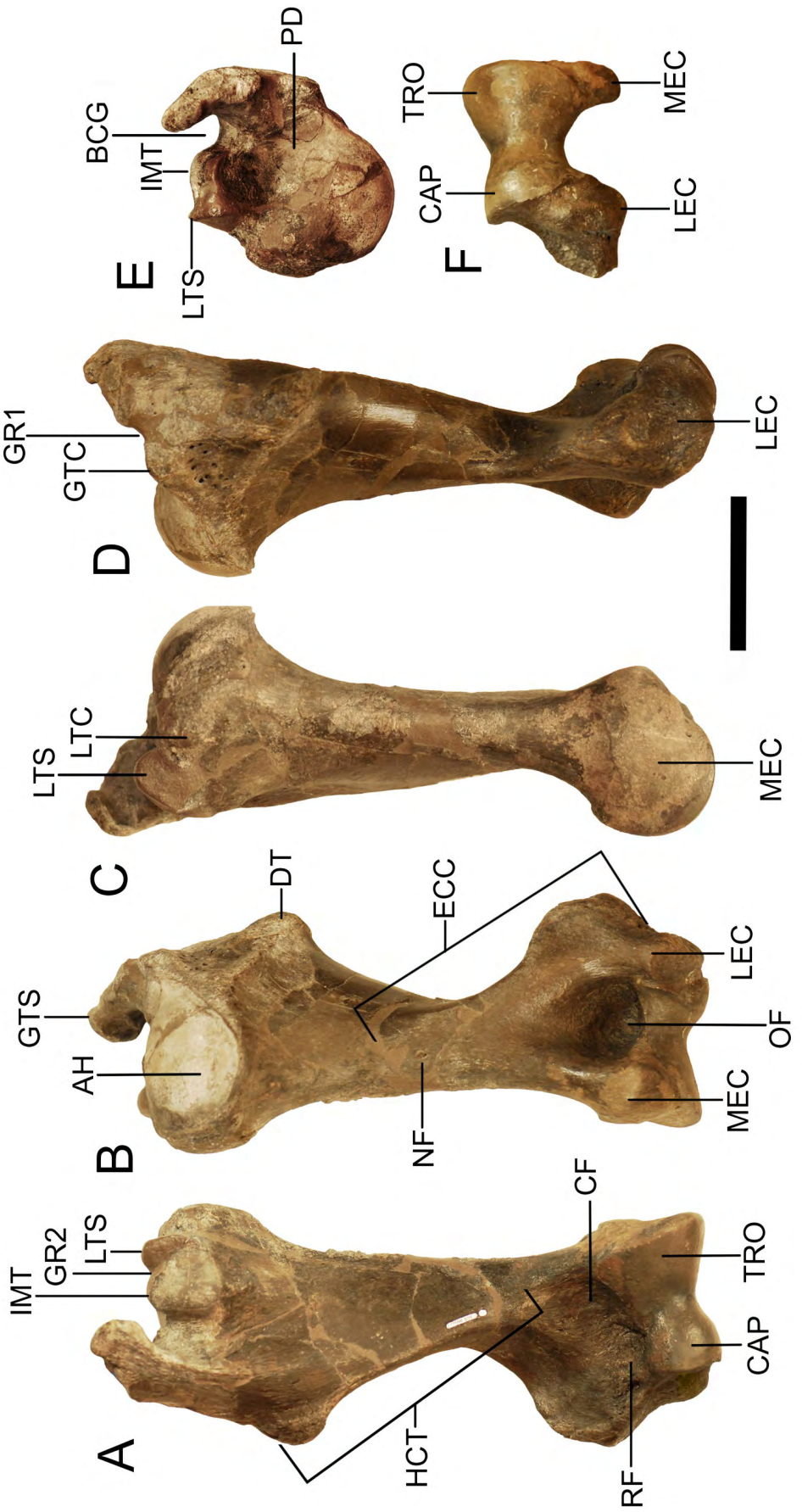

Figure 41. Right humerus of ETMNH 609. Views: A, anterior; B, posterior; C, medial; D, lateral; E, proximal; F, distal. Abbreviations: AH, articular head; BCG, bicipital groove; CAP, capitulum; CF, coronoid fossa; HCT, humeral crest; DT, deltoid tuberosity; ECC, epicondylar crest; GR1, groove one; GR2, groove two; GTC, greater tuberosity convexity; GTS, greater tuberosity summit; IMT, intermediate tubercle; LEC, lateral epicondyle; LTC, lesser tuberosity convexity; LTS, lesser tuberosity summit; MEC, medial epicondyle; NF, nutrient foramen; OF, olecranon fossa; PD, proximal depression; RF, radial fossa; TRO, trochlea. Scale bar = 10 cm.

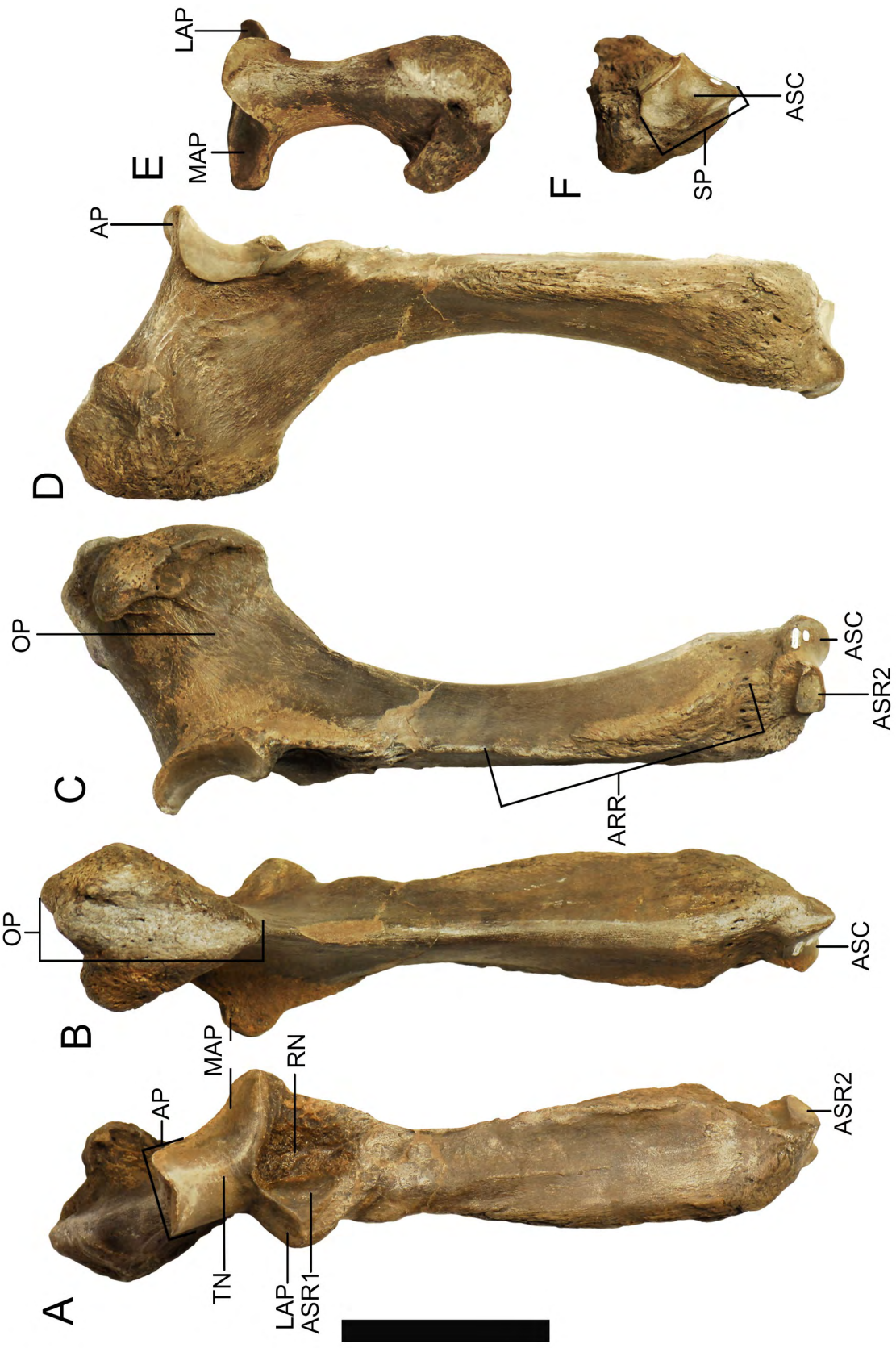

Figure 42. Right ulna of ETMNH 609. Views: A, anterior; B, posterior; C, medial; D, lateral; E, proximal; F, distal. Abbreviations: AP, anconeal process; ARR, articular rugose bone for radius; ASC, articular surface for cuneiform; ASR1–2, articular surfaces for radius 1–2; LAP, lateral articular process; MAP, medial articular process; OP, olecranon process; RN, radial notch; SP, styloid process; TN, trochlear notch. Scale bar = 10 cm.

Figure 43. Right radius of ETMNH 609. Views: A, anterior; B, posterior; C, medial; D, lateral; E, proximal; F, distal. Abbreviations: ASU1–3, articular surfaces for the ulna 1–3; ASC, articular surface for the capitulum; ASL, articular surface for the lunar; ASS, articular surface for the scaphoid; AST, articular surface for the trochlea; CP, radial coronoid process; NK, radial neck; RCT, radial crest; RTB, radial tuberosity. Scale bar = 10 cm.

Figure 44. Articulated carpal bones of ETMNH 609 in anterior view. Abbreviations: CUN, cuneiform; LUN, lunar; MAG, magnum; SCA, scaphoid; TRD, trapezoid; TRM, trapezium; UNC, unciform. The pisiform is not visible in this view. Scale bar = 10 cm.

ally and flares posteriorly (Figs. 44, 48). An anterior articular surface for the cuneiform is round proximally and square distally. ETMNH 601 has an additional small, round anterolateral articular surface for the ulna that does not occur in ETMNH 609.

Trapezium.—The trapezium is a small, rugose bone with a 'V'-shape pointed distally (Figs. 44, 49). An oval articular surface for the trapezoid is present on the lateral side. ETMNH 601 has a distally extended articular surface for a slight articulation with the second metacarpal.

Trapezoid.—A rugose prominence occurs on the anterior surface (Figs. 44, 50). The proximal articular surface for the scaphoid is square with a convexly rounded medial edge and is depressed mediolaterally. At the posteromedial corner of this facet, it forms a ridge with a round, medial articular surface for the trapezium. Distally, the trapezium articular surface folds laterally into the convex, ovate distal articular surface for the second metacarpal. Laterally, this distal articular surface forms an edge with the lateral kidney-shaped articular surface for the magnum.

Magnum.—The magnum is narrower across the mediolateral axis than the anteroposterior axis (Figs. 44, 51). Anteroproximally, there is an articular surface for the scaphoid that is triangular with

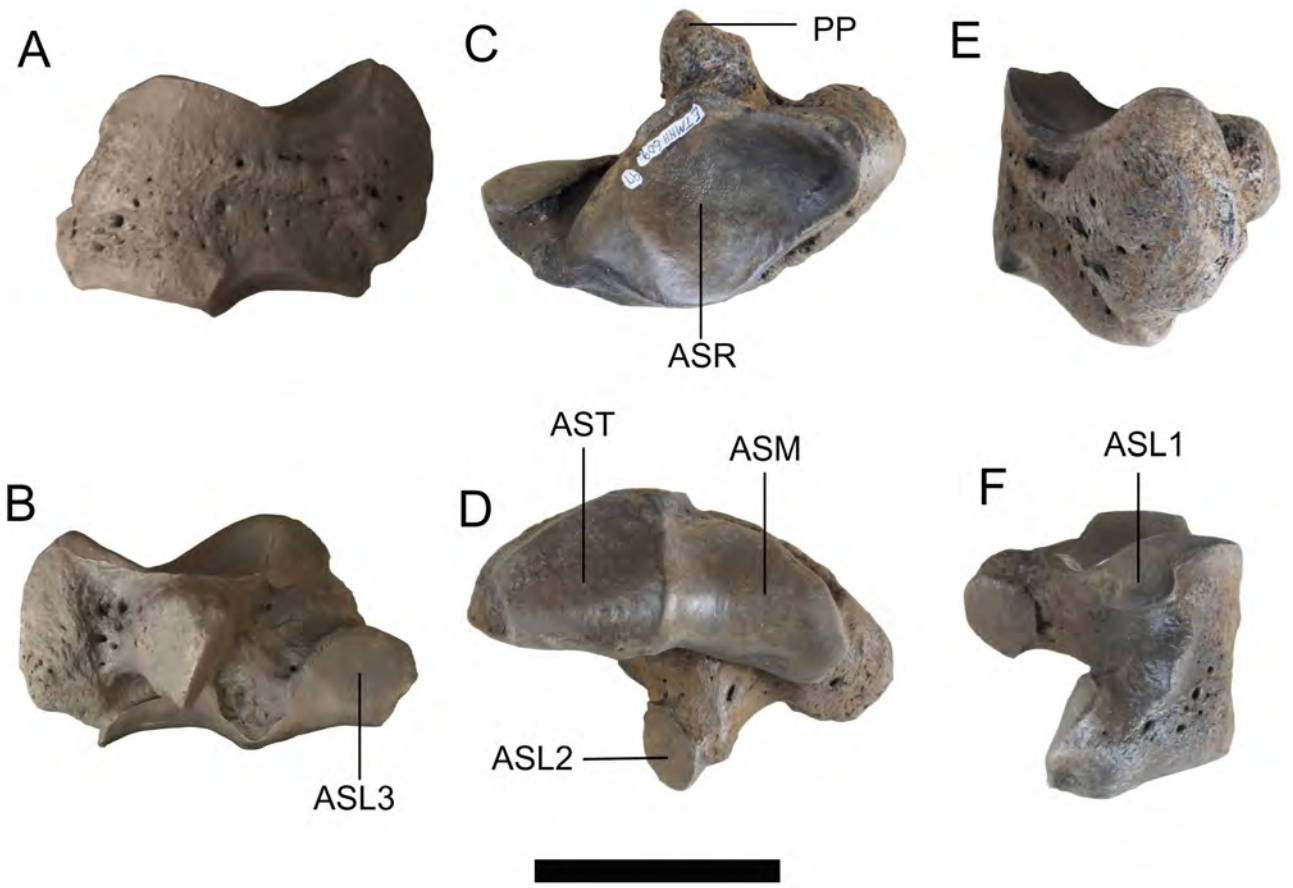

Figure 45. Right scaphoid of ETMNH 609. Views: A, anterior; B, posterior; C, proximal; D, distal; E, medial; F, lateral. Abbreviations: ASL1–3, articular surfaces for lunar 1–3; ASM, articular surface for magnum; ASR, articular surface for radius; AST, articular surface for trapezoid; PP, posterior process. Scale bar = 5 cm.

an anterior straight edge and posterior point that is laterally raised. This raised portion forms a ridge with the triangular posteroproximal articular surface, which is saddled over a proximally raised process, for articulation with the lunar. On the medial surface, there is a kidney-shaped articular surface that articulates with the trapezoid and forms an edge with the anteroproximal facet. Along its distal edge, this articular surface contacts a small, rectangular articular surface for the second metacarpal. One articular surface for the third metacarpal covers most of the distal surface of the magnum. Posteriorly, this articular surface extends along a small distal process that mirrors the proximal process. This facet is slightly curved anteriorly and has a straight medial edge with the second metacarpal facet. On the lateral side, there is another kidney-shaped articular surface for the unciform. The magna from the GFS lack a posterior process resembling those discussed by Harrison and Manning (1983).

Unciform.—All of the articular surfaces are on the anterior portion of the unciform and are distolaterally curved (Figs. 44, 52). The posterior portion of the unciform consists of a rugose process that can be variable within a population as demonstrated by Harrison and Manning (1983), but it is consistent within the limited sample from the GFS. Two articular surfaces meet at a ridge on the proximal side of the anterior portion. The proximolateral articular surface for the cuneiform is slightly convex anteroposteriorly and comes to a rounded point on the lateral side. The proximomedial articular surface is round, longer anteroposteriorly, and

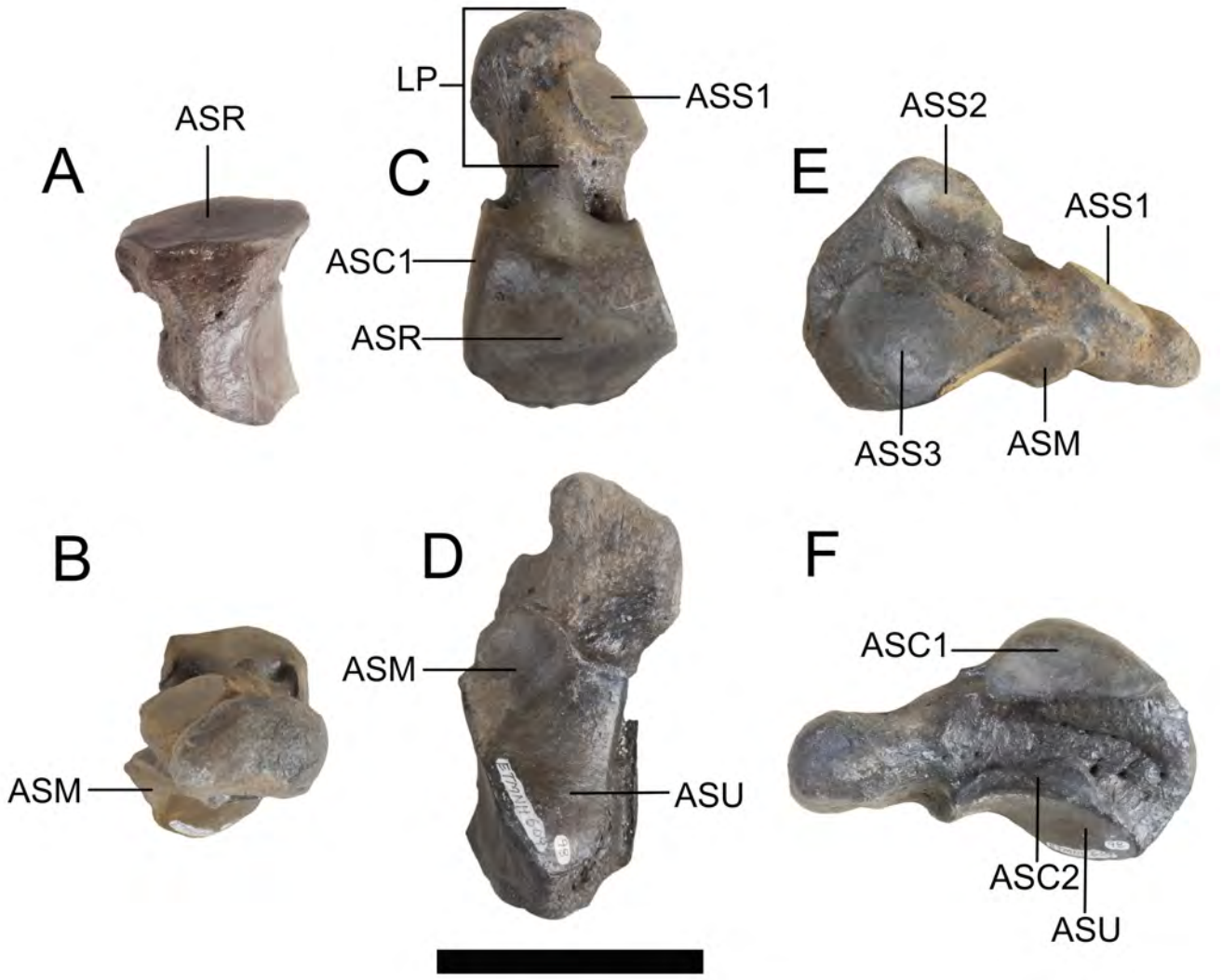

Figure 46. Right lunar of ETMNH 609. Views: A, anterior; B, posterior; C, proximal; D, distal; E, medial; F, lateral. Abbreviations: ASC1–2, articular surfaces for cuneiform 1–2; ASM, articular surface for magnum; ASR, articular surface for radius; ASS1–3, articular surfaces for scaphoid 1–3; ASU, articular surface for unciform; LP, lunar process. Scale bar = 5 cm.

articulates with the lunar. A second medial articular surface is distal to the lunar facet and is 'C'-shaped for articulation with the magnum. On the distal surface, articular facets are present for the third, fourth, and, on ETMNH 601, fifth metacarpals. The more medial third metacarpal and the lateral fourth metacarpal share the articular surface without a dividing ridge; however, there is an indicative line formed by wear. Overall, the articular surface is triangular with a small convexity along the medial edge near where it contacts the medial articular surface for the magnum. This lateral indentation articulates with the fifth metacarpal or the proximal expansion present on some fourth metacarpals.

Second Metacarpal.—Both medial and lateral edges are slightly curved medially so the sides appear pinched anteroposteriorly (Fig. 53). There is a slight posterior ridge just medial to the midline of the bone that extends from proximal to distal and, at the posterodistal facets, matches with the intermediate relief. On the proximal end, there are three primary articular surfaces. A roughly square medial articular surface for the trapezoid is the largest and has a slight depression in the middle. The lateral edge of this facet is raised to form a ridge with the rectangular proximomedial articular surface for the

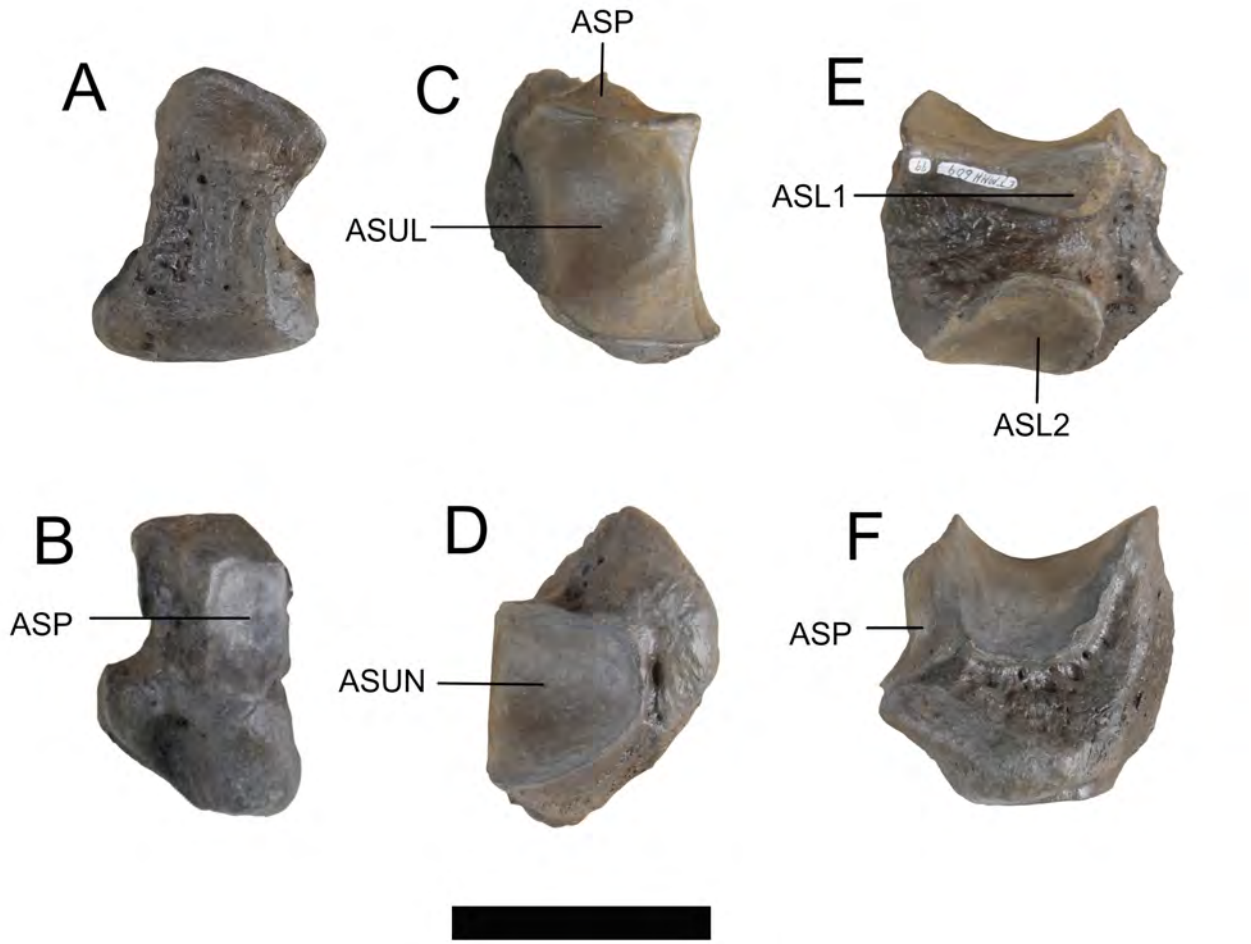

Figure 47. Right cuneiform of ETMNH 609. Views: A, anterior; B, posterior; C, proximal; D, distal; E, medial; F, lateral. Abbreviations: ASL1–2, articular surfaces for lunar 1–2; ASP, articular surface for pisiform; ASUL, articular surface for ulna; ASUN, articular surface for unciform. Scale bar = 5 cm.

Figure 48. Right pisiform of ETMNH 609. Views: A, anterior; B, dorsal; C, lateral. Abbreviations: ASC, articular surface for cuneiform. Scale bar = 5 cm.

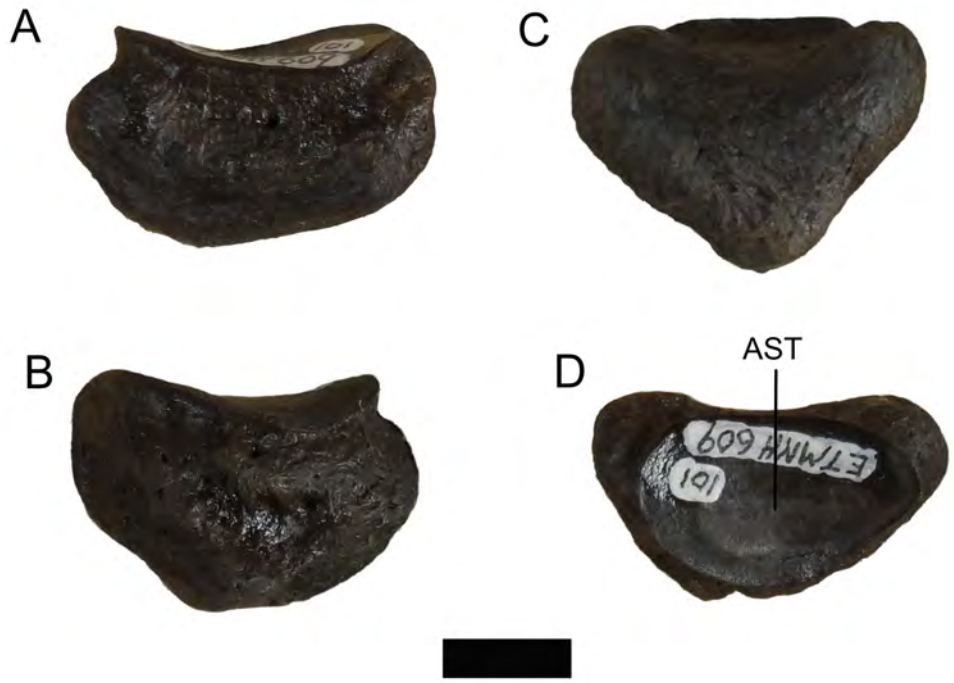

Figure 49. Right trapezium of ETMNH 609. Views: A, proximal; B, distal; C, medial; D, lateral. Abbreviation: AST, articular surface for trapezoid. Scale bar = 1 cm.

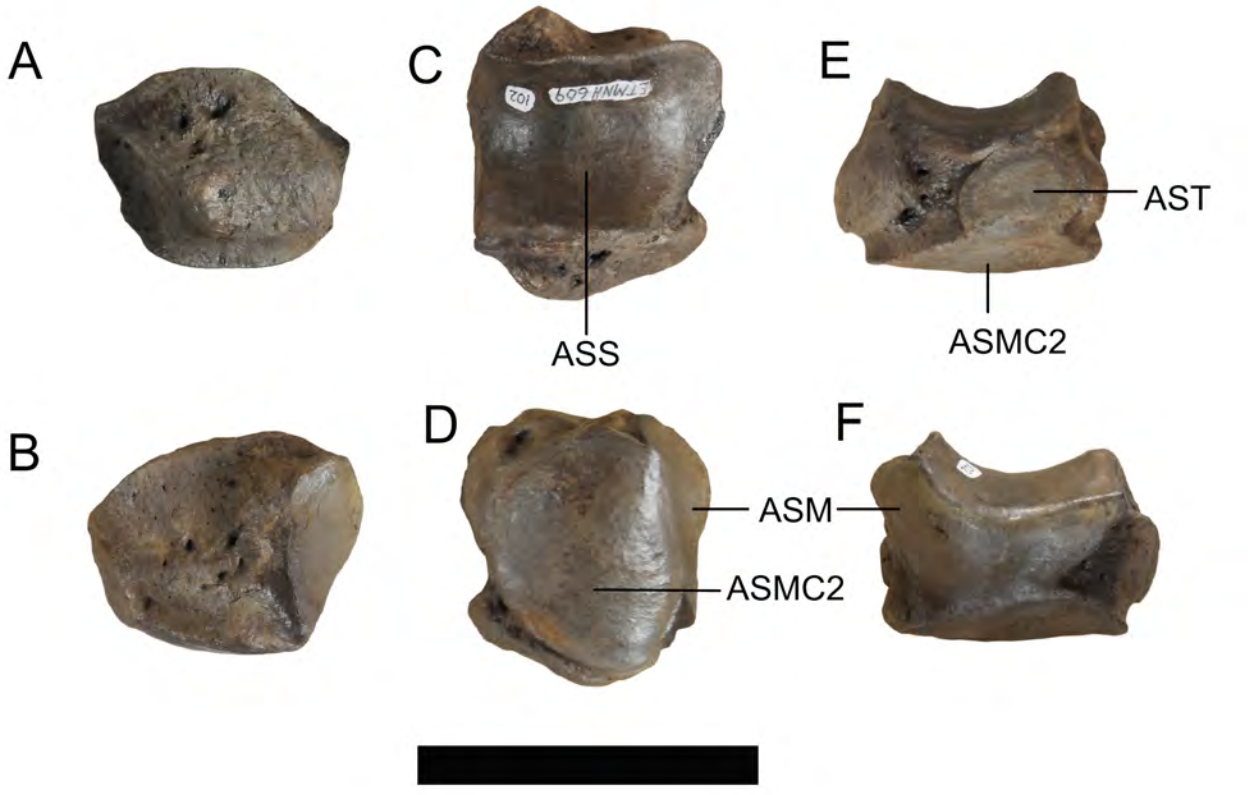

Figure 50. Right trapezoid of ETMNH 609. Views: A, anterior; B, posterior; C, proximal; D, distal; E, medial; F, lateral. Abbreviations: ASM, articular surface for magnum; ASMC2, articular surface for second metacarpal; ASS, articular surface for scaphoid; AST, articular surface for trapezium. Scale bar = 5 cm.

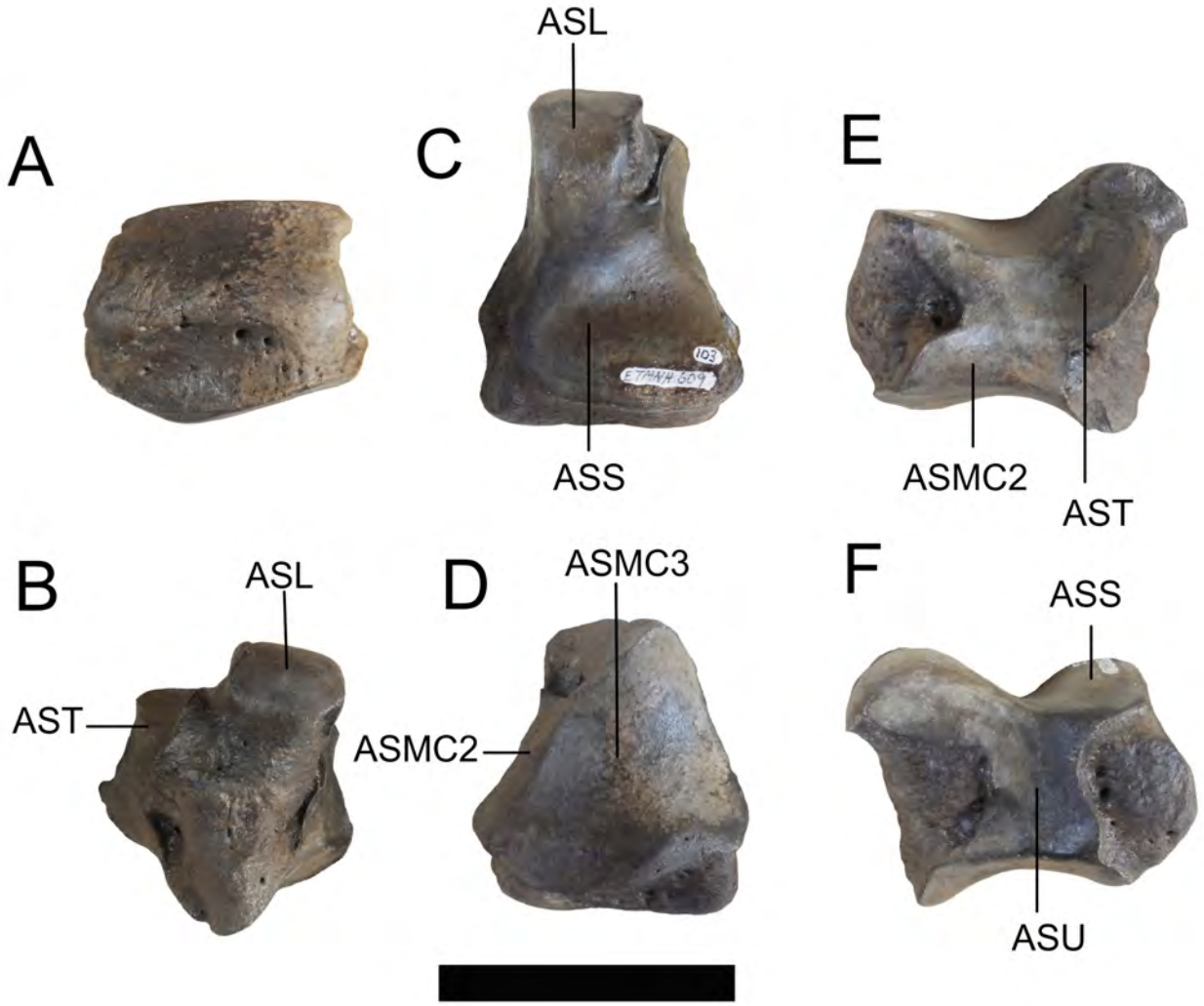

Figure 51. Right magnum of ETMNH 609. Views: A, anterior; B, posterior; C, proximal; D, distal; E, medial; F, lateral. Abbreviations: ASL, articular surface for lunar; ASMC2–3, articular surfaces for second and third metacarpals; ASS, articular surface for scaphoid; AST, articular surface for trapezoid; ASU, articular surface for unciform. Scale bar = 5 cm.

magnum, which slopes distally and laterally from the ridge. At the distal edge, this facet folds into the lateral-most articular surface of the proximal end. This lateral articular surface for the third metacarpal is rectangular. At the distal end, the anterior articular surface for the proximal phalanx is smooth and, though the lateral edge is parallel to the axis of the bone, the medial edge curves laterally creating a half-dome shape. On the posterior articular surface, two facets are separated by the intermediate relief. Both facets are oval with slight depressions along their midlines, are slanted from proximomedial to distolateral, and each articulates with one sesamoid.

Third Metacarpal.—On the anterior surface of the proximal end, there are two rugose knobs that serve as sites of muscle attachment (Fig. 54). Similar rugosities are on the posterior surface as well. In posterior view, a nutrient foramen is present at the midpoint of the diaphysis along a posterior ridge that separates a pair of depressions proximal to the distal articular surface. These depressions are not as pronounced as those seen in other species of *Teleoceras*. On the medial and lateral sides of the bone, there are proximal rectangular articular surfaces for the second and fourth meta-

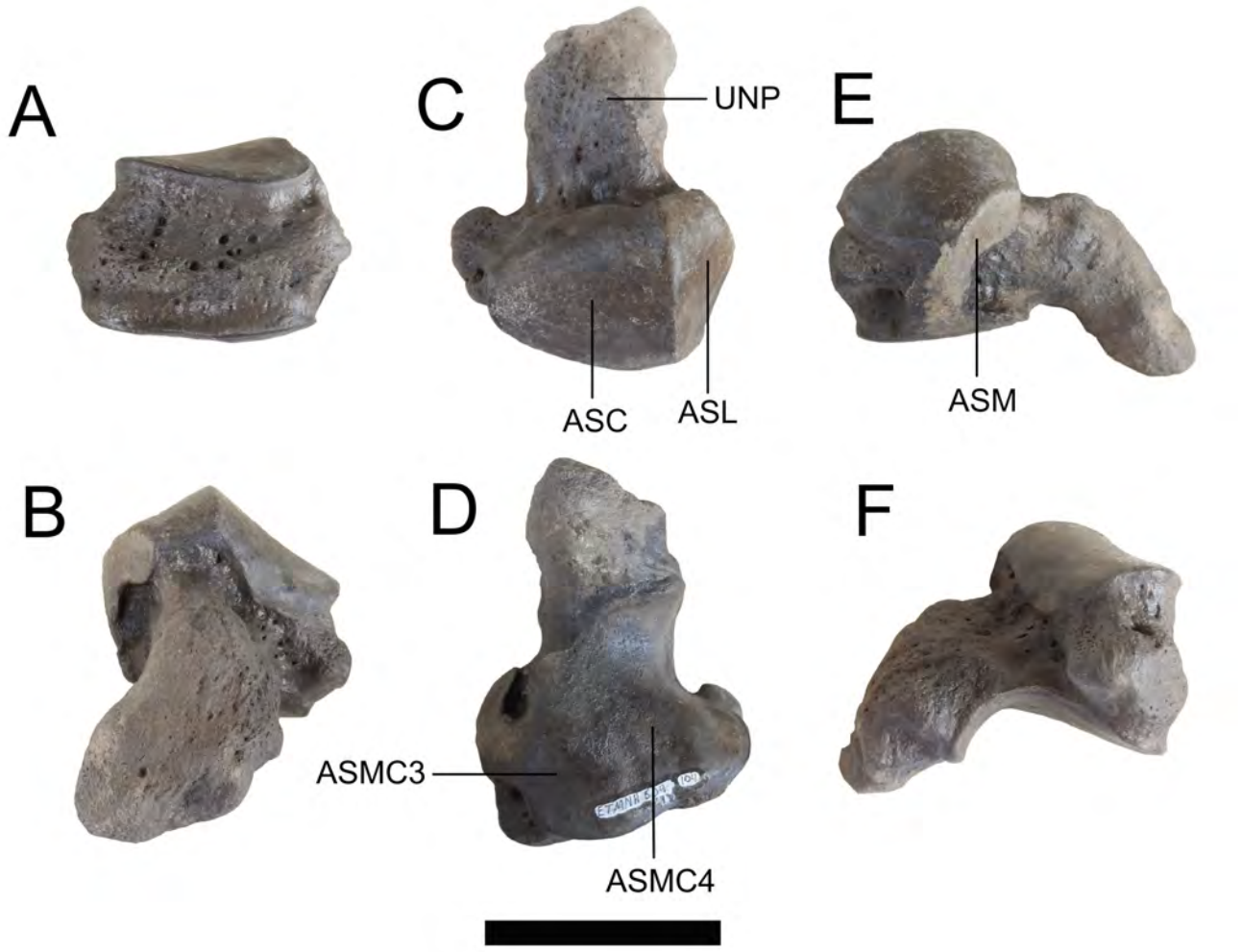

Figure 52. Right unciform of ETMNH 609. Views: A, anterior; B, posterior; C, proximal; D, distal; E, medial; F, lateral. Abbreviations: ASC, articular surface for cuneiform; ASL, articular surface for lunar; ASM, articular surface for magnum; ASMC3–4, articular surfaces for third and fourth metacarpals; UNP, unciform process. Scale bar = 5 cm.

carpals, respectively. A triangular articular surface for the magnum is on the medial side of the proximal end and has a concavity at the narrow posterior end. The lateral proximal articular surface for the unciform is medially domed with a straight lateral edge and a pinched posterior point. Distally, the anterior articular surface for the proximal phalanx of the third digit is smooth and domed proximally. Posteriorly, an intermediate relief divides the distal articular surface into two oval facets for articulation with the two sesamoids.

Fourth Metacarpal.—Along the diaphysis, the narrower lateral side is more concave than the rugose medial side (Fig. 55). Both the proximal and the distal ends curve further posteriorly than the diaphyseal area giving the appearance that the midsection is depressed. Two articular surfaces are on the proximal end of the fourth metacarpal. Medially, there is a rectangular articular surface for the third metacarpal. The proximal edge of this facet forms a ridge with the medial edge of the proximal articular surface. This proximal articular surface for the unciform is the larger of the two and is indented along the lateral edge. Posteriorly, it folds over a raised portion that forms a tight articulation with the unciform. On ETMNH 601, there is an articular notch lateral to this facet where the fifth metacarpal articulates; however, on ETMNH 609, a remnant

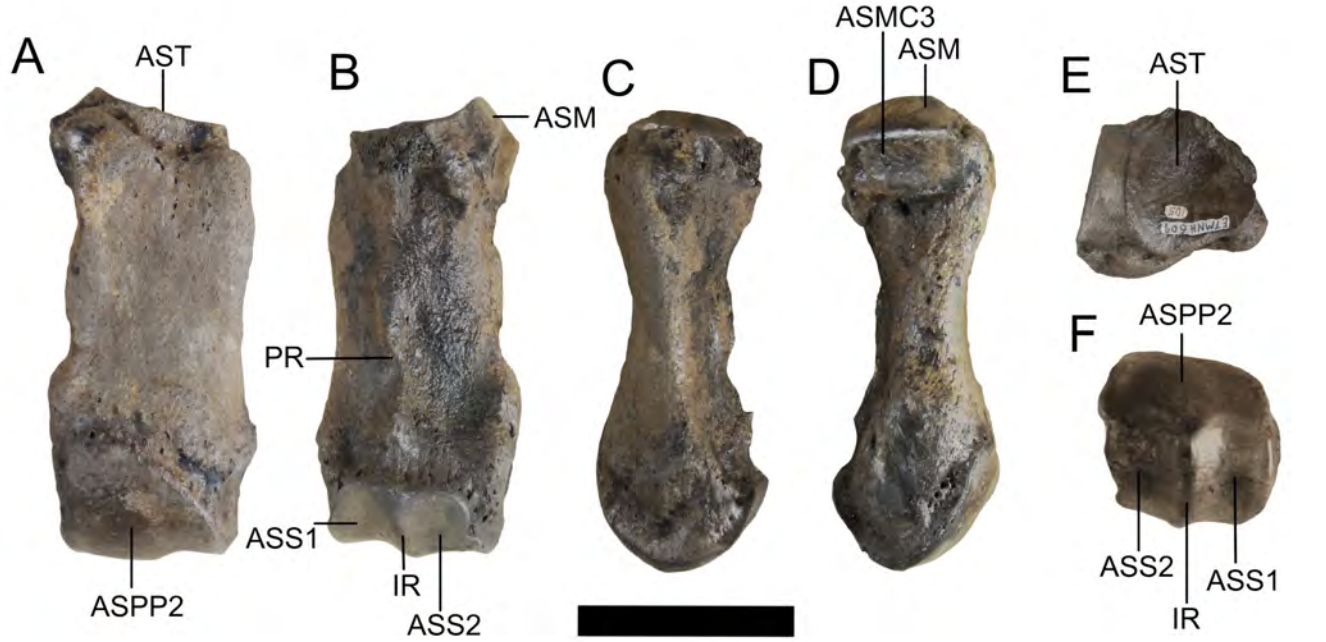

Figure 53. Right second metacarpal of ETMNH 609. Views: A, anterior; B, posterior; C, medial; D, lateral; E, proximal; F, distal. Abbreviations: ASM, articular surface for magnum; ASMC3, articular surface for third metacarpal; ASPP2, articular surface for proximal phalanx of the second digit; ASS1–2, articular surfaces for sesamoids 1–2; AST, articular surface for trapezoid; IR, intermediate relief; PR, posterior ridge. Scale bar = 5 cm.

Figure 54. Right third metacarpal of ETMNH 609. Views: A, anterior; B, posterior; C, medial; D, lateral; E, proximal; F, distal. Abbreviations: ASM, articular surface for magnum; ASMC2, articular surface for second metacarpal; ASMC4, articular surface for fourth metacarpal; ASPP3, articular surface for proximal phalanx of third digit; ASS1–2; articular surface for sesamoids 1–2; ASU, articular surface for unciform; IR, intermediate relief; NF, nutrient foramen; PR, posterior ridge. Scale bar = 5 cm.

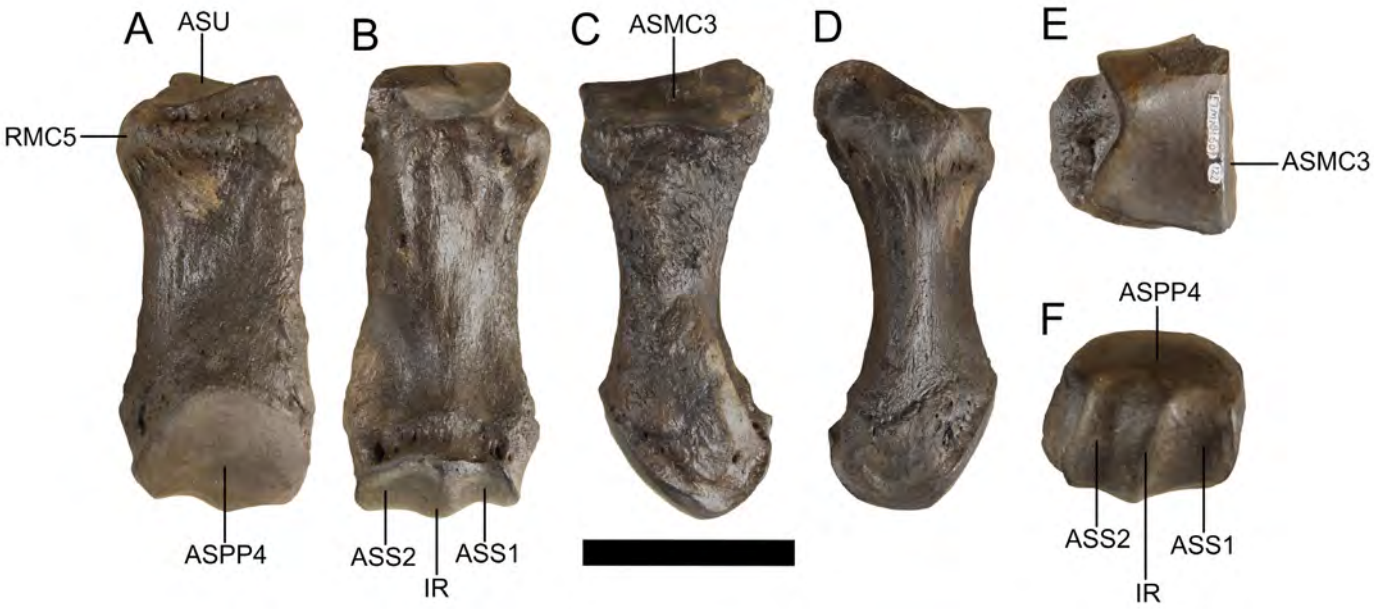

Figure 55. Right fourth metacarpal of ETMNH 609. Views: A, anterior; B, posterior; C, medial; D, lateral; E, proximal; F, distal. Abbreviations: ASMC3, articular surface for third metacarpal; ASPP4, articular surface for proximal phalanx of fourth digit; ASS1–2, articular surfaces for sesamoids 1–2; ASU, articular surface for unciform; IR, intermediate relief; RMC5, remnant of fifth metacarpal. Scale bar = 5 cm.

of the fifth metacarpal is fused to the fourth metacarpal in place of the notch. At the distal end, the anterior articular surface for the proximal phalanx is smooth and proximally domed with only a slight lateral curvature. Two facets are on the posterior surface and are separated by an intermediate relief that slants from proximomedial to distolateral creating slanted facets for articulation with the two sesamoids.

Fifth Metacarpal.—Each manus of ETMNH 601 has a fifth metacarpal (Fig. 56) that was first described by Wallace (2006). A proximal articular surface for the unciform has a posterior convex fold. There is medial rugose bone that articulates with a proximolateral depression on the fourth metacarpal. On ETMNH 609 and 8271, the fourth metacarpals have expanded lateral knobs, which are believed to be the remnants of the fifth metacarpals. Neither the isolated nor the fused fifth metacarpals have evidence of a distal articular surface for a proximal phalanx.

Though similar in morphology, metacarpals are noticeably larger than metatarsals (Fig. 57). Distal to the metacarpals, each digit consists of three phalanges and two sesamoids. Phalanges and sesamoids of the manus and pes are nearly indistinguishable except for by size (Fig. 58), so a combined description will be provided following the description of the hind limb.

Hind Limb

Innominate.—It is difficult to differentiate the three bones—ilium, ischium, and pubis—that make up each innominate due to the degree of fusion (Fig. 59). The acetabulum is round with the acetabular incision on the lateral edge of the obturator foramen. There is a small fossa on the articular surface of the acetabulum. The ilium is the largest of the innominate bones and expands into a broad wing. Laterally, the iliac wing is smooth, but the medial iliac wing is rugose for articulation with the sacrum. The iliac crest is rounded at the dorsocranial spine and makes a nearly straight edge to the ventrocranial spine. A sciatic eminence is prominent on the dorsocranial spine and the greater

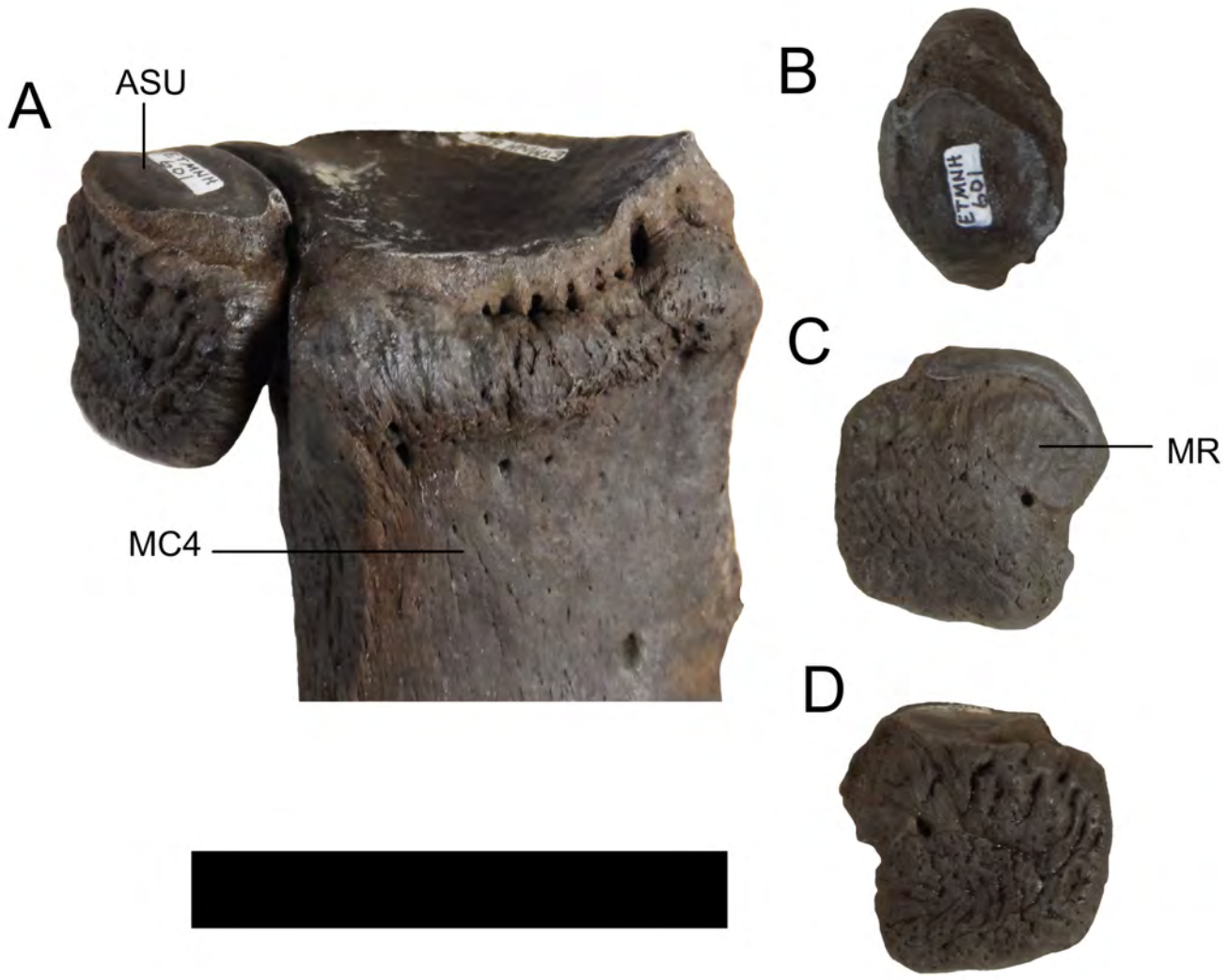

Figure 56. Right fifth metacarpal of ETMNH 601. Views: A, anterolateral showing articulation with fourth metacarpal; B, dorsal; C, medial; D, lateral. Abbreviations: ASU, articular surface for unciform; MC4, fourth metacarpal; MR, medial rugose bone. Scale bar = 5 cm.

sciatic notch is deep. A thin, smooth ischium forms the symphysis, which is small relative to the overall size of the innominate. The ischial arch occurs between this symphysis and the rugose ischiatic tuberosity. There is no evidence of an ilio-pubic eminence between the ilium and the pubis, which has a broad body and slender branches.

Femur.—The diaphysis is slightly curved in the parasagittal plane (Fig. 60). The posterior surface of the femur is nearly flattened, but the anterior surface is more rounded. At the proximal end, there is a minimal trochanteric fossa along the posterior edge of the greater trochanter. A round articular head extends only minimally proximal to the greater trochanter. Along the medial edge, the head forms a lip that overlies the suture line. There is no obvious fovea capitis on the femoral head. A shallow depression is the only evidence of a femoral neck between the head and the greater trochanter. There is a blunt greater trochanter without a definite summit and with only a minimal crest at the latero-distal point. There is an elongate, rugose lesser trochanter on the medial surface that does not extend more medially than the femoral head. An elongate third trochanter is on the lateral surface but does not extend as far laterally as the greater trochanter.

Figure 57. Right metapodials of ETMNH 609 in anterior view. A, metacarpals; B, metatarsals. Scale bar = 5 cm.

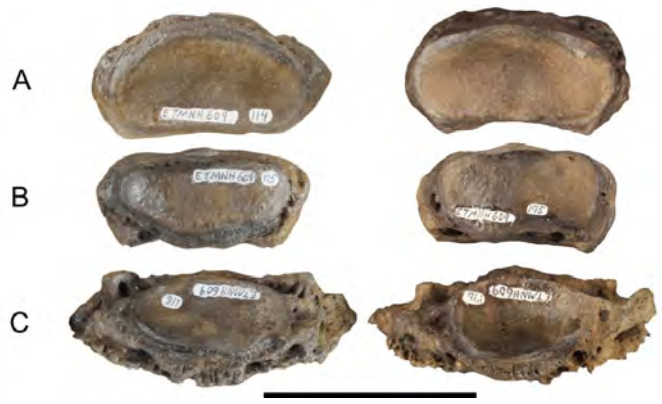

Figure 58. Right phalanges of third digits of ETMNH 609. Left, front phalanges; Right, hind phalanges. A, proximal phalanges; B, medial phalanges; C, distal phalanges. Scale bar = 5 cm.

The third trochanter is reduced among rhinocerotids but is larger than those seen in most other species of *Teleoceras.*

Distally, medial and lateral trochlear tubercles are present on the anterior surface and are separated by a trochlear groove. There is a pronounced femoral ridge that extends from the medial trochlear tubercle along the diaphysis to the head. In anterior view, the more prominent medial trochlear tubercle is also more rounded compared to the smaller and more angular lateral trochlear tubercle. It is possible that this medial trochlear tubercle acted as a locking mechanism as found in derived equids (Hermanson and MacFadden, 1996). On the posterodistal surface, a larger lateral condyle slants slightly compared to the smaller medial condyle, which is more aligned with the diaphyseal axis. A deep intercondylar fossa extends medially and laterally beneath the edges of the articular condyles. Both epicondyles have large muscle scars on the outer surface. Most femoral muscle attachments are well-defined, especially the supracondylar fossa on the posterior surface just proximal to the condyles.

Patella.—Patellae are massive, rugose bones that articulate with the femoral trochlear tubercles (Fig. 61). A distinct point is formed by the apex at the distal end, but the base forms a rounded angle at the proximal end. The base does not extend much further proximally than the posterior articular surface does. This articular surface covers nearly the entire posterior surface and has two convexities

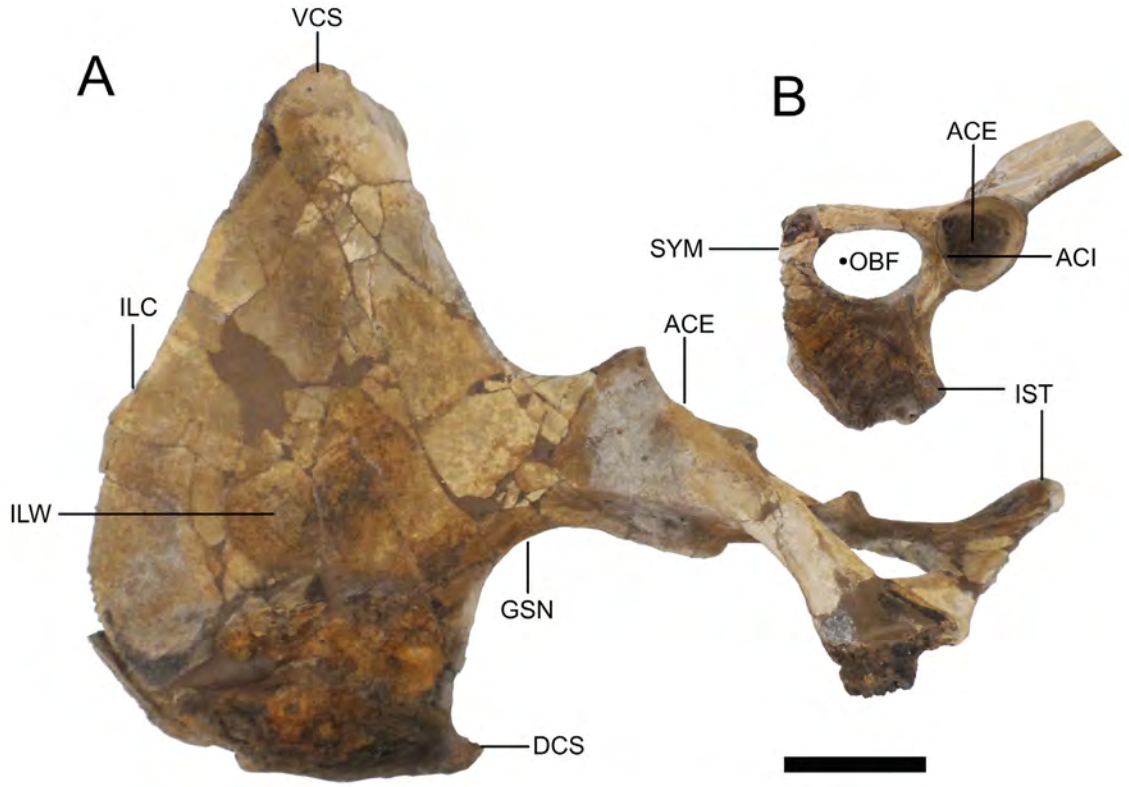

Figure 59. Left innominate of ETMNH 609. Views: A, anterodorsal; B, anteroventral. Abbreviations: ACE, acetabulum; ACI, acetabular incision; DCS, dorsocranial spine; GSN, greater sciatic notch; ILC, iliac crest; ILW, iliac wing; IST, ischiatic tuberosity; OBF, obturator foramen; SYM, symphysis; VCS, ventrocranial spine. Scale bar = 10 cm.

that extends from proximal to distal for articulation with the femoral trochlear tubercles. A rounded lateral angle is present but not pronounced. In contrast, the medial angle is a well-defined prominence that forms a distomedial point.

Tibia.—The proximal end is larger than the distal and, for articulation with the femur, it has two large articular surfaces separated by a minimal popliteal notch on the posterior surface (Fig. 62). The lateral articular surface is a rounded triangle whereas the medial articular surface is smaller, more rounded, and more centrally depressed than the lateral articular surface. A cranial intercondylar area is present between the anterior portions of the medial and lateral articular surfaces. A narrow depression—the central intercondylar area—is bordered by the lateral and medial intercondylar eminences to separate the lateral articular surface from the medial articular surface and. There is also a smaller, flatter caudal intercondylar area between the posterior portions of the articular surfaces. Between the medial and lateral tibial tuberosities, there is a shallow tibial tuberosity groove. Though the medial tibial tuberosity is slightly rugose and aligned with the diaphysis, the lateral tibial tuberosity is more prominent, more rugose, and protrudes laterally from the diaphysis. Proximolaterally, there is a fibular articular surface that is shaped like an upside-down teardrop as seen on ETMNH 609. Rather than being smooth as most articular surfaces are, this is rugose for a tight articulation that becomes fused with age as seen on ETMNH 601.

In cross-section, the diaphysis is triangular as the tibial crest extends for nearly the entire length of the bone. The medial side of the diaphysis is nearly straight, but the lateral side is concave with a slight projection near the midpoint of the diaphysis. Distally, there is a parallelogram-shaped articu-

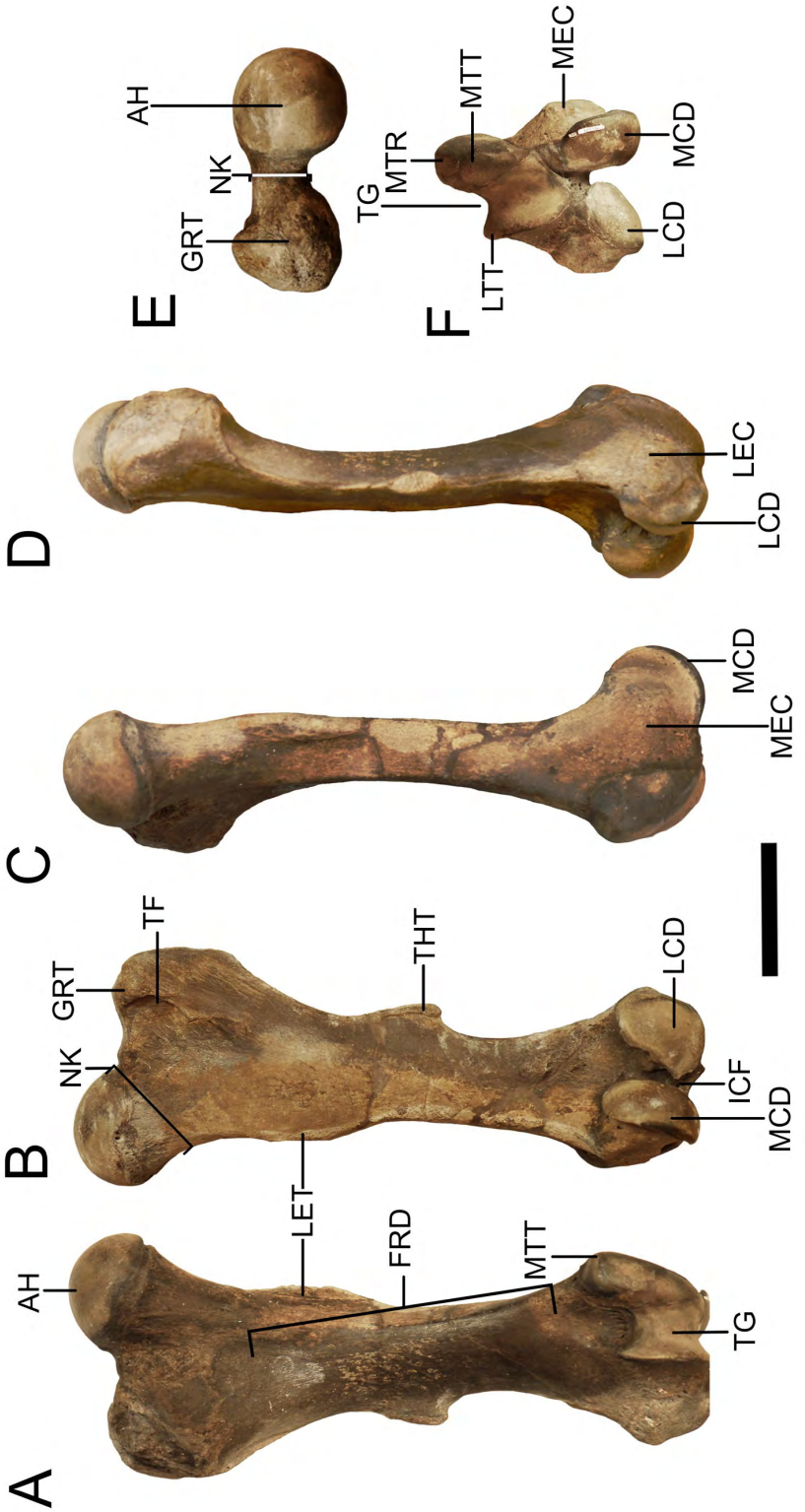

Figure 60. Right femur of ETMNH 609. Views: A, anterior; B, posterior; C, medial; D, lateral; E, proximal; F, distal. Abbreviations: AH, articular head; FRD, femoral ridge; GRT, greater trochanter; ICF, intercondylar fossa; LCD, lateral condyle; LEC, lateral epicondyle; LET, lesser trochanter; LTT, lateral trochlear tubercle; MCD, medial condyle; MEC, medial epicondyle; MTR, medial trochlear ridge; MTT, medial trochlear tubercle; NK, neck; TF, trochanteric fossa; TG, trochlear groove; THT, third trochanter. Scale bar = 10 cm.

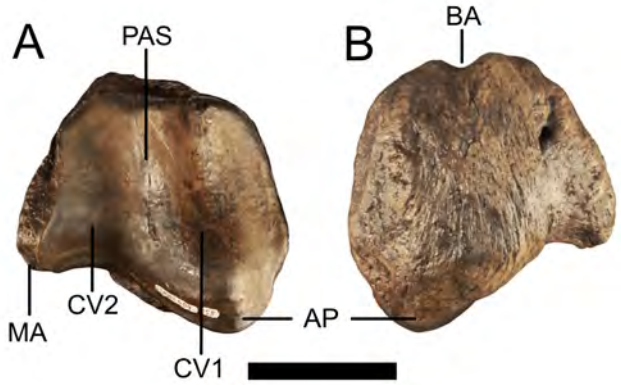

Figure 61. Left patella of ETMNH 609 flipped to appear as right. Views: A, posterior; B, anterior. Abbreviations: AP, apex; BA, base; CV1 and CV2, patellar convexity 1 and 2; MA, medial angle; PAS, posterior articular surface. Scale bar = 5 cm.

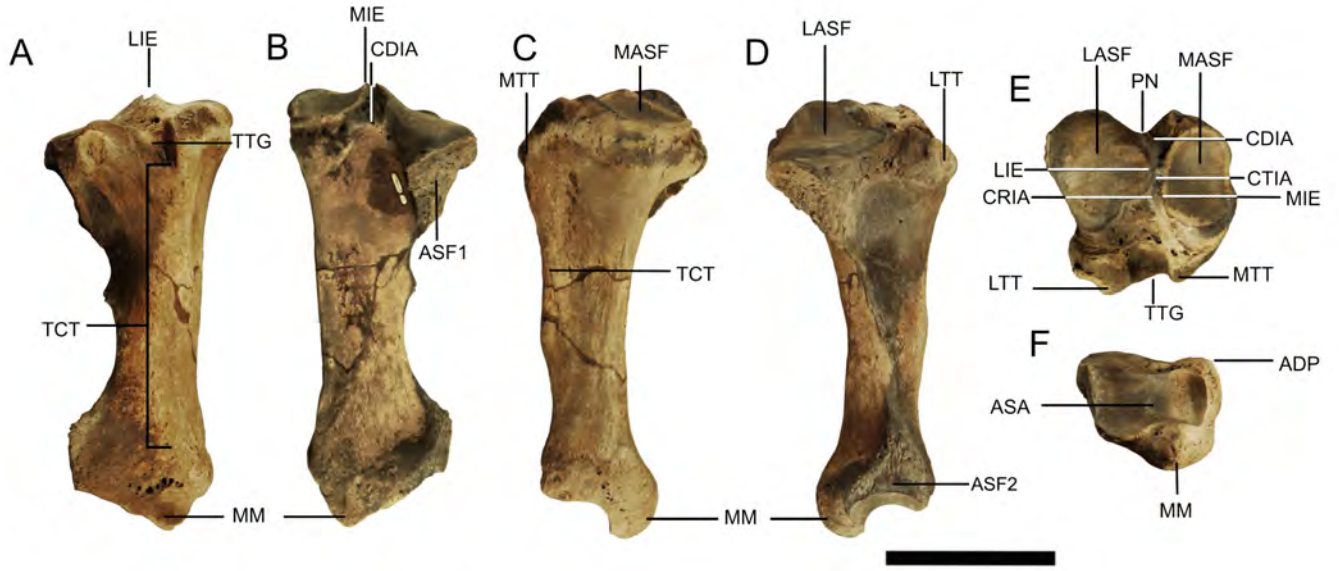

Figure 62. Right tibia of ETMNH 609. Views: A, anterior; B, posterior; C, medial; D, lateral; E, proximal; F, distal. Abbreviations: ADP, anterodistal process; ASA, articular surface for astragalus; ASF1–2, articular surfaces for fibula 1–2; CDIA, caudal intercondylar area; CRIA, cranial intercondylar area; CTIA, central intercondylar area; LASF, lateral articular surface for femur; LIE, lateral intercondylar eminence; LTT, lateral tibial tuberosity; MASF, medial articular surface for femur; MIE, medial intercondylar eminence; MM, medial malleolus; MTT, medial tibial tuberosity; PN, popliteal notch; TCT, tibial crest; TTG, tibial tuberosity groove. Scale bar = 10 cm.

lar surface for the astragalus. Depressions for the astragalar trochlea are slanted from anterolateral to posteromedial and are separated by a raised ridge that appears to be pinched anteroposteriorly. Posteromedially to this articular surface is the medial malleolus, which is the distal-most point of the tibia. On the lateral surface, there is a small, domed articular surface for the fibula that contacts the astragalar facet along its distal edge. A triangle of rugose bone extends proximal to the fibular facet to form a tighter articulation with the fibula. A ridge connects the proximal and distal fibular facets as it runs the length of the diaphysis, including the lateral projection that matches the medial protuberance of the fibula.

Fibula.—Fibulae have rugose ends with an

Figure 63. Left fibula of ETMNH 609 flipped to appear as right. Views: A, lateral; B, medial. Abbreviations: ASA, articular surface for astragalus; AST1–2, articular surfaces for tibia 1–2; LML, lateral malleolus. Scale bar = 10 cm.

anteroposteriorly compressed proximal end of the diaphysis and a triangular distal end of the diaphysis with rounded angles (Fig. 63). The proximal articulation site for the tibia is shaped like an upside-down teardrop, whereas the distal articulation site is semi-circular. A small, round articular surface is present on the distal lateral malleolus for articulation with the astragalus. It is continuous with the corresponding distolateral articular facet on the tibia. A ridge curves from the proximal posterolateral articulation site to the distolateral articulation site. Along this ridge, there is a small protuberance that, when articulated with the tibia, is only slightly distal to a corresponding projection on the lateral side of the tibial diaphysis. The fibulae of ETMNH 601 are proximally fused to the tibiae as seen in some species of *Teleoceras* (Prothero, 2005).

Calcaneum.—The calcaneum is the largest of the tarsal bones (Figs. 64, 65). It is important to note that the articular surfaces of the calcanea display a large amount of variation in their size and shape. Heavily rugose bone covers the distal end of the calcaneal tuber and forms a ridge along the lateral surface of the diaphysis, which appears compressed mediolaterally. On the medial surface, the sustentaculum is prominent and rugose with only a slight tendon groove. A dorsal, roughly rounded articular surface for the astragalus is present on the sustentaculum. Lateral to the sustentaculum is a second articular surface for the astragalus. This facet is ovate, slants toward the sustentaculum, and is depressed along a mediolateral fold. The lateral edge of this articular surface folds over into a variably-shaped fibular articular surface. There is a small knob of rugose bone lateral to the fibular facet. On the medial side of the proximal process, there is a small facet that articulates with the astragalus. This facet folds into the oval articular surface for the cuboid on the plantar side of the calcaneum.

Astragalus.—The proximal side of the astragalus forms a trochlea that provides the articular surface for the tibia (Figs. 64, 66). The larger, lateral portion of the trochlea extends more proximally than the smaller, medial portion. A wide trochlear groove separates the lateral and medial portions of the trochlea. The articular surface of the lateral trochlea folds posterolaterally to form a second proximal articular surface that, with the calcaneum, contributes to an articular surface for the fibula. The astragalar base is distal to the trochlea and has two articular surfaces separated by a raised ridge. Medially, there is a square surface with rounded medial corners for articulation with the navicular. The lateral articular surface for the cuboid is rectangular with the long axis oriented anteroposteriorly, is nearly flat at the level of the ridge formed with the medial articular surface, and folds proximolaterally. On the posterior surface of the astragalus, there is an oval articular surface for

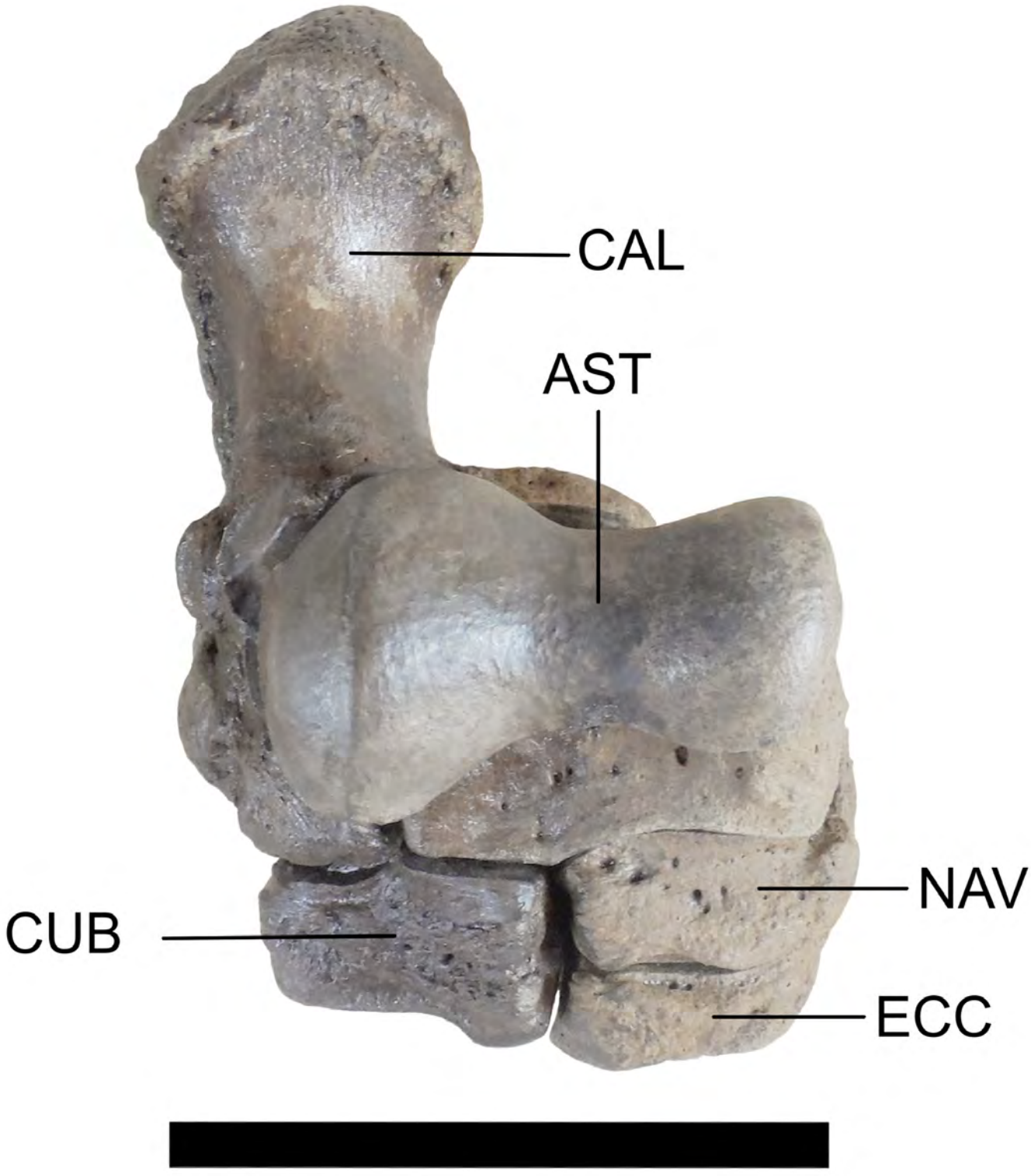

Figure 64. Articulated right tarsal bones of ETMNH 609 in anterior view. Abbreviations: AST, astragalus; CAL, calcaneum; CUB, cuboid; ECC, ectocuneiform; NAV, navicular. The mesocuneiform and entocuneiform are not visible in this view. Scale bar = 10 cm.

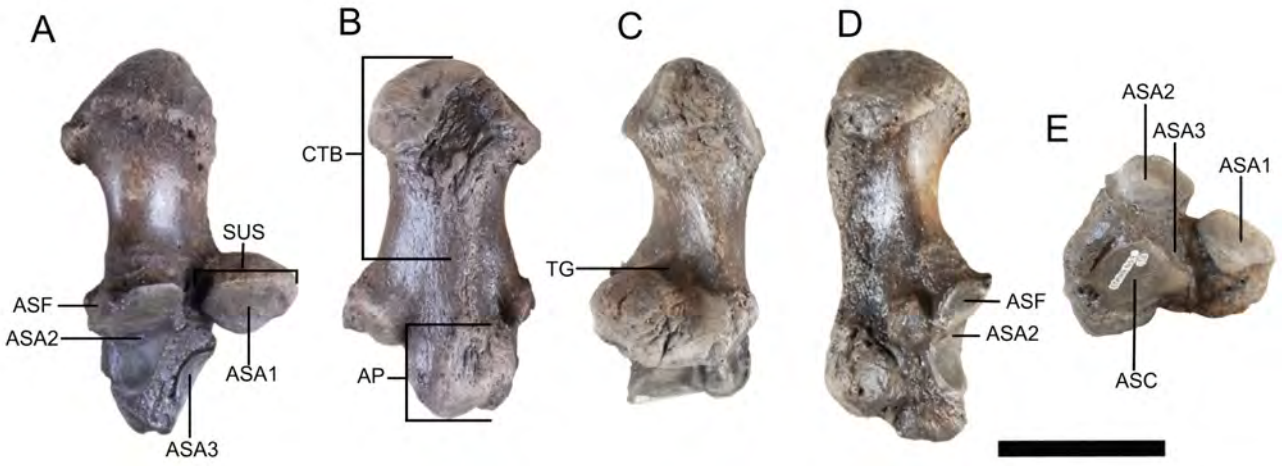

Figure 65. Right calcaneum of ETMNH 609. Views: A, dorsal; B, ventral; C, medial; D, lateral; E, distal. Abbreviations: AP, anterior process; ASA1–3, articular surfaces for astragalus 1–3; ASC, articular surface for cuboid; ASF, articular surface for fibula; CTB, calcaneal tuber; SUS, sustentaculum; TG, tendon groove. Scale bar = 5 cm.

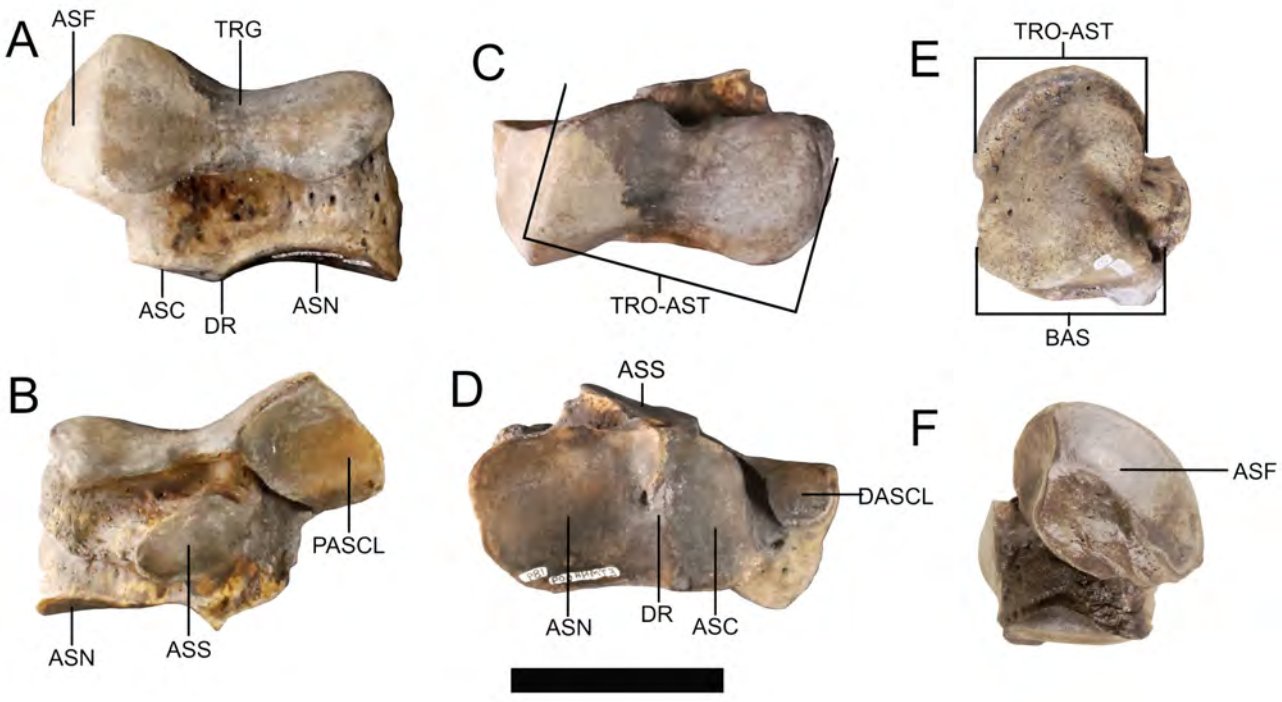

Figure 66. Left astragalus of ETMNH 609 flipped to appear as right. E and F are the right astragalus of the same specimen. Views: A, anterior; B, posterior; C, proximal; D, distal; E, medial; F, lateral. Abbreviations: ASC, articular surface for cuboid; ASF, articular surface for fibula; ASN, articular surface for navicular; ASS, articular surface for sustentaculum; AST, articular surface for tibia; BAS, base; DASCL, distal articular surface for calcaneum; DR, distal ridge; PASCL, proximal articular surface for calcaneum; TRG, trochlear groove; TRO, trochlea. Scale bar = 5 cm.

the sustentaculum of the calcaneum that is positioned superior to the midpoint of the base and inferior to the trochlear groove. Laterally, there is a large, oblong articular surface for the calcaneum proximolateral to the astragalar base.

Navicular.—In general, the navicular is a square bone and is compressed proximodistally (Figs. 64, 67). One articular surface for the astragalus covers nearly the entire proximal side. This surface slants from the posteromedial corner to the anterolateral corner. At its anterolateral corner, this articular surface folds into a small, lateral articular surface for the cuboid. There is another small, round articular surface on the posterolateral side that forms a second articulation with the cuboid. The two lateral articular surfaces are separated by a depression, but both form an edge with the distal articular surface. There is a small medial protuberance on the posterior surface with a small, round, distal articular surface for the entocuneiform. Distally, the smaller, round, medial articular surface for the mesocuneiform is separated from the larger, triangular, lateral articular surface for the ectocuneiform by a slight ridge. There is a concavity on the lateral edge of the ectocuneiform articular surface that corresponds to the depression between the lateral cuboid articular surfaces.

Cuboid.—This bone is compressed proximodistally but is elongated anteroposteriorly (Figs. 64, 68). A nearly triangular portion extends into a posterior, rugose process with a distal curvature. On the medial side of the posterior process, there

Figure 67. Right navicular of ETMNH 609. Views: A, anterior; B, posterior; C, proximal; D, distal; E, medial; F, lateral. Abbreviations: ASA, articular surface for astragalus; ASC1–2, articular surfaces for cuboid 1–2; ASEC, articular surface for ectocuneiform; ASEN, articular surface for entocuneiform; ASM, articular surface for mesocuneiform; MPT, medial process. Scale bar = 5 cm.

is a single anteromedial articular surface divided into two semi-circular facets. The proximal surface articulates with the navicular and the distal articulates with the ectocuneiform. Two articular surfaces are present on the proximal surface of the anterior portion; both are triangular and are divided by a ridge. The medioproximal articular surface articulates with the astragalus and the lateroproximal articular surface articulates with the calcaneum. A small, proximal articular surface for the navicular is on the medial surface of the anterior portion. Distal to this facet is a domed articular surface for articulation with the ectocuneiform. This facet folds onto the distal surface into two articular surfaces that are separated by a slight ridge. The smaller medial articular surface for the third metatarsal is a slender rectangle with the long axis oriented anterolateral to posteromedial. Laterally, a larger, triangular articular surface is present for articulation with the fourth metatarsal.

Entocuneiform.—This is a small, rugose bone that curves distolaterally (Fig. 69). An oval anterolateral surface articulates with the mesocuneiform and a small round proximal surface articu-

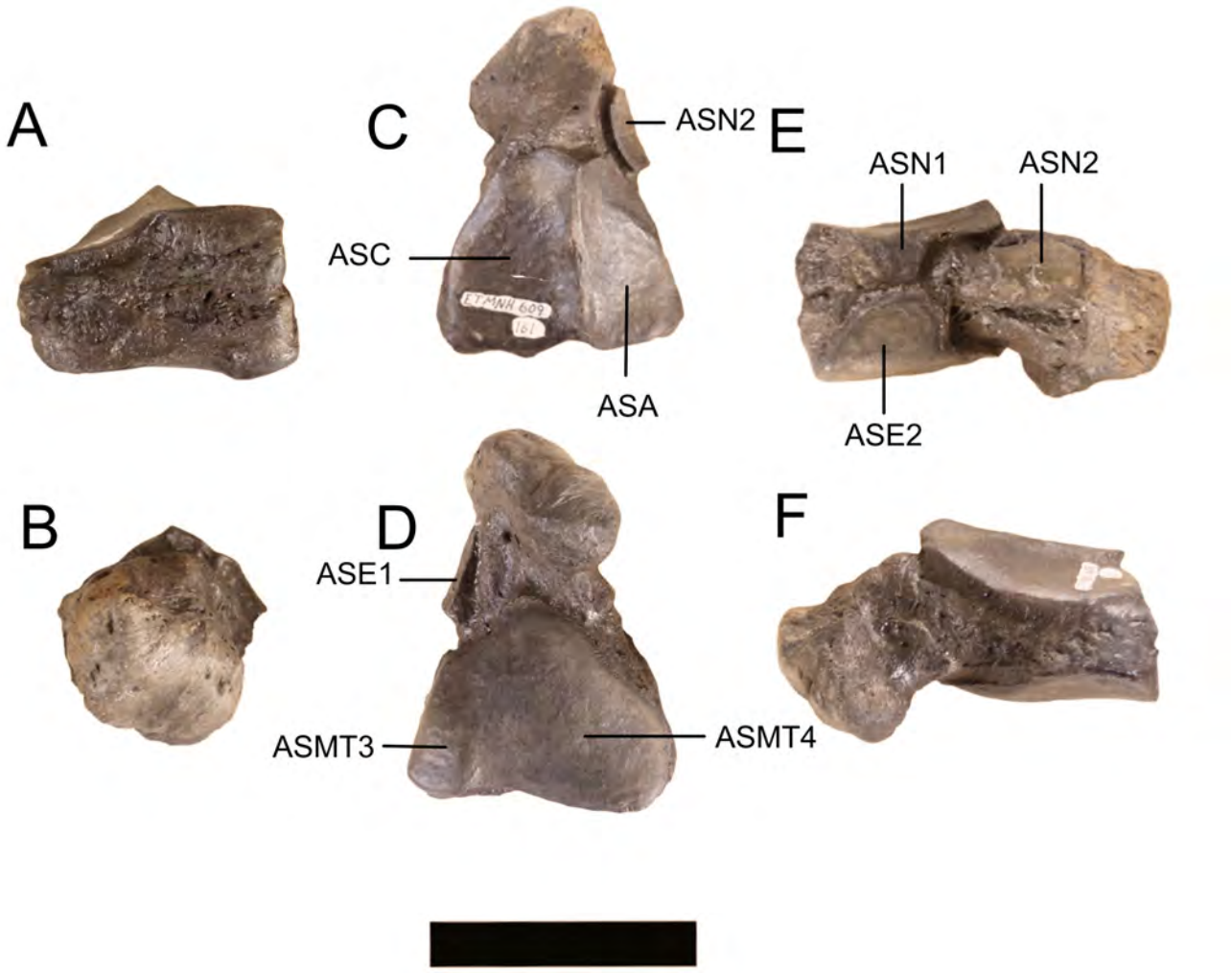

Figure 68. Right cuboid of ETMNH 609. Views: A, anterior; B, posterior; C, proximal; D, distal; E, medial; F, lateral. Abbreviations: ASA, articular surface for astragalus; ASC, articular surface for cuboid; ASN1–2, articular surfaces for navicular 1–2; ASE1–2, articular surface for ectocuneiform 1–2; ASMT3, articular surface for third metacarpal; ASMT4, articular surface for fourth metacarpal. Scale bar = 5 cm.

lates with the navicular.

Mesocuneiform.—A rugose knob is present on the anteromedial face of the mesocuneiform (Fig. 70). The mesocuneiform proximally articulates with the navicular and distally with the second metatarsal. From the distal articular surface, the lateral edge folds proximally into an articular surface for the ectocuneiform. Also from the distal articular surface, the posteromedial edge folds proximally into an articular surface for the entocuneiform. Articular surfaces of the mesocuneiform are extremely variable in size and shape.

Ectocuneiform.—A raised, rugose knob is present on the anterior surface of the ectocuneiform (Figs. 64, 71). There is a concavity just posterior to the midpoint on the lateral edge that corresponds to the concavity on the lateral edge of the navicular. Proximally, there is one articular surface for the navicular that covers nearly the entire surface and has both the posterior and medial corners turned proximally. On the posterior portion of the proximal surface, an edge is formed with the slender, elongate, lateral articular surface for the cuboid. There is a small, semi-circular articular surface on the posteromedial edge for articulation with the mesocuneiform. This articular surface folds distally into a rectangular articular surface for articulation with the second metatarsal. The articular surface for the second metatarsal forms a lateral edge with the distal, triangular articular surface for the third metatarsal. On the lateral edge, this distal articular surface forms an anterolateral edge with a second, round articular surface for the cuboid. On the ectocuneiforms of ETMNH 601, the more anterior of the two cuboid articulations is also in contact with the proximal navicular articular surface.

Second Metatarsal.—There is a small rugose prominence on the anterolateral side of the distal end and a second rugose knob on the posterior surface (Fig. 72). Three articular surfaces are present on the proximal end of the second metatarsal. Medially, there is a round articular surface for the mesocuneiform. This facet forms a medial edge with a posteriorly rounded, rectangular proximolateral articular surface for the ectocuneiform. On the lateral side of the proximal end, the ectocunei-

Figure 69. Right entocuneiform of ETMNH 609. Views: A, anterolateral; B, posteromedial. Abbreviations: ASM, articular surface for mesocuneiform; ASN, articular surface for navicular. Scale bar = 1 cm.

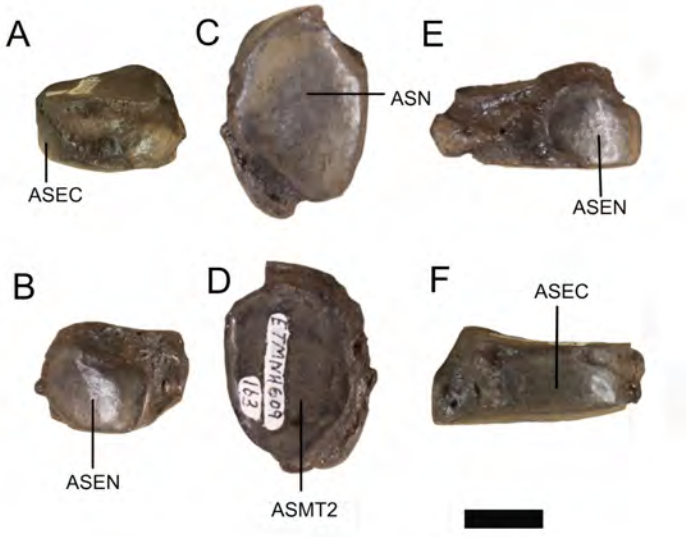

Figure 70. Right mesocuneiform of ETMNH 609. Views: A, anterior; B, posterior; C, proximal; D, distal; E, medial; F, lateral. Abbreviations: ASEC, articular surface for ectocuneiform; ASEN, articular surface for entocuneiform; ASMT2, articular surface for second metatarsal; ASN, articular surface for navicular. Scale bar = 1 cm.

Figure 71. Right ectocuneiform of ETMNH 609. Views: A, anterior; B, posteromedial; C, proximal; D, distal; E, medial; F, lateral. Abbreviations: ASC1–2, articular surfaces for cuboid 1–2; ASM, articular surface for mesocuneiform; ASMT2, articular surface for second metatarsal; ASMT3, articular surface for third metatarsal; ASN, articular surface for navicular. Scale bar = 5 cm.

form facet forms an edge with a small, triangular articular surface for the third metatarsal. Distally, the anterior articular surface for the proximal phalanx is smooth and angled distomedially from the anterolateral prominence. On the posterior surface, the distal articular surface is divided into two facets by the intermediate relief, which is aligned with medial rugose bone along the posterior surface. The facets slant proximomedially and each articulates with a sesamoid.

Third Metatarsal.—The proximal end is positioned slightly posterior to the distal creating the slant seen in the articulated pes (Fig. 73). Nutrient foramina are near the anterior and posterior midpoints on the third metatarsals. On the proximomedial surface, a slender articular surface extends anteroposteriorly for the second metatarsal. The proximal edge of this surface contacts the larger, rectangular proximolateral articular surface for the ectocuneiform. A raised ridge occurs between the proximolateral articular surface and the narrow, proximomedial articular facet for the cuboid. On the lateral side of the proximal end, there is

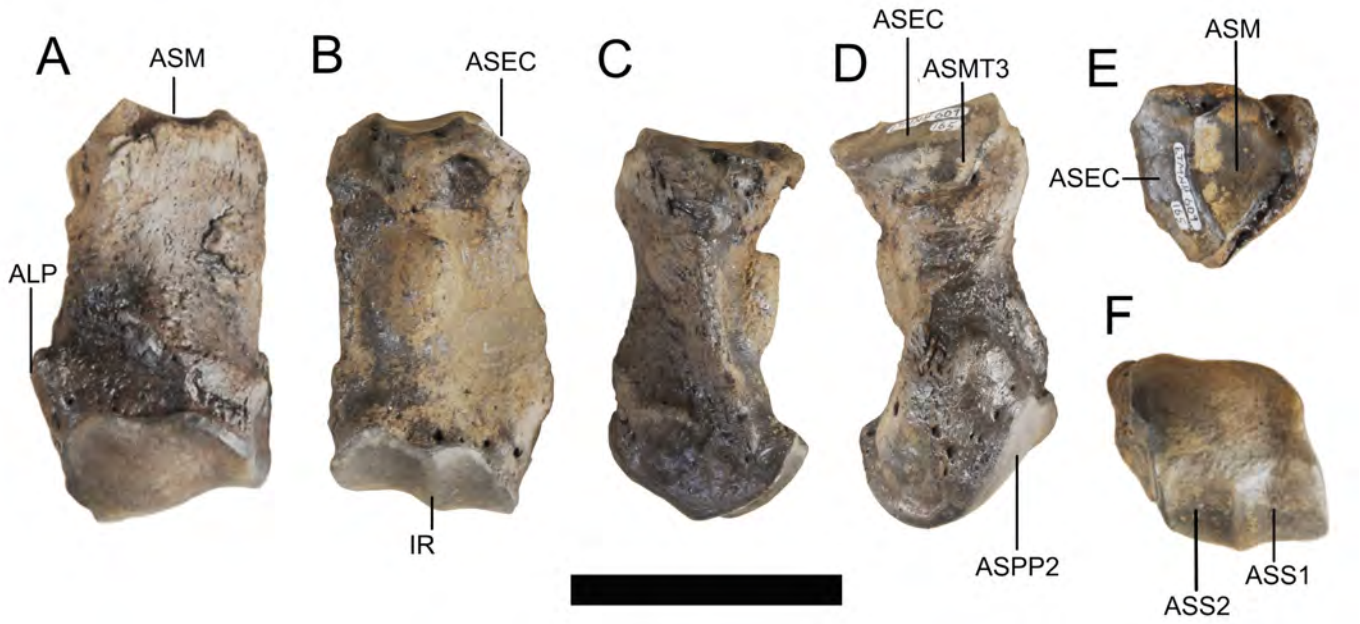

Figure 72. Right second metatarsal of ETMNH 609. Views: A, anterior; B, posterior; C, medial; D, lateral; E, proximal; F; distal. Abbreviations: ALP, anterolateral process; ASEC, articular surface for ectocuneiform; ASM, articular surface for mesocuneiform; ASMT3, articular surface for third metatarsal; ASPP2, articular surface for proximal phalanx of second digit; ASS1–2, articular surfaces for sesamoids 1–2; IMR, intermediate relief. Scale bar = 5 cm.

Figure 73. Right third metatarsal of ETMNH 609. Views: A, anterior; B, posterior; C, medial; D, lateral; E, proximal; F, distal. Abbreviations: ASC, articular surface for cuboid; ASEC, articular surface for ectocuneiform; ASMT2, articular surface for second metatarsal; ASMT4, articular surface for fourth metatarsal; ASPP3, articular surface for proximal phalanx of the third digit; ASS1–2, articular surfaces for sesamoids 1–2; IR, intermediate relief; NF, nutrient foramen. Scale bar = 5 cm.

an articular surface for the fourth metatarsal that has two rounded portions—anterior and posterior. A straight proximal edge contacts the lateral edge of the proximal cuboid articular facet. At the distal end of the third metatarsal, paired, round rugosities are on the anterior surface and extend distally around their respective edges forming rugosities on either side. There is no distinct ridge along the midline of the posterior side of the diaphysis as on metapodials of other species, but there is a slight pair of depressions proximal to the distal facets. The anterior articular surface for the proximal phalanx is smooth and domed proximally with edges that are variable in shape. Posteriorly, an intermediate relief that is slanted slightly laterally as it extends proximally separates the distal articular surface into two facets that each articulate with one sesamoid.

Fourth Metatarsal.—The lateral edges of the fourth metatarsals appear pinched anteroposteriorly (Fig. 74), and ETMNH 609 has a slight inward curvature that is more pronounced than that of ETMNH 601. On the posterior surface, there is a rugose bump at the proximal end along the midline of the diaphysis. Only two articular surfaces are on the proximal end of the fourth metatarsal. A slightly depressed triangular facet covers the proximal surface for articulation with the cuboid. The straight medial edge of this facet forms an edge with the medial articular surface for the third metatarsal. This facet consists of two rounded portions—anterior and posterior. The posterior portion forms a process that extends posteriorly, and the anterior articular surface, which articulates with the proximal phalanx, is smooth and domed proximally with a slant from proximomedial to distolateral. An intermediate relief divides the posterior articular surface of the distal end into two facets that each articulate with one sesamoid.

Phalanges and Sesamoids

Because the phalanges and sesamoids of the

manus and pes are so similar (Fig. 58), they will be described together. Phalanges and sesamoids of the second and fourth digits are larger in the manus than in the pes. In the third digits, the phalanges and sesamoids of the manus are approximately the same sizes as those in the pes. Typical of *Teleoceras*, the phalanges are compressed so the second and fourth digits are longer than the third to support the digitigrade splay of the manus and pes. In the manus and pes, the third digit is the most compressed. It is important to note that, on the second digit of the left pes of ETMNH 601, the phalanges are pathological so that the distal and medial phalanges are completely fused and the proximal phalanx is remodeled (Fig. 75).

Proximal Phalanges.—Phalanges of the second and fourth digits are nearly mirror images of each other and are blocky with heavy rugosities on the non-articular surfaces (Fig. 76). Distally, these phalanges slope anteriorly so that the posterior edge is positioned superior to the anterior edge. Shapes of the articular surfaces are variable within and between individuals; proximal articular surfaces vary between round and square whereas distal articular surfaces are more ovate with a small concavity in the center and a notch on the posterior edge. Proximal phalanges of the third digits are more compressed anteroposteriorly but wider mediolaterally.

Medial Phalanges.—Medial phalanges are much more compressed than the proximal phalanges and have rugosities present on every non-articular surface (Fig. 77). However, like with the proximal phalanges, the medial phalanges of the second and fourth digits are nearly mirror images of each other. In anterior view, these phalanges are domed proximally. Like with the proximal phalanges, the shapes of the articular surfaces are variable within and between individuals; proximal articular surfaces are more ovate whereas the distal articular surfaces are convex anterior to posterior and just barely curve over the anterior edges. Medial phalanges of the third digits are more compressed than those of the second and fourth digits.

Distal Phalanges.—All of the distal phalanges are rugose and porous to allow blood vessels

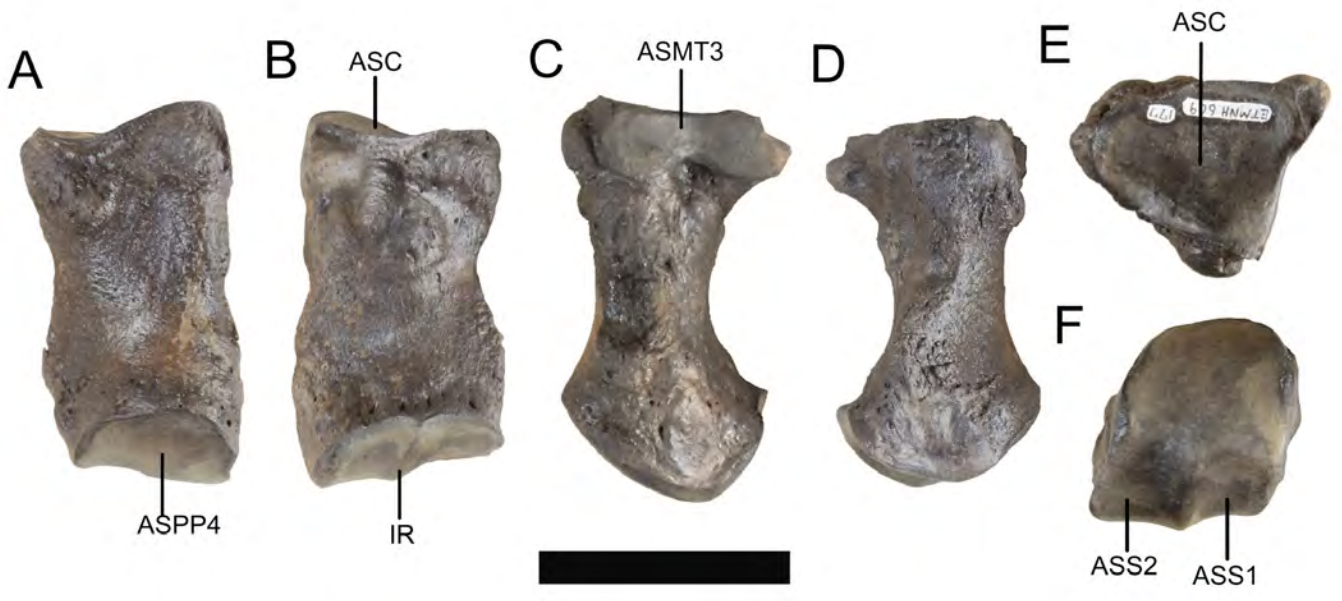

Figure 74. Right fourth metatarsal of ETMNH 609. Views: A, anterior; B, posterior; C, medial; D, lateral; E, proximal; F, distal. Abbreviations: ASC, articular surface for cuboid; ASMT3, articular surface for third metatarsal; ASPP4, articular surface for proximal phalanx of digit four; ASS1–2, articular surfaces for sesamoids 1–2; IR, intermediate relief. Scale bar = 5 cm.

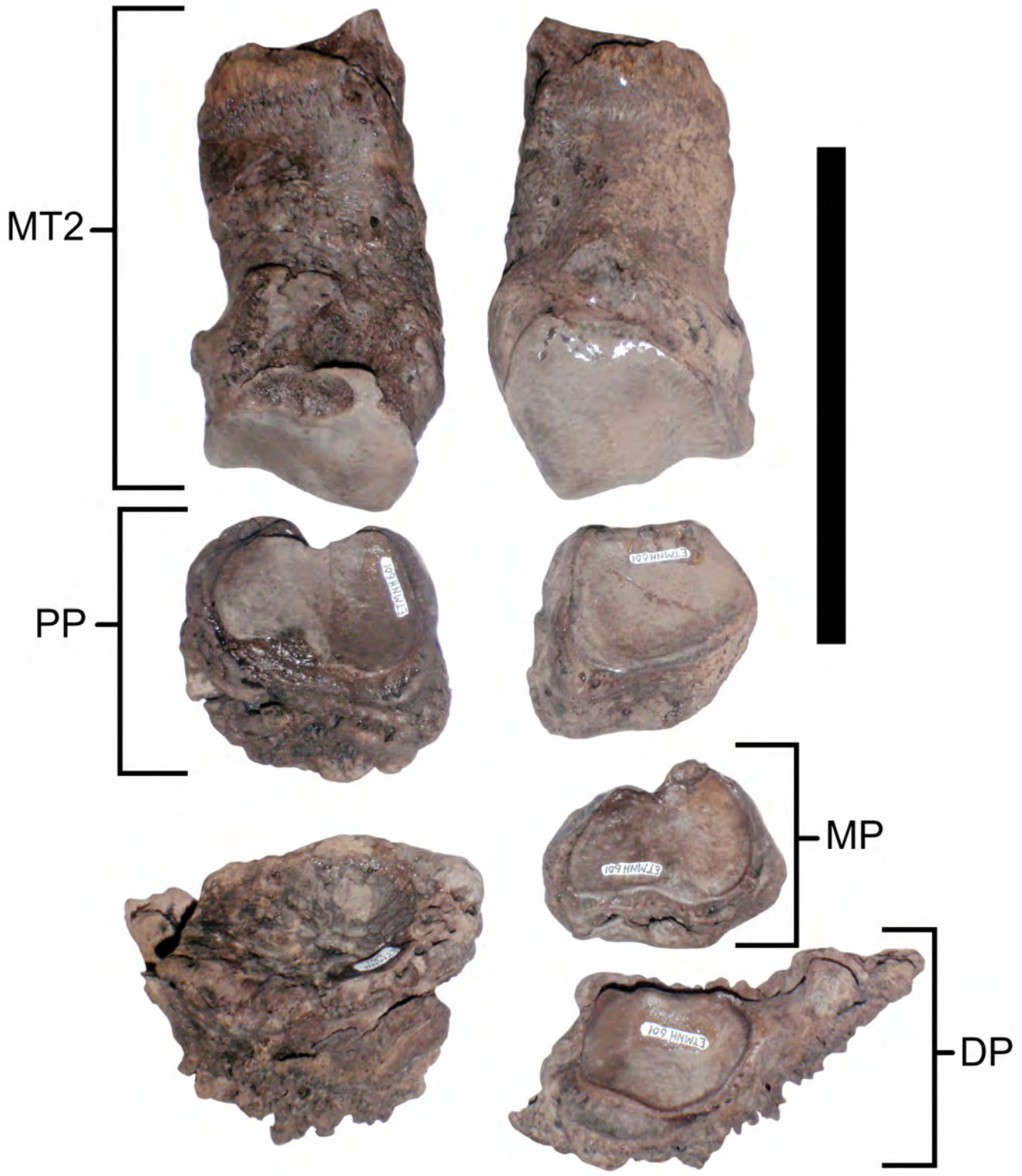

Figure 75. Pathological phalanges of the left hind second digit of ETMNH 601 with healthy phalanges of the right hind second digit. Notice that the left medial and distal phalanges are fused together. Abbreviations: DP, distal phalanx; MP, medial phalanx; PP, proximal phalanx; MT2, second metatarsal. Scale bar = 10 cm.

Figure 76. Proximal phalanges of the right manus of ETMNH 609. Views: A, anterior; B, posterior; C, proximal; D, distal. Abbreviations: II, second digit; III, third digit; IV, fourth digit. Scale bar = 5 cm.

to reach the hoof structure (Fig. 78; Engiles et al., 2015). Distal phalanges of the second and fourth digits arc medially and laterally, respectively, and narrow to a point giving them a triangular appearance. Shapes of the proximal articular surfaces are variable within and between individuals, but tend to be round to ovate and slightly raised along the anterior edge.

Sesamoids.—All of the sesamoids are rugose bones with concave articular surfaces for articulation with the metapodials (Fig. 79).

DISCUSSION

The occurrence of *Teleoceras aepysoma* in the Appalachian Mountains is unique within a genus typically found in the Great Plains (Prothero, 2005).

Figure 77. Medial phalanges of the right manus of ETMNH 609. Views: A, anterior; B, posterior; C, proximal; D, distal. Abbreviations: II, second digit; III, third digit; IV, fourth digit. Scale bar = 5 cm.

It is possible this unusual habitat contributed to the atypical morphology. For example, though the GFS population has many of the characters previously described as typical of *Teleoceras*, it lacks features that can now no longer be used as synapomorphies for the genus (Table 3). Specifically, *Teleoceras aepysoma* exhibits, as adults: unfused nasals without a nasal horn and a less rotund body with longer, more gracile limbs. Limb elements of *Teleoceras aepysoma* are considerably elongated, which is noteworthy in a genus characterized by "short, robust limbs" (Prothero, 2005:94). Elongated limb bones during the late Hemphillian are also in contrast to the trend toward an increased "shortening and stumpiness" of *Teleoceras* limbs postulated by Prothero (2005:207; Fig. 80). These proportional differences are accompanied by other skeletal and dental characters that differentiate the GFS taxon and warrant the designation of a new species of *Teleoceras*. There are also unusual characters that are not true apomorphies, such as the presence of fifth metacarpals on ETMNH 601 and p2s on ETMNH 609 and 21659.

Difficulties encountered while trying to clas-

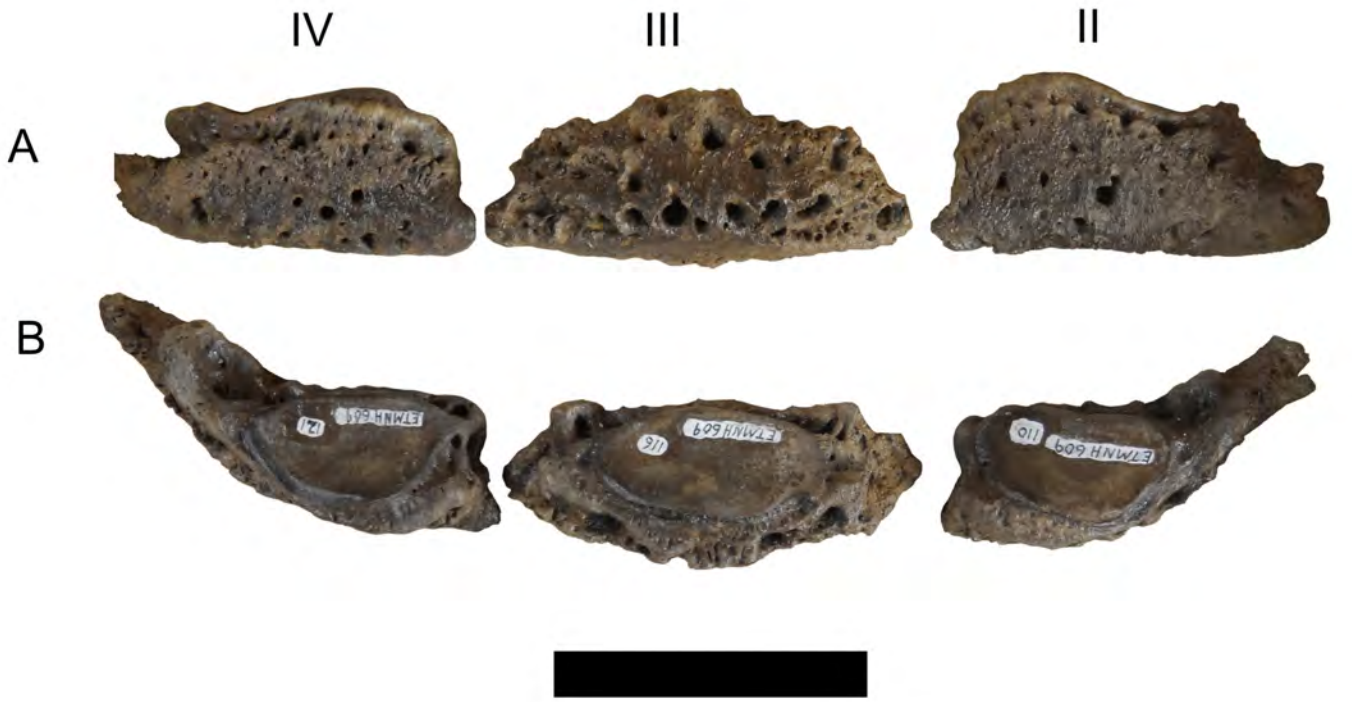

Figure 78. Distal phalanges of the right manus of ETMNH 609. Views: A, anterior; B, proximal. Abbreviations: II, second digit; III, third digit; IV, fourth digit. Scale bar = 5 cm.

Figure 79. Posterior view of sesamoids articulated with the fourth metacarpal. Scale bar = 5 cm.

sify *Teleoceras aepysoma* make it clear that the genus *Teleoceras* should be revised. For instance, Prothero (2005:94) describes the nasal incision as "retracted to anterior P3" as a Teleoceratini synapomorphy, but this feature appears to be defined incorrectly because most, if not all, *Teleoceras* crania, including those from the GFS, have a nasal incision that extends posterior to the P3. The presence of the GFS population illustrates the wide-degree of genus-level variation and brings attention to the necessity of reexamining previously known populations for similarly variable character states. Because of the small sample size of the GFS specimens, no robust statistical analyses were performed. These analyses will be possible following further excavation of the site and recovery of additional elements.

Although Madden and Dalquest (1990:266) discussed potentially "the last rhinoceros in North America" from Blancan sediments in Texas, this is only a small, isolated tooth fragment identified as *Teleoceras* based on size, and it is possible that

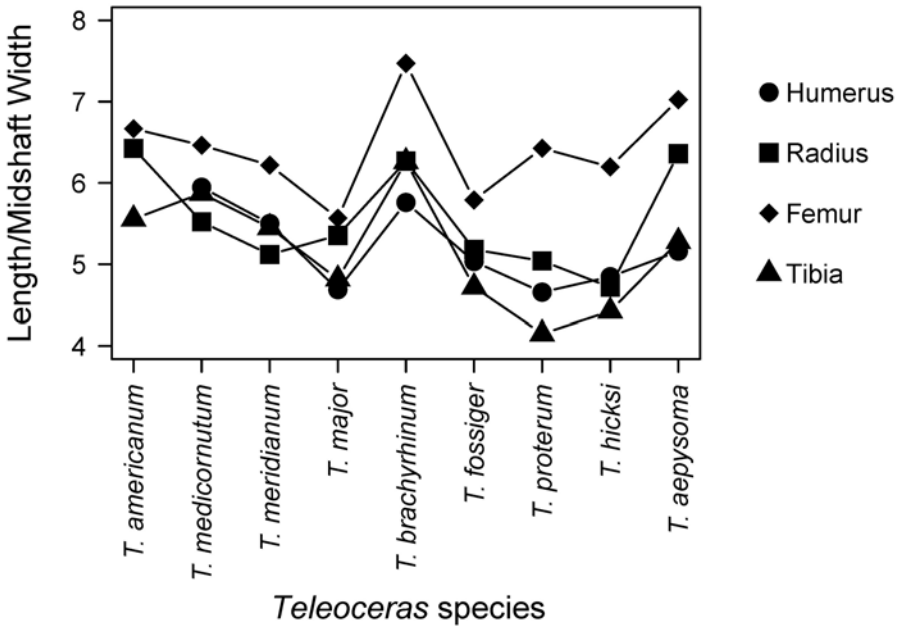

Figure 80. Ratios of length to midshaft width of humerus, radius, femur, and tibia. Except *Teleoceras aepysoma*, all measurements are from Prothero (2005). *Teleoceras guymonense* is excluded because of lack of data.

it may have been reworked (Prothero, 2005). Gustafson (2012) made similar claims about an early Blancan *Teleoceras* tooth from Washington with similar reworking potential. Until more material is found, these specimens do not justify extending the temporal range of *Teleoceras* beyond the end of the Hemphillian. Therefore, the Gray Fossil Site can be added to the latest Hemphillian localities that contain the last of the North American rhinos: the Mount Eden Fauna of California, USA; the Yepómera (Rincon) Fauna of Chihuahua, Mexico; the Rancho El Ocote Fauna of Guanajuato, Mexico; and the Palmetto Fauna of Florida, USA (Tedford et al., 2004; Webb et al., 2008).

ACKNOWLEDGEMENTS

The authors would like to thank the numerous museum staff, students, and volunteers who were involved in this work from the discovery of the fossils to the publication of this manuscript. We thank J. Mead and B. Schubert for their comments on a previous version of this manuscript. A. Joyner provided an initial map, and B. Compton, S. Haugrud, and A. Nye provided research assistance at the Gray Fossil Site. Additionally, we are especially grateful for the access provided to museum collections by J. Galkin (AMNH), R. Hulbert (FLMNH), C. Ito (NMNH), L. Ivy (DMNS), and L. Wilson (FHSM). Finally, the authors thank K. Jansky, L. Burns, S. Cox, and J. Martin for their support of this research. This research was supported by a National Science Foundation grant to S. Wallace and B. Schubert (EAR-0958985), the ETSU Office of Research and Sponsored Programs, the ETSU Department of Geosciences, and the Don Sundquist Center of Excellence in Paleontology.

LITERATURE CITED

Anderson, J. F., A. Hall-Martin, and D. A. Russell. 1985. Long-bone circumference and weight in mammals, birds and dinosaurs. Journal of Zoology 207:53–61.

Barone, R. 1999. Anatomie Comparée des Mammifères Domestiques, Tome 1: Osteologie.

Vigot Freres, Paris, 761 pp.

Christiansen, P. 2002. Locomotion in terrestrial mammals: the influence of body mass, limb length and bone proportions on speed. Zoological Journal of the Linnean Society 136(4):685–714.

Cook, H. J. 1927. A new rhinoceros of the genus *Teleoceras* from Colorado. Proceedings of the Colorado Museum of Natural History 7:1–5.

Cope, E. D. 1878. Descriptions of new extinct Vertebrata from the upper Tertiary and Dakota Formations. Bulletin of the US Geological and Geographical Survey of the Territories, 4:379–396.

DeSantis, L. R. G., and S. C. Wallace. 2008. Neogene forests from the Appalachians of Tennessee, USA: geochemical evidence from fossil mammal teeth. Palaeogeography, Palaeoclimatology, Palaeoecology 266:59–68.

Dinerstein, E. 1991. Sexual dimorphism in the greater one-horned rhinoceros (*Rhinoceros unicornis*). Journal of Mammalogy 72(3):450–457.

Doughty, E. M., S. C. Wallace, B. W. Schubert, and L. M. Lyon. 2018. First occurrence of the enigmatic peccaries *Mylohyus elmorei* and *Prosthennops serus* from the Appalachians: latest Hemphillian to early Blancan of Gray Fossil Site, Tennessee. PeerJ 6:e5926.

Engiles, J. B., H. L. Galantino-Homer, R. Boston, D. McDonald, M. Dishowitz, and K. D. Hankenson. 2015. Osteopathology in the equine distal phalanx associated with the development and progression of laminitis. Veterinary Pathology 52(5):928–944.

Farlow, J. O., J. A. Sunderman, J. J. Havens, A. L. Swinehart, J. A. Holman, R. L. Richards, N. G. Miller, R. A. Martin, R. M. Hunt Jr., G. W. Storrs, B. B. Curry, R. H. Fluegeman, M. R. Dawson, and M. E. T. Flint. 2001. The Pipe Creek Sinkhole biota, a diverse late Tertiary continental fossil assemblage from Grant County, Indiana. American Midland Naturalist 145(2):367378.

Flower, W. G. 1876. On some cranial and dental characters of the existing species of rhinoceroses. Proceedings of the Scientific Meetings of the Zoological Society of London 44(1):443–457.

Garutt, N. V. 1994. Dental ontogeny of the woolly rhinoceros *Coelodonta antiquitatis* (Blumenbach, 1799). Cranium 11(1):37–48.

Gustafson, E. P. 2012. New records of rhinoceroses from the Ringold Formation of central Washington and the Hemphillian-Blancan boundary. Journal of Vertebrate Paleontology 32(3):727–731.

Harrison, J. A., and E. M. Manning. 1983. Extreme carpal variability in *Teleoceras* (Rhinocerotidae, Mammalia). Journal of Vertebrate Paleontology 3(1):58–64.

Hatcher, J. B. 1894. A median horned rhinoceros from the Loup Fork Beds of Nebraska. The American Geologist 13(3):149–150.

Heller, E. 1914. The White Rhinoceros: With Thirty-One Plates, Volume 61. Smithsonian Institution, Washington DC, 77 pp.

Hermanson, J. W., and B. J. MacFadden. 1992. Evolutionary and functional morphology of the shoulder region and stay-apparatus in fossil and extant horses (Equidae). Journal of Vertebrate Paleontology 12(3):377–386.

Hermanson, J. W., and B. J. MacFadden. 1996. Evolutionary and functional morphology of the knee in fossil and extant horses (Equidae). Journal of Vertebrate Paleontology 16(2):349–357.

Hitchins, P. M. 1978. Age determination of the black rhinoceros (*Diceros bicornis* Linn.) in Zululand. South African Journal of Wildlife Research 8(2):71–80.

Hulbert Jr., R. C., and F. C. Whitmore Jr. 2006. Late Miocene mammals from the Mauvilla Local Fauna, Alabama. Bulletin of the Florida Museum of Natural History 46(1):1–28.

Hulbert Jr., R. C., S. C. Wallace, W. E. Klippel, and P. W. Parmalee. 2009. Cranial morphology and systematics of an extraordinary sample of the late Neogene dwarf tapir, *Tapirus polkensis* (Olsen). Journal of Paleontology 83(2):238–262.

Leidy, J. 1865. [Descriptions of *Rhinoceros meridianus* and *R. hesperius*.] Proceedings of the Academy of Natural Sciences of Philadelphia

17(4):176–177.

Leidy, J. 1885. *Rhinoceros* and *Hippotherium* from Florida. Proceedings of the Academy of Natural Sciences of Philadelphia 37:32–33.

MacFadden, B. J., and R. C. Hulbert Jr. 1990. Body size estimates and size distributions of ungulate mammals from the Late Miocene Love Bone Bed of Florida. Pp. 337–363 *in* J. Damuth, and B. J. MacFadden (eds.), Body Size in Mammalian Paleobiology: Estimation and Biological Implications. Cambridge University Press, Cambridge, United Kingdom.

Madden, C. T., and W. W. Dalquest. 1990. The last rhinoceros in North America. Journal of Vertebrate Paleontology 10(2):266–267.

McFadyean, J. 1908. The Comparative Anatomy of the Domesticated Animals, Part 1: Osteology and Arthrology. William R. Jenkins Co., New York, 208 pp.

Mead, A. J. 2000. Sexual dimorphism and paleoecology in *Teleoceras*, a North American Miocene rhinoceros. Paleobiology 26(4):689–706.

Mead, J. I., B. W. Schubert, S. C. Wallace, and S. L. Swift. 2012. Helodermatid lizard from the Mio-Pliocene oak-hickory forest of Tennessee, eastern USA, and a review of monstersaurian osteoderms. Acta Palaeontologica Polonica 57(1):111–121.

Mihlbachler, M. C. 2003. Demography of late Miocene rhinoceroses (*Teleoceras proterum* and *Aphelops malacorhinus*) from Florida: linking mortality and sociality in fossil assemblages. Paleobiology 29(3):412–428.

Ochoa, D., M. Whitelaw, Y.-S. Liu, and M. Zavada. 2012. Palynology of Neogene sediments at the Gray Fossil Site, Tennessee, USA: floristic implications. Review of Palaeobotany and Palynology 184:36–48.

Ochoa, D., M. S. Zavada, Y. Liu, and J. O. Farlow. 2016. Floristic implications of two contemporaneous inland upper Neogene sites in the eastern US: Pipe Creek Sinkhole, Indiana, and the Gray Fossil Site, Tennessee (USA). Palaeobiodiversity and Palaeoenvironments 96(2):239–254.

Osborn, H. F. 1898a. The extinct rhinoceroses. Memoirs of the American Museum of Natural History 2(3):75–164.

Osborn H. F. 1898b. A complete skeleton of *Teleoceras*, the true rhinoceros from the upper Miocene of Kansas. Science 7:554–557.

Osborn, H. F. 1904. New Miocene rhinoceroses with revision of known species. Bulletin of the American Museum of Natural History 20(27):307–326.

Parmalee, P. W., W. E. Klippel, P. A. Meylan, and J. A. Holman. 2002. A late Miocene-early Pliocene population of *Trachemys* (Testudines: Emydidae) from East Tennessee. Annals of Carnegie Museum 71(4):233–239.

Prothero, D. R. 1998. Rhinocerotidae. Pp. 595–605 *in* C. M. Janis, K. M. Scott, and L. L. Jacobs (eds.), Evolution of Tertiary Mammals of North America, Volume 1: Terrestrial Carnivores, Ungulates, and Ungulate-like Mammals. Cambridge University Press, Cambridge, United Kingdom.

Prothero, D. R. 2005. The Evolution of North American Rhinoceroses. Cambridge University Press, Cambridge, United Kingdom, 218 pp.

R Core Team. 2016. R: A language and environment for statistical computing. R Foundation for Statistical Computing, Vienna, Austria. Available at https://www.r-project.org/

Samuels, J. X., K. E. Bredehoeft, and S. C. Wallace. 2018. A new species of *Gulo* from the early Pliocene Gray Fossil Site (Eastern United States); rethinking the evolution of wolverines. PeerJ 6:e4648.

Shunk, A. J., S. G. Driese, and G. M. Clark. 2006. Latest Miocene to earliest Pliocene sedimentation and climate record derived from paleosinkhole fill deposits, Gray Fossil Site, northeastern Tennessee, USA. Palaeogeography, Palaeoclimatology, Palaeoecology 231:265–278.

Shunk, A. J., S. G. Driese, and J. A. Dunbar. 2009. Late Tertiary paleoclimatic interpretation from lacustrine rhythmites in the Gray Fossil Site, northeastern Tennessee, USA. Journal of Paleolimnology 42:11–24.

Strömberg, C. A. E., and F. A. McInerney. 2011. The Neogene transition from C_3 to C_4 grasslands in North America: assemblage analysis of fossil phytoliths. Paleobiology 37(1):50–71.

Tedford, R. H., L. B. Albright III, A. D. Barnosky, I. Ferrusquia-Villafranca, R. M. Hunt Jr., J. E. Storer, C. C. Swisher III, M. R. Voorhies, S. D. Webb, and D. P. Whistler. 2004. Mammalian biochronology of the Arikareean through Hemphillian interval (late Oligocene through early Pliocene epochs). Pp. 169–231 *in* M. O. Woodburne (ed.), Late Cretaceous and Cenozoic Mammals of North America: Biostratigraphy and Geochronology. Columbia University Press, New York.

Voorhies, M. R., and S. G. Stover. 1978. An articulated fossil skeleton of a pregnant rhinoceros, *Teleoceras major* Hatcher. Proceedings of the Nebraska Academy of Sciences 88:47–48.

Wallace, S. C. 2006. A new population of *Teleoceras* (Mammalia: Rhinocerotidae) from the Southern Appalachians (Gray, Tennessee). Geological Society of America Abstracts with Programs 38:85.

Wallace, S., B. Schubert, J. Mead, R. Short, J. Doby, and S. Swift. 2014. Recent finds from the latest Miocene/early Pliocene Gray Fossil Site Lagerstätten of eastern Tennessee, southern Appalachians, USA. Journal of Vertebrate Paleontology, Program and Abstracts, 251.

Wallace, S. C., and X. Wang. 2004. Two new carnivores from an unusual late Tertiary forest biota in eastern North America. Nature 431:556–559.

Webb, S. D., R. C. Hulbert Jr., G. S. Morgan, and H. F. Evans. 2008. Terrestrial mammals of the Palmetto Fauna (early Pliocene, latest Hemphillian) from the Central Florida Phosphate District. Pp. 93–312 *in* X. Wang, and L. G. Barnes (eds.), Geology and Vertebrate Paleontology of Western and Southern North America: Contributions in Honor of David P. Whistler. Natural History Museum of Los Angeles County, Science Series 41.

Whitelaw, J. L., K. Mickus, M. J. Whitelaw, and J. Nave. 2008. High-resolution gravity study of the Gray Fossil Site. Geophysics 73(2):B25–B32.

Yatkola, D., and L. G. Tanner. 1979. *Brachypotherium* from the Tertiary of North America. Occasional Papers of the Museum of Natural History, University of Kansas 77:1–11.

Zobaa, M. K., M. S. Zavada, M. J. Whitelaw, A. J. Shunk, and F. E. Oboh-Ikuenobe. 2011. Palynology and palynofacies analyses of the Gray Fossil Site, eastern Tennessee: their role in understanding the basin-fill history. Palaeogeography, Palaeoclimatology, Palaeoecology 308:433–444.

Appendix 1. Measurements used for scatterplots (mm). *Teleoceras aepysoma* data are results of this research. All other data are from Prothero (2005: tables 4.9, 4.10, 4.11, 5.7, 5.8, 5.9).

	T. americanum	*T. medicornutum*	*T. meridianum*	*T. major*	*T. brachyrhinum*	*T. fossiger*	*T. proterum*	*T. hicksi*	*T. guymonense*	*T. aepysoma*
Skull										
P2 to occiput	444	482	--	471	428	--	475	511	--	519.76
lambdoid crest to nasals	435	488	--	483	403	--	--	490	--	455.49
width at zygoma	320	350	323	333	353	355	--	356	--	357.18
width of occiput	163	200	170	209	200	207	184	226	--	235.61
height of occiput	161	239	--	203	180	217	210	198	--	196.54
Dentition										
P2–M3	227	236	--	243	256	305	328	254	--	265.99
P2–P4	97	94	--	99	109	129	104	100	--	116.29
M1–M3	136	140	138	143	149	178	150	152	159	158.85
p3–m3	210	242	--	220	243	250	242	241	--	246.84
p3–p4	72	72	--	71	83	79	82	72	--	82.33
m1–m3	141	155	--	148	165	173	159	172	140	165.74
Humerus										
Length	--	333	264	314	311	307	284	315	--	392.5
Distal Width	--	101	88	97	83	99	91	99	--	154.1
Midshaft Width	--	56	48	67	54	61	61	65	--	76.08
Ulna										
Length	305	310	--	293	294	260	262	279	270	389.3
Midshaft Width	29	41	--	42	31	35	38	42	38	59.20
Radius										
Length	257	265	215	257	257	259	252	250	235	310.6
Distal Width	75	86	77	94	73	99	92	95	87	97.9
Midshaft Width	40	48	42	48	41	50	50	53	52	48.84
Metacarpal 3										
Length	120	134	104	118	113	115	105	115	117	125.6
Proximal Width	39	51	44	49	42	52	50	51	54	69.8
Femur										
Length	340	433	398	384	396	440	392	440	--	491.6
Distal Width	133	121	110	123	98	113	102	115	--	134.4
Midshaft Width	51	67	64	69	53	76	61	71	--	69.99

Appendix 1. Continued.

	T. americanum	*T. medicornutum*	*T. meridianum*	*T. major*	*T. brachyrhinum*	*T. fossiger*	*T. proterum*	*T. hicksi*	*T. guymonense*	*T. aepysoma*
Tibia										
Length	250	276	218	236	263	236	195	230	220	271.5
Distal Width	70	88	70	85	74	87	75	86	76	90.1
Midshaft Width	45	47	40	49	42	50	47	52	40	51.44
Calcaneum										
Length	85	105	--	125	94	130	124	125	--	140.2
Width at Sustentaculum	54	63	--	74	55	78	70	74	--	77.06
Metatarsal 3										
Length	102	110	87	98	99	109	86	84	--	105.2
Proximal Width	37	48	32	44	37	50	40	39	--	54.3